



universität  
wien

# MASTERARBEIT

Titel der Masterarbeit

„Mutational analysis and post-transcriptional modification  
of human telomerase RNA“

verfasst von

Stefan Handl

angestrebter akademischer Grad

Master of Science (MSc)

Wien, 2015

Studienkennzahl lt. Studienblatt: A 066 834

Studienrichtung lt. Studienblatt: Masterstudium Molekulare Biologie

Betreut von: Mag. Dr. Christina Waldsich, Privatdoz.

# Table of Contents

<b>Abbreviations.....</b>	<b>2</b>
<b>1 Introduction .....</b>	<b>3</b>
1.1 Human telomerase – a ribonucleoprotein-complex.....	3
1.1.1 Biogenesis and recruitment of human telomerase to telomeres .....	4
1.1.2 The catalytic cycle of telomerase .....	6
1.2 Structural organization of the human telomerase reverse transcriptase .....	9
1.3 The architecture of the human telomerase RNA .....	11
1.3.1 Structural feature of the Core domain .....	12
1.3.2 Structure of the stem terminus element (STE) .....	14
1.3.3 The H/ACA scaRNA domain is essential for biogenesis .....	15
1.4 Pseudouridines (Ψ) – a prominent post-transcriptional modification in hTR .....	16
1.5 Disease-related phenotypes of human telomerase mutations .....	16
1.6 RNA folding .....	18
<b>2 Scientific aims of this project.....</b>	<b>19</b>
<b>3 Materials .....</b>	<b>20</b>
3.1 Plasmid constructs .....	20
3.1.1 Plasmids encoding mutated variants of hTR .....	20
3.2 Cell lines and bacterial strains.....	20
<b>4 Methods.....</b>	<b>22</b>
4.1 Fast cloning .....	22
4.2 Transformation of <i>E. coli</i> .....	23
4.3 Miniprep and sequencing of plasmid DNA.....	23
4.4 Cell culture .....	23
4.4.1 Transient transfection with FuGENE® .....	24
4.4.2 RNA extraction.....	24
4.4.3 Preparation of cell extracts under native conditions.....	25
4.5 Direct telomerase activity assay (DTA) .....	26
4.6 Chemical probing .....	27
4.6.1 <i>In vivo</i> DMS mapping .....	27
4.6.2 Pseudouridine mapping .....	27
4.6.3 Reverse transcription of chemically modified RNA .....	28
4.6.4 8% denaturing polyacrylamide gel electrophoresis (PAGE).....	30
4.6.5 Quantification of DMS modification pattern.....	31
<b>5 Results .....</b>	<b>32</b>
5.1 Mutational analysis of human telomerase RNA.....	32
5.1.1 Experimental setup .....	32
5.1.2 The C123A mutation in hTR significantly reduces telomerase activity.....	34
5.1.3 The intracellular structure of hTR in complex with hTERT .....	36
5.1.4 The C123A mutation causes misfolding in the core domain of hTR .....	37
5.2 Post-transcriptional modification of human telomerase RNA .....	42
5.2.1 Pseudouridines detected with CMCT probing.....	42
<b>6 Discussion .....</b>	<b>44</b>
<b>7 References .....</b>	<b>47</b>
<b>8 Acknowledgements.....</b>	<b>57</b>
<b>9 Appendix .....</b>	<b>58</b>
9.1 Abstract .....	58
9.2 Zusammenfassung .....	59
9.3 Book Chapter: Mapping RNA structure <i>In vitro</i> using Nucleobase-specific probes .....	60
9.4 Curriculum Vitae .....	76

## Abbreviations

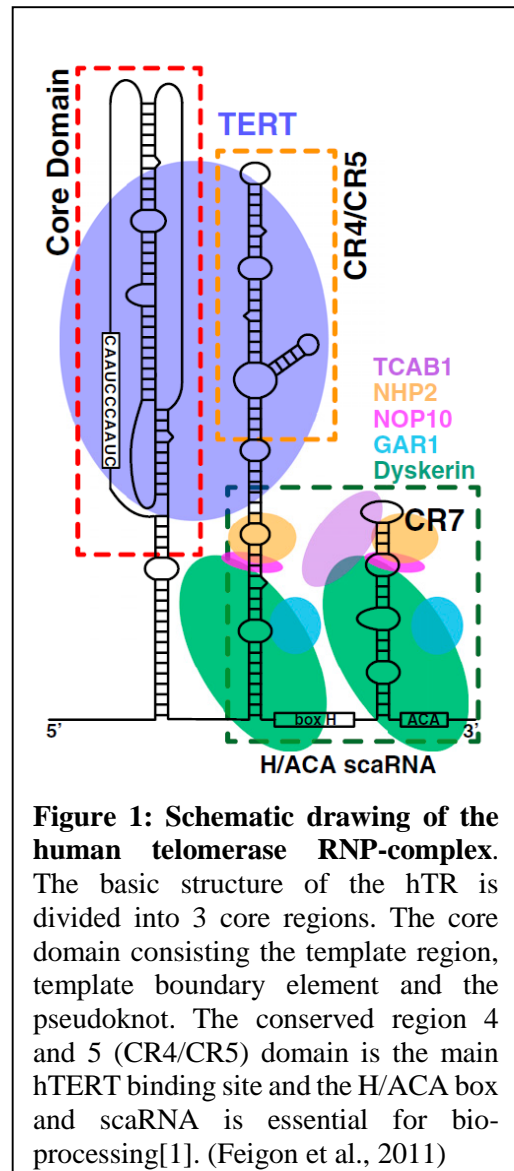
---

A.....	adenine
aa.....	amino acid
AA.....	aplastic anemia
asp .....	aspartic acid
ATM.....	ataxia telangiectasia mutated
ATR .....	ataxia telangiectasia and Rad3-related
bp .....	base-pair
C.....	cytosine
CMCT .....	N-cyclohexyl-N'-(2-morpholinoethyl)carbodiimide metho-p-toluenesulfonate
CTE.....	C-terminal element
G.....	guanosine
DC.....	dyskeratosis congenital
DDR .....	DNA damage response
DMS.....	dimethyl sulfate
DNA.....	deoxyribonucleic acid
ds.....	double stranded
HEK .....	human embryonic kidney
hTERT .....	human telomerase reverse transcriptase
hTR .....	human telomerase RNA
IFD .....	'insertion in fingers' domain
IPF.....	idiopathic pulmonary fibrosis
me.....	methyl group
NAP .....	nucleotide addition processivity
nt .....	nucleotide
NTE.....	N-terminal element
OH.....	hydroxyl group
Ψ .....	pseudouridine
PAGE .....	polyacrylamide gel electrophoresis
PCR.....	polymerase chain reaction
RAP.....	repeat addition processivity
RNA .....	ribonucleic acid
RNP.....	Ribonucleoprotein
RT .....	reverse transcriptase
scaRNA.....	small cajal body-specific RNA
ss .....	single strand
STE .....	stem terminus element
TBE.....	template boundary element
TERT .....	telomerase reverse transcriptase
TRBD.....	telomerase RNA binding domain
U.....	uracil

# 1 Introduction

## 1.1 Human telomerase – a ribonucleoprotein-complex

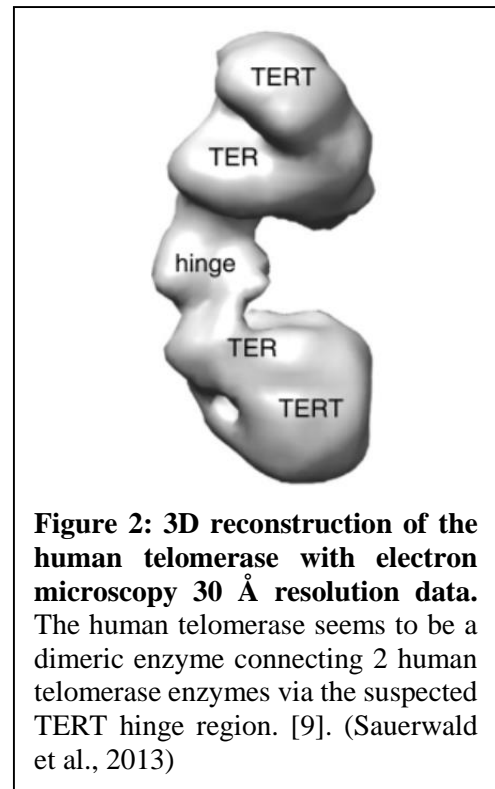
The human telomerase is a ribonucleoprotein-complex (RNP-complex) consisting of the catalytic protein part, the human telomerase reverse transcriptase (hTERT), the template RNA part, the human telomerase RNA (hTR) and several accessory proteins (Dyskerin, NOP10, NHP2, TCAB1 and GAR1) (**Figure 1**) [1][2][3][4]. In general the telomerase enzyme was found in extracts of *Tetrahymena thermophila* by C. W. Greider and E. H. Blackburn in 1985 and was awarded with the Noble prize in 2009 [5]. The telomerase itself is a eukaryotic specific feature due to the fact that it is part of the protection mechanism to guard the end of linear chromosomes [6]. The main function of the telomerase is the maintenance of the telomeres by *de novo* synthesis of telomeric repeats. For this the telomerase reverse transcriptase uses the template sequence of the telomerase RNA for recognition and elongation of the telomeres [7]. The telomerase RNA and telomerase reverse transcriptase share a strong co-evolution which makes it impossible that the TR or TERT of different species work together for a fully functioning telomerase enzyme [8]. Further investigations and structural probing of human telomerase revealed that it may also act as a dimer *in vivo* (**Figure 2**) [9][10][11].



Telomeres are a region at the end of chromosomes consisting of hexanucleotide repeats (5'-TTAGGG-3') [12][13]. The amount of telomere repeats are species specific and can, for example, range up to many kilobases in human. In addition the telomeres are protected by a multi-protein-complex called shelterin (TIN2, TPP1, POT1, TRF1, TRF2 and Rap1) [14][15]. The shelterin complex induce a specific structure at the end of chromosomes by looping the single stranded end back into the double stranded telomeres. As the single-strand (ss) end intervenes the double strand (ds), a structure forms, which is called T-loop. These can vary in length from 1 kb to 25 kb [16]. This is important because this loop formation together with the shelterin complex protect the end of chromosomes from automated DNA damage repair pathways and therefore solve the 'end-protection problem' in mammals [17]. Not only steric protection is granted by the shelterin complex but also proteins like TIRF1 and POT1 repress ATR and ATM pathways that are associated with DNA damage responses (DDR)[18]. It has also been shown that PPT1 and POT1 together play a crucial role

in recruiting telomerase to the telomeres [19][20]. Telomerase recruitment is important because after each replication cycle the telomeres are shortened due to the ‘end-replication problem’, which is caused by the lack of Okazaki fragments at the end of chromosomes and therefore shorten the chromosomes in each replication cycle, or through nucleases which are specialized to target terminal DNA elements [21][22]. This problem describes the shortening of chromosomes after each replication for about 50-100 base pairs (bp) per cycle due to the lack of RNA primers at the very end of the lagging strand [23]. Short telomeres causes instability of the chromosomes and forces the cell into a stage of senescence [24][25][26][27]. Therefore in highly proliferative cells, like stem, hematopoietic and cancer cells the expression of telomerase is up-regulated. Interestingly, the expression of telomerase in cancer cells is much higher

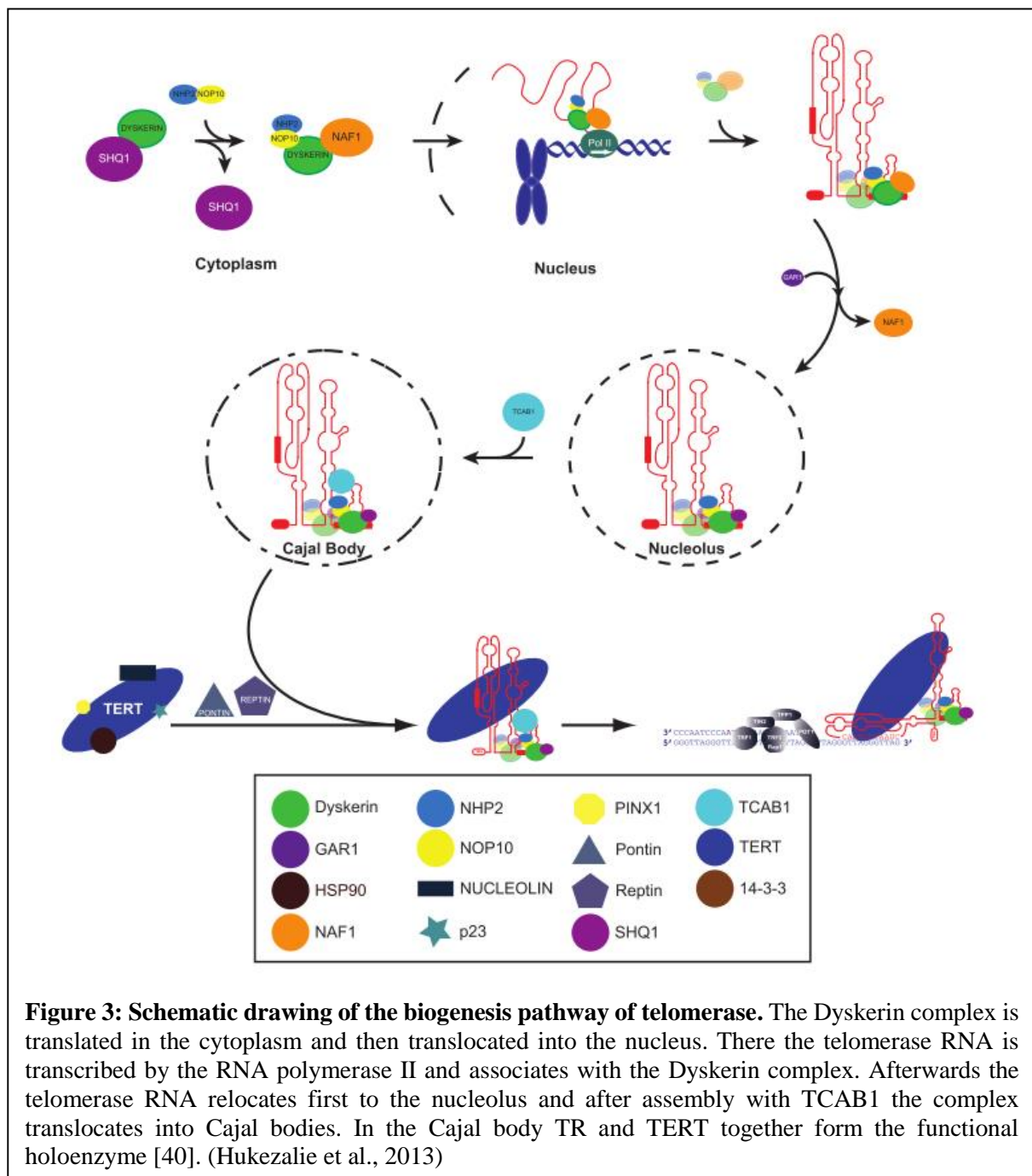
than in stem cells [28]. In the case of cancer cells, 90 % have up regulated telomerase expression [29]. This discovery shifted the focus of cancer research to telomerase as a therapeutic target to inhibit this ability to endlessly replicate [28][30]. The expression of TERT is strictly regulated and it seems to be tied to the telomerase activity [31]. Therefore in somatic cells where no telomerase activity is detectable, the expression is mostly suppressed [32][33]. There is also speculation that the expression of hTERT is connected to telomerase activity and therefore indicates tumorigenesis in form of a biomarker [34]. Despite of cancer there are other inheritable diseases like dyskeratosis congenita (DC), aplastic anemia (AA) and idiopathic pulmonary fibrosis (IPF) which are all connected to the activity deficiency of human telomerase [35][36][37]. Despite the knowledge we obtained about telomerase biogenesis, its role in disease and maintenance of telomere homeostasis, there is little known about functions not related to telomere homeostasis. This is interesting because hTERT also harbors a mitochondrial localization sequence despite the fact that the before mentioned functions are all in the nucleus [30]. There might also be evidence that telomerase plays a crucial role in apoptosis, DNA damage response and gene expression [30]. Therefore is still a lot unknown about the telomerase-RNP-complex [38].



### 1.1.1 Biogenesis and recruitment of human telomerase to telomeres

The biogenesis of human telomerase is a multi-step process which includes hTR transcription/maturation, hTERT translation and co-localization of both into the nucleus, as the main steps. In the cajal bodies hTR and hTERT form the functional holoenzyme (**Figure 3**)[39][40]. Interestingly, the biogenesis of hTR is not tied to the expression of hTERT [41].

The biogenesis of human telomerase starts with the translation of Dyskerin, Nhp2, Nop10 and Naf1 which translocate into the nucleus and bind co-transcriptionally to hTR, which is transcribed by RNA polymerase II [40][42]. In the nucleus they bind to the H/ACA domain of hTR and form the TR-H/ACA-RNP [40]. The formation of the TR-H/ACA-RNP is mainly controlled by the BIO box sequence (5'-CUGU-3') [43]. Gar1 recruits the hTR-H/ACA-RNP into the nucleolus by replacing Naf1 [40]. Together with Gar1 the Dyskerin complex is complete [44][45]. The formation of this complex is also very important for stability and maturation of hTR [46]. The main function of the Dyskerin complex is to guide the pseudouridylation and provide stability of hTR [47]. TCAB1 promotes translocation of the RNP into the Cajal bodies controlled via the CAB box signal sequence (5'-ugAG-3'), which also categorizes hTR as an scaRNA [48][49]. Despite the complex relocation into the Cajal bodies, this step does not seem to be necessary for full assembly of the telomerase holoenzyme, as cells lacking Cajal



bodies still manage to elongate the telomeres [40][50]. The localization to the Cajal bodies is a scaRNA feature and is also connected to the pseudouridylation of snRNAs [51].

The human telomerase reverse transcriptase is translated in the cytoplasm and then, passing through nuclear pores, brought into the nucleus, specifically into the nucleolus [52]. Afterwards the assembly of hTR-H/ACA-RNP and hTERT into a holoenzyme takes place and is managed by two ATPases (Pontin and Reptin) [53]. These ATPases bind hTR and hTERT independently and dissociate after the telomerase complex is formed [40]. On a side note it is interesting that expression studies of telomerase revealed that the expression of telomerase seems to be regulated by hTERT mRNA [54]. Another interesting fact is that co-purification experiments have shown that active telomerase complex is often co-purified with NAT10 and GNL3L which suggests that the telomerase could travel freely between nucleolus and cajal bodies [55]. Additionally this proteins complex enhances the activity of telomerase suggesting that these are part of the catalytically active telomerase complex [40]. This completes the biogenesis of human telomerase and the telomerase is ready for recruitment to the telomeres.

The re-localization of telomerase to the telomeres is a highly regulated process. For example FISH studies have shown that TR containing Cajal bodies co-localize with telomeres during the S-phase [56][57][58][59][60]. On the other hand the enrichment of telomerase in cajal bodies is neither necessary for activity nor for correct biogenesis of human telomerase [61]. Furthermore mutational analysis of the CAB signal has shown that a dysfunctional CAB signal does not interfere with the accumulation of the telomerase RNP but impairs telomere elongation [50]. It seems that for recruitment of telomerase to the telomeres the shelterin complex plays a much more important role [40]. Therefore it has been shown that TPP1 and POT1, part of the shelterin complex, not only are crucial for recruitment but also the presence enhances the telomerase activity [62].

### 1.1.2 The catalytic cycle of telomerase

The maintenance of the telomeres and the catalytic activity of telomerase is a highly regulated and orchestrated event which involves at least hTERT, hTR, shelterin complex and the DNA of the chromosome [6]. The enzymatic catalysis consist of 3 major steps: substrate recognition, nucleotide addition and translocation for repeat (**Figure 4**) [4][40].

To determine the telomerase activity there are 2 important aspects to differentiate: the nucleotide addition processivity (NAP) and the repeat addition processivity (RAP) [63][40]. The former determines the ability of the telomerase to add nucleotides onto the 3'OH end of the substrate DNA. The latter assesses the function of translocation and addition of multiple full repeats of 5'-TTAGGG-3' [63]. Specific amino acids of the TERT and specific structural elements of TR are important for NAP and RAP, respectively [40]. For example, template recognition and addition of nucleotides are restricted by the helix P1b [22][23]. The template region (3'-GTTAGGGTTAG-5') is split into a substrate recognition part (first 5 nucleotides from the 3' end) and the template itself.

In the first step of the catalytic cycle the telomerase recognizes the templates and aligns the first 5 nucleotides of the template region with the telomeres [40]. In the second step telomerase adds nucleotides onto the 3'-OH end of the telomere in a complementary manner to the template sequence (3'-GTTAG-5'). The elongation stops due to the template boundary element (TBE) [40]. In the last step the telomerase has to translocate and re-aligns the substrate to the template region to allow for the next round of elongation or it dissociate from the telomeres completely [40]. Translocation and repeat addition is a very unique feature of telomerase RTs compare to other RTs [63].

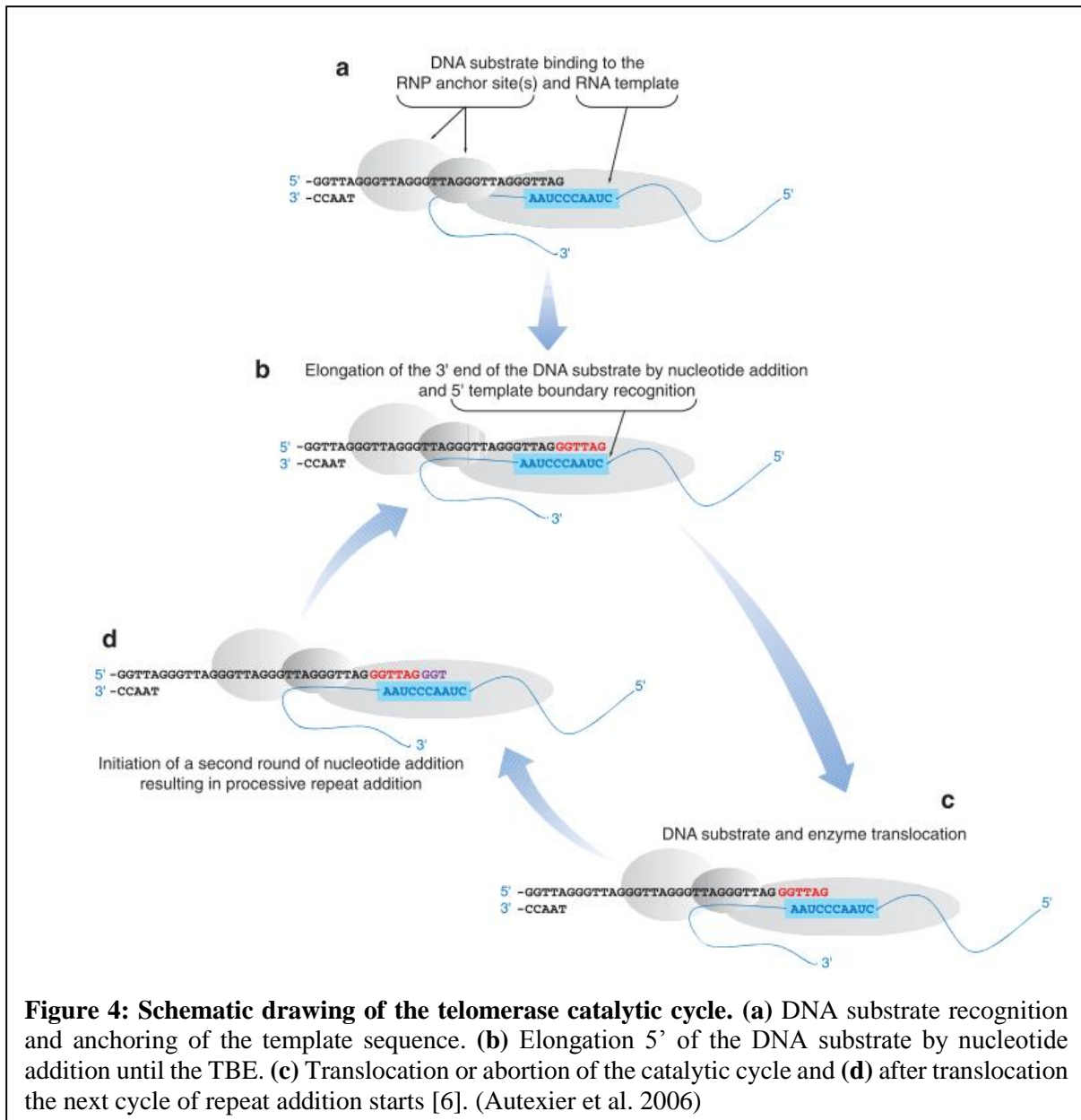


**Figure 4: Schematic drawing of the telomerase catalytic cycle. (a)** DNA substrate recognition and anchoring of the template sequence. **(b)** Elongation 5' of the DNA substrate by nucleotide addition until the TBE. **(c)** Translocation or abortion of the catalytic cycle and **(d)** after translocation the next cycle of repeat addition starts [6]. (Autexier et al. 2006)

The telomerase activity is very delicate process which is regulated by many factors. It is very interesting to note that Cajal bodies are not necessary for elongation and activity of telomerase, but the nuclear localization signal is very important for correct function of telomerase [61][65]. Also, *in vitro* only hTERT and hTR are required for activity but *in vivo* accessory proteins are required as well



[4][66][67][68]. An additional factor in processivity is the shelterin complex, which is responsible for recruitment of telomerase to telomeres but the POT1-TPP1-telomere complex seems to directly enhance the telomerase activity as well [69].

Importantly, the two distinct catalytic aspects (RAP and NAP) of telomerase activity are independently controlled and regulated. There are mutations in hTERT which enhance repeat addition processivity (**Figure 5**) [70]. Recent analysis of hTERT has shown that translocation is the rate limiting step in repeat addition processivity [70]. Also hTR mutations can cause either RAP or NAP or both processivities to go down and up. For example, recent analysis of the AA disease related mutation G305A showed a reduction in overall nucleotide addition processivity but seemed to not affect repeat addition processivity [71]. Further investigations have to be done to obtain more knowledge how this distinct processes are controlled.

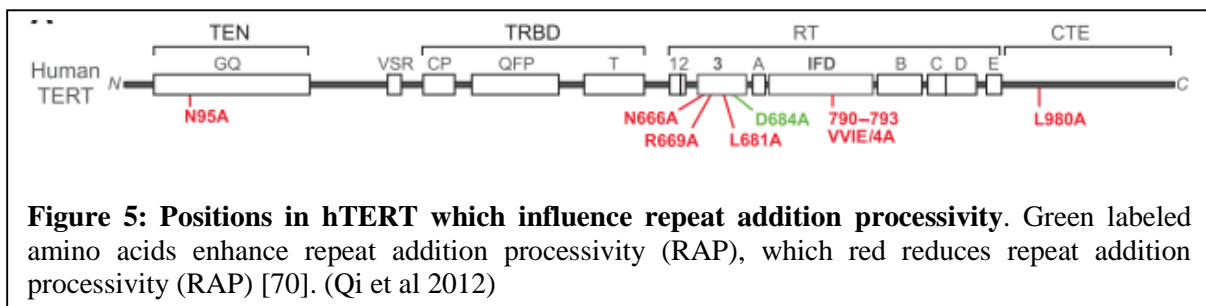


**Figure 5: Positions in hTERT which influence repeat addition processivity.** Green labeled amino acids enhance repeat addition processivity (RAP), which red reduces repeat addition processivity (RAP) [70]. (Qi et al 2012)

## 1.2 Structural organization of the human telomerase reverse transcriptase

The human telomerase reverse transcriptase (hTERT) consists of 1132 aa and harbors the conserved RT motif, which are flanked by the TEN and TRBD motifs in the N-terminal domain and the C-terminal element [2][65]. TERT is conserved throughout species although some lack the N-terminal element (**Figure 6**). The importance of TERT in the cell seems evident due to the fact that overexpression of TERT in many primary cell lines immortalizes them [72][73][74]. Currently there is no crystal structure of hTERT, but there is an high resolution structure of *Tribolium castaneum* TERT which lacks the TEN and linker domain [75]. Given the evolutionary difference of vertebrate and insects it is still a matter of debate how divergent the architecture of *Tribolium castaneum* and hTERT is (**Figure 2**) [9][76]. A special structural feature of TERT is its ring like substructure which is formed by the TRBD, the finger, palm and thumb motifs (**Figure 7**) [75]. This structural feature has also been seen in the human variant of TERT [77]. The inner side of this ring substructure is composed of amino acids known to preferentially interact with nucleic acids [78][79]. The fingers and palm motifs harbor aa which interact in nucleotide addition from the RT domain and TRBD interacting aa interact with the telomerase RNA.

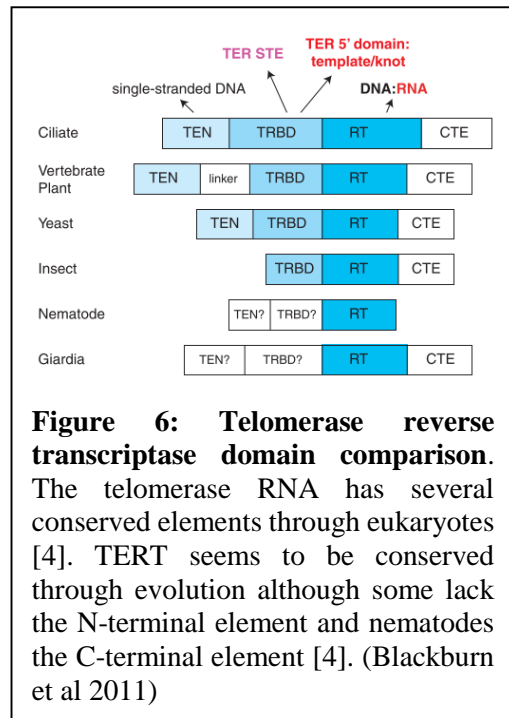


**Figure 6: Telomerase reverse transcriptase domain comparison.** The telomerase RNA has several conserved elements through eukaryotes [4]. TERT seems to be conserved through evolution although some lack the N-terminal element and nematodes the C-terminal element [4]. (Blackburn et al 2011)

The N-terminal domain consists of the telomerase essential N-terminal motif (TEN) and the telomerase RNA binding domain (TRBD) (**Figure 8**). TEN itself has been identified to bind preferentially to telomeric DNA [80]. Together the TEN and the TRBD domain coordinate binding of TR and correct positioning of the template in the active center of the telomerase [76]. The TRBD is a universally conserved RNA binding domain, which plays a role in RNP assembly and repeat addition processivity [81][82][83]. It interacts with the telomerase RNA with the pseudoknot/template domain and the CR4/CR5 domain [84]. The TEN domain is involved in binding of ssDNA and repeat addition processivity, suggesting that it maintains the contact to chromatin during translocation of the telomerase [85][86][87]. For example, at position 13 and 14 requires a leucine retains RAP but decreases overall processivity by only adding one repeat onto the DNA primer [76][88]. Another important amino acid in the TEN region is glycine 169 (G169). Mutating this residue reduces telomerase activity *in vivo* and *in vitro* [89]. In hTERT an unstructured linker region is located between the TEN and the TRBD motif

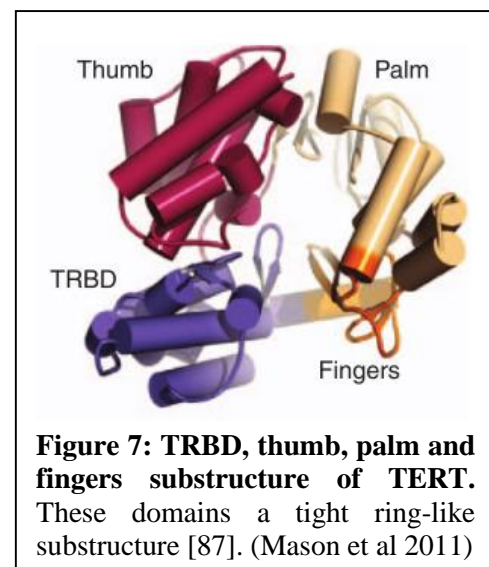
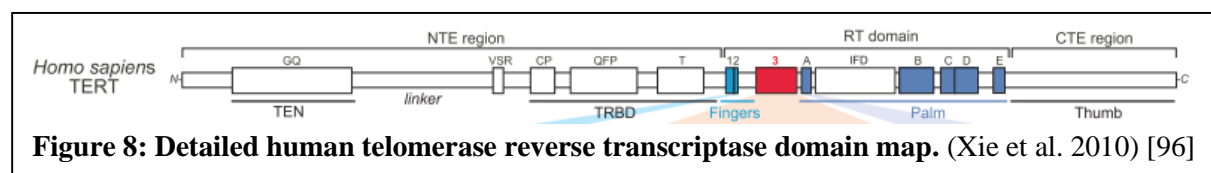


**Figure 7: TRBD, thumb, palm and fingers substructure of TERT.** These domains a tight ring-like substructure [87]. (Mason et al 2011)

which allows conformational flexibility within TERT [76]. Specific telomerase motifs in TRBD (CP, T and QFP) are important for TR binding and activity of telomerase [90][91][92]. Thus far TR and TRBD of TERT are known binding partners but there have been ongoing investigations on how they interact. For example, the TBE of hTR interacts with TBRD and contributes to RAP [64][93]. On that matter it has also been shown that the T-motif of TRBD not only binds to hTR but is also important during catalysis *in vitro* [83].

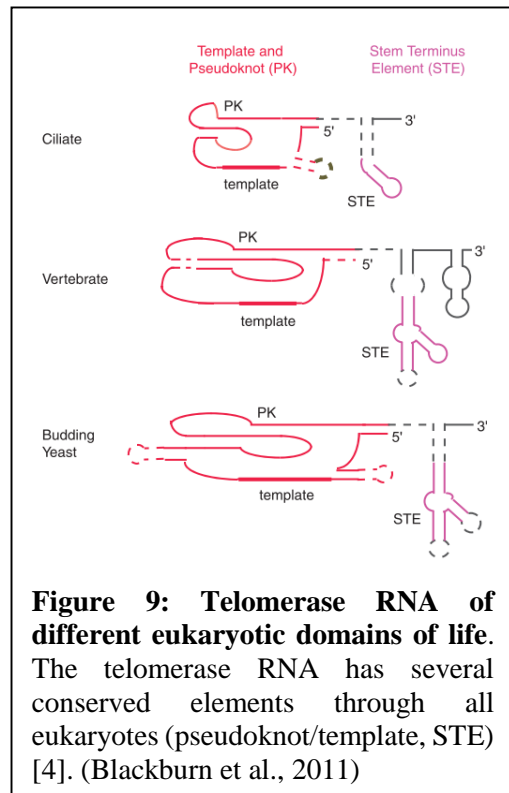
The RT domain is responsible for the catalytic function of the telomerase and is the most best-studied part of the TERT [76][94]. It consists of 7 functionally important and conserved RT motifs and is conserved throughout all RTs (**Figure 8**) [2][76]. The unique feature of the telomerase RT is the IFD (‘insertion in fingers domain’) which is located between the A and B’ motifs [76]. This IFD consists of 4 antiparallel  $\alpha$ -helices, of which one is assumed to interact with the backbone of the DNA substrate and thus to be important for catalytic function [75]. The active site of this RNA-dependent DNA polymerase is composed of 3 invariant aspartic acid residues and magnesium ions to stabilize the transition state [6][95]. One of the 3 is located in motif A and the other two in motif C [6][95]. Mutational analysis of motif 3 in the RT domain revealed that distinct residues are essential for either repeat addition processivity or nucleotide addition processivity [96]. While the conserved RT motifs are made up of the finger and palm structure, the thumb is formed by the C-terminal element. Although the C-terminal element contributes to the ring-like substructure of RT, this domain only shows weak conservation. [76]

Multiple hTERT pre-mRNA variants have been found which give evidence that changes in the splicing pattern may also alter telomerase function [97]. One alternative splicing pattern found is the  $\beta$ -isoform of hTERT [98]. This isoform does not contain an RT domain but is able to translocate and bind hTR. It was suggested to be a negative inhibitor of normal form of telomerase but seemed not to affect telomere maintenance in cancer cells [99]. Despite its obvious use in telomerase-RNP-complex recent investigations showed that hTERT might also have different functions in the cell. hTERT has been identified to play a role in post-transcriptional gene-silencing in the mitochondria opening new possibilities of interaction facettes for hTERT [100].



### 1.3 The architecture of the human telomerase RNA

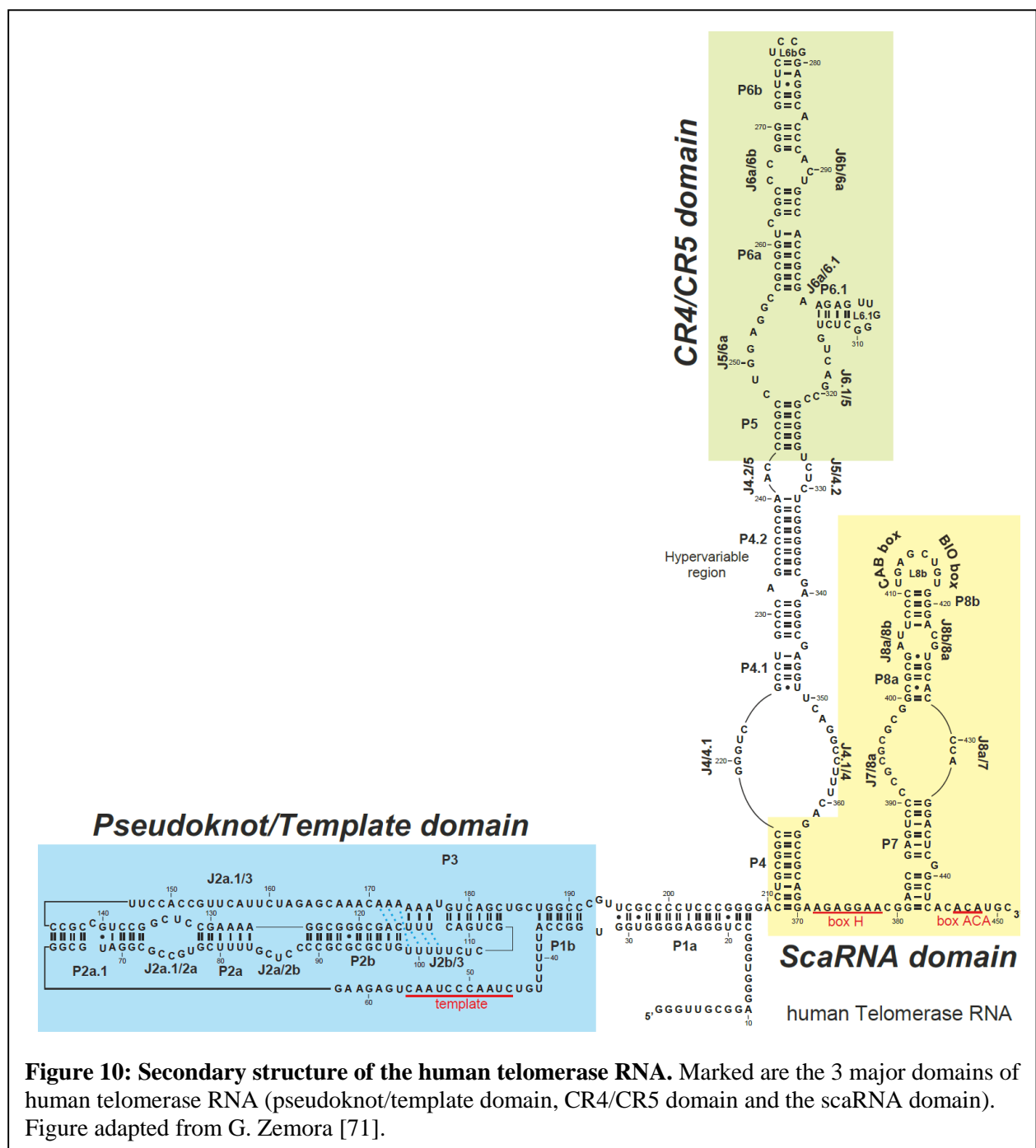
The telomerase RNA varies greatly in size in different eukaryotic species from small ciliated protozoa (147-209 nt), vertebrates (312-559 nt) and the longest in budding yeast (779-1817 nt) [4][101][102][103]. Despite their difference in length the telomerase RNAs have conserved regions throughout the eukaryotes. In the year 2000 Chen et al. published a minimum consensus structure of vertebrate telomerase through phylogenetic comparative analysis consisting only of the pseudoknot, parts of the CR4/CR5 domain and the H/ACA domain [104]. The human telomerase RNA consist of 3 important structurally conserved domains, which are also the consensus minimum telomerase RNA elements in vertebrates, which is also referred to as the pseudoknot/template domain (nucleotide 33-191), STE domain (CR4/CR5) (nucleotides 243-326) and the scaRNA domain (nucleotides 211-237 and 334-451) (**Figure 10**) [1][104][105]. Early mutational analysis showed that for a functional human telomerase the pseudoknot and template domain in addition to the STE are essential [68][106]. This study has also shown that mutations in the triple helix and template boundary element abolishes telomerase activity [68]. The pseudoknot/template domain carries the template sequence which is crucial for telomerase activity and substrate recognition and has shown to have the most conserved nucleotides in the entire telomerase RNA [104]. The pseudoknot/template domain and the CR4/CR5 domain interact independently with hTERT [66]. Notably CR4/CR5 domain has been proposed to constitute the main binding site [107]. The last important domain is the scaRNA domain, which has a typical H/ACA RNA structure [56]. Despite the conserved H/ACA boxes this domain harbors the CAB box, which allows



localization of telomerase RNA to Cajal bodies. Thus, this domain is important for biogenesis and maturation of hTR [56].

### 1.3.1 Structural feature of the Core domain

The core domain of the human telomerase RNA has received the most attention due to the fact that it plays a crucial role in telomerase activity and most of the disease related mutations are found in the pseudoknot region [1][37]. From a structural perspective it consists of 3 main elements: template region, the P1b helix (TBE) and the P2/P3 pseudoknot (**Figure 11**)[1]. The most crucial role of the core domain and its vast structural features is the positioning of the template in the active site of the telomerase.



Biochemical studies of the pseudoknot have revealed that the minimum functioning pseudoknot domain in hTR *in vitro* consists only of nucleotides 33 to 191 including 5 intact helices (P2a.1, P2a, P2b, P3 and P1b) [1][106][108]. Especially the structure of the 5 helices is crucial for telomerase activity [1][106]. One important structural feature of the core domain is the triple helix formed between Watson-Crick base pairs in the pseudoknot and nucleotides in junctions J2b/3 and J2a.1/3. (**Figure 11**, blue dashed lines) [109][110]. A triple helix is a special conformation of U·A·U Hoogsteen base triples

and is a common feature of non-coding RNAs [111]. Disrupting the triple helix drastically reduces the activity of telomerase and compensatory mutations can partially restore the function of the telomerase [112][110][113]. This strengthened the hypothesis that the tertiary interactions of the pseudoknot are important for telomerase function [110]. Similarly, removing the bulge adjacent to the triple helical scaffold U177 drastically reduces the activity of telomerase and substituting the 2'OH of A176 with a 2'OMe group reduces the telomerase activity by 50 % [109][112]. Interestingly, as U177 is bulged out,

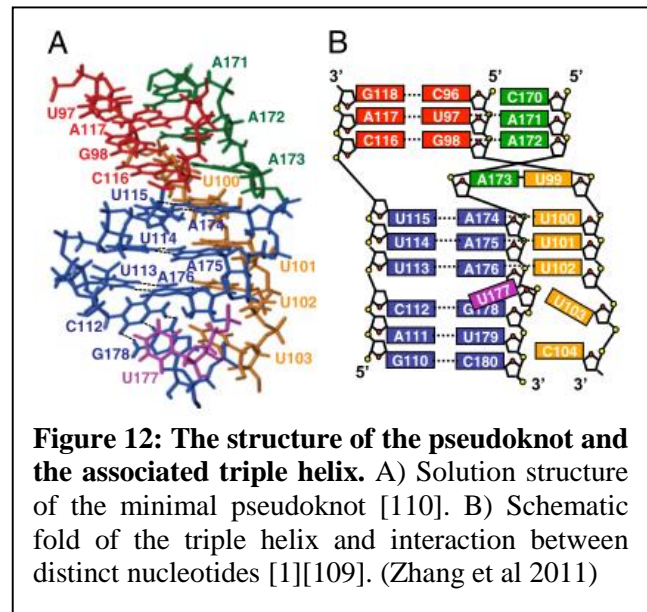


**Figure 12: The structure of the pseudoknot and the associated triple helix.** A) Solution structure of the minimal pseudoknot [110]. B) Schematic fold of the triple helix and interaction between distinct nucleotides [1][109]. (Zhang et al 2011)

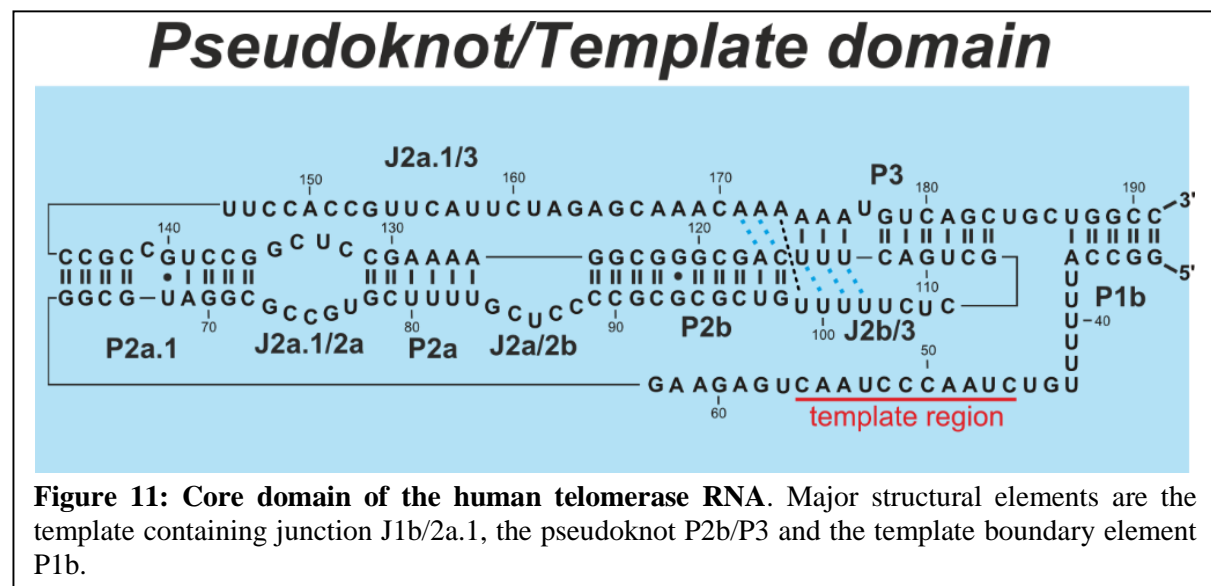


**Figure 11: Core domain of the human telomerase RNA.** Major structural elements are the template containing junction J1b/2a.1, the pseudoknot P2b/P3 and the template boundary element P1b.

the base seems to cover the 2'OH of A176 potentially preventing A176 to take part in the catalysis. However, NMR spin relaxation experiments revealed that U177 provides backbone flexibility to A176 and therefore facilitate catalysis [110]. While the interaction between the pseudoknot and the TRBD domain have been studied, the nucleotides responsible for direct interaction between hTR and hTERT have not been identified yet [106]. Among other reasons, this could be due to hTERT only interacting with the backbone of the pseudoknot nucleotides.

The template region is located in a large junction connecting stems P1b and P2a.1. Interestingly this 26 nucleotide junction J1b/2a.1 constrains the 40 nucleotide long junction J2a.1/3 and P3 seemingly forcing it into a tight fold (**Figure 11**) [1]. The template boundary element (TBE), which is formed by P1b in case of hTR, is responsible for proper template recognition and elongation [64]. The 5 nt junction J2a/2b, between P2a and P2b, induces a  $\sim 90^\circ$  kink in the core domain thereby significantly shaping the architecture of the pseudoknot domain [114]. As such it is not surprising that this junction is necessary for telomerase function [114]. Interestingly the telomerase activity can be enhanced by inserting more Cs in the J2a/2b junction [114].

Recently, SHAPE probing of the core domain *in vitro* proposed a slightly different structure of the core domain [115]. For example, stem P2a.1 is elongated by base-pairs U146-G63 and reduces junction J2a.1 by base pairing C136-G73 and C132-G76 [115]. However, it remains an open question if *in vitro* folded hTR adopts the same fold as *in vivo*. This is of particular interest, as there is evidence that TR folds in a stepwise protein-mediated manner [116].

### 1.3.2 Structure of the stem terminus element (STE)

The stem terminus element (STE), which is composed of the CR4/CR5 domain in hTR, is the second domain, which interacts independently with hTERT and is important for catalytic activity [1][66]. The STE is suggested to play an important role in the catalytic activity of telomerase by positioning TERT and the template relative to each other [4]. Importantly in human telomerase, the CR4/CR5 has been suggested to be the main binding site of hTR [66]. In hTR, the major structural element of the CR4/CR5 domain is the 3-way junction consisting of the helices P6a, P6.1 and P5 connected by the junctions J6a/6.1, J6.1/5 and J5/6a (**Figure 13**) [1]. UV crosslinking studies showed that nucleotides U182, U187 and U205 (in hTR U261, U276 and U308) seem to interact with the TRBD domain of TERT in Medaka telomerase [117]. Recently, the x-ray crystal structure of the CR4/CR5 element in couple with the TRBD domain of the Medaka telomerase has been published [118]. One hallmark of this high resolution structure was the G-A non-canonical base pair (hTR: A301-G305; medakaTR A199-G213) at the base of P6.1, whereby A199 makes a direct contact to Phe496 of TRBD [118]. If this is also true for the human variant remains to be resolved.



P6.1 harbors most of the highly conserved nucleotides in this domain and is therefore the best-studied section in this domain [1]. Out of this 13 nt 8 form the helix and are invariant, which is a rather unusual [1]. It has been shown that formation of these base pairs are crucial for telomerase function and telomerase assembly [1][119][107]. Nucleotides U306 and G310 in L6.1 form a wobble base pair and the remaining 3 nucleotides form a small loop which is a well-known conformation and has been suggested to be responsible for co-interaction of TR with TERT [110]. It remains to be addressed whether a similar architecture and interactions with TRBD occur in human telomerase [1].

P6 is a long stem consisting of P6a and P6b, which are connected by an asymmetric internal loop (J6a/6b and J6b/6a) (**Figure 13**) [1]. Removal of more than the cap sequence L6b (UCCG) of P6 abolishes telomerase activity presumably due to the loss of TERT-CR5/CR5 interactions [66]. Further base pair substitutions in this structure did not affect telomerase activity [66].

### CR4/CR5 domain

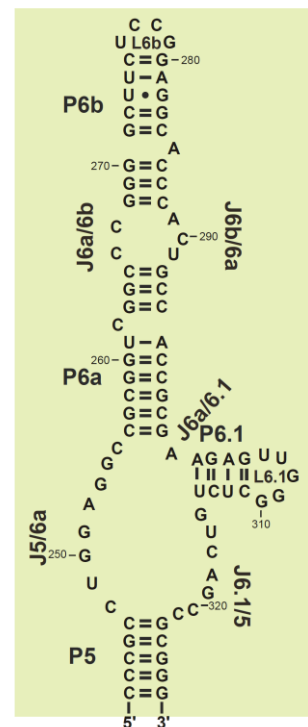
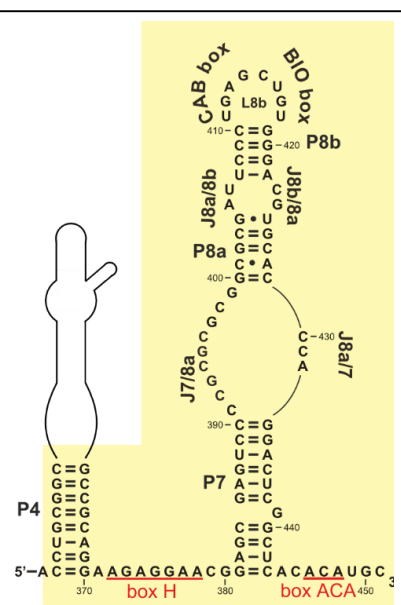


**Figure 13: Secondary structure of the human telomerase RNA CR4/CR5 domain.** The main structural feature is the P5-P6a-P6.1 three-way junction of CR4/CR5.

### 1.3.3 The H/ACA scaRNA domain is essential for biogenesis

The last major domain of the human telomerase RNA is the scaRNA domain. It is characterized by the typical H/ACA snoRNA-like fold and associated conserved sequence motifs, the H box and the ACA box in J4/7 and at the very 3' end of the hTR, respectively [104]. A CAB box was identified in L8b, thus this domain was described as a scaRNA [47]. In fact, like scaRNAs hTR was found to relocate to Cajal bodies [40]. The main function of this domain is the accumulation and maturation of the human telomerase RNA [39]. Thus this domain harbors essential sequences for biogenesis and maturation of hTR [1][47]. The H box (ANANNA; N = any base) and the ACA box are a very common motif in vertebrate non-coding RNAs, the snoRNAs known to guide pseudouridylation of rRNAs [44][120]. The closing loop L8b contains the CAB box element (consensus sequence: ugAG), which recruits TCAB1 and localizes hTR to the Cajal bodies [49][121]. The BIO box signal is also found in



### ScaRNA domain

**Figure 14: Secondary structure of the scaRNA domain of human telomerase RNA.**



loop L8b, but does not occur in other H/ACA RNAs. The BIO box is responsible for accumulation of vertebrate TRs and their maturation [121]. Both of these signals seem to operate on their own, but the solution structure CR7 shows a wobble configuration between U411 and G417 [121]. Disrupting the helix P8b to distort the loop reduces hTR accumulation and in turn telomerase activity [121].

## 1.4 Pseudouridines (Ψ) – a prominent post-transcriptional modification in hTR

Post-transcriptional modifications are modifications to RNA transcript right after transcription. Widely known are the modification of mRNA (3'-polyadenylation, 5'-capping and splicing). Additionally there are modifications which directly affect the chemistry of the nucleobases or sugars directly. Pseudouridylation is 1 of the 109 known post-transcriptional modification in all phylogenetic branches [122]. Pseudouridylation is an isomerization reaction which modifies uridines by turning the pyrimidine 180° around the N3-C6 axis

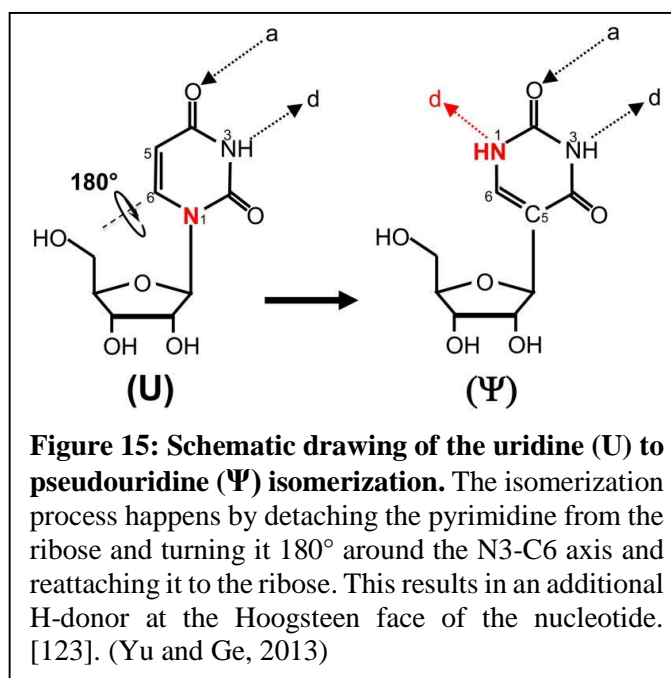


(**Figure 15**) [123]. This creates an additional imino group and therefore an H-bond donor at the Hoogsteen face of the nucleotide. This results in the possibility for new inter- and intramolecular interactions. It has also been shown that Ψs are necessary for function in rRNAs [124]. Specifically Ψs induce a different fold of the RNA, thereby directly affecting the function of the ribosome [124]. This seems also to be valid for Ψs in rRNAs and snRNAs [125]. Also, for hTR there is evidence that Ψs play a crucial role in adopting structure by stabilizing the P6.1 stem and rearranging the nucleotides in the loop and so enhancing the overall stability of this substructure [126]. The pseudouridylation in human telomerase RNA happens during the maturation process in the cajal bodies through the H/ACA-Dyskerin-RNP [44]. Along this line it is interesting to note that pseudouridylation can be induced by environmental stress in *Saccharomyces cerevisia* [123].

## 1.5 Disease-related phenotypes of human telomerase mutations

The importance of telomerase in the human organism has already been shown earlier. Dysfunction of such an important enzyme can have severe effects and causes diseases like dyskeratosis congenita (DC),

aplastic anemia (AA) and idiopathic pulmonary fibrosis (IPF), which are also called by their related effect of ‘premature ageing effect’. It has also been shown that in 90% of all cancer telomerase activity is up-regulated [127][128]. A few of these disease phenotypes are characterized and have undergone intense investigations [129].

Dyskeratosis congenita (DC) was first found in patients carrying the X-linked form of DKC1 encoding the protein Dyskerin [130]. Later on mutations conferring the same disease were identified in hTR and hTERT as well accessory proteins and the shelterin-complex (**Figure 16**)[35][131][132][133][134]. The symptoms are nail dystrophy, abnormal skin pigmentation, oral leukoplakia, fatal bone marrow failure, pulmonary fibrosis and high rates of cancer [135][136][137]. On the molecular and genetic level the identification of DC is characterized by short telomeres in peripheral blood lymphocytes [135][138]. The crystal structure of Dyskerin revealed that DKC1 mutations impair RNA binding of Dyskerin [139]. The onset and severity of DC is determined by the location of the mutation; i.e. whether the mutation effects telomerase activity or biogenesis. Mutations in the hTERT and hTR have often a later onset and milder symptoms [135]. On the other hand mutations in TCAB1, which is important for recruitment of hTR to the Cajal bodies results in a very early onset and extreme phenotypes [134]. In general, it is necessary to distinguish between mutations in hTR which impair biogenesis (scaRNA domain) and those

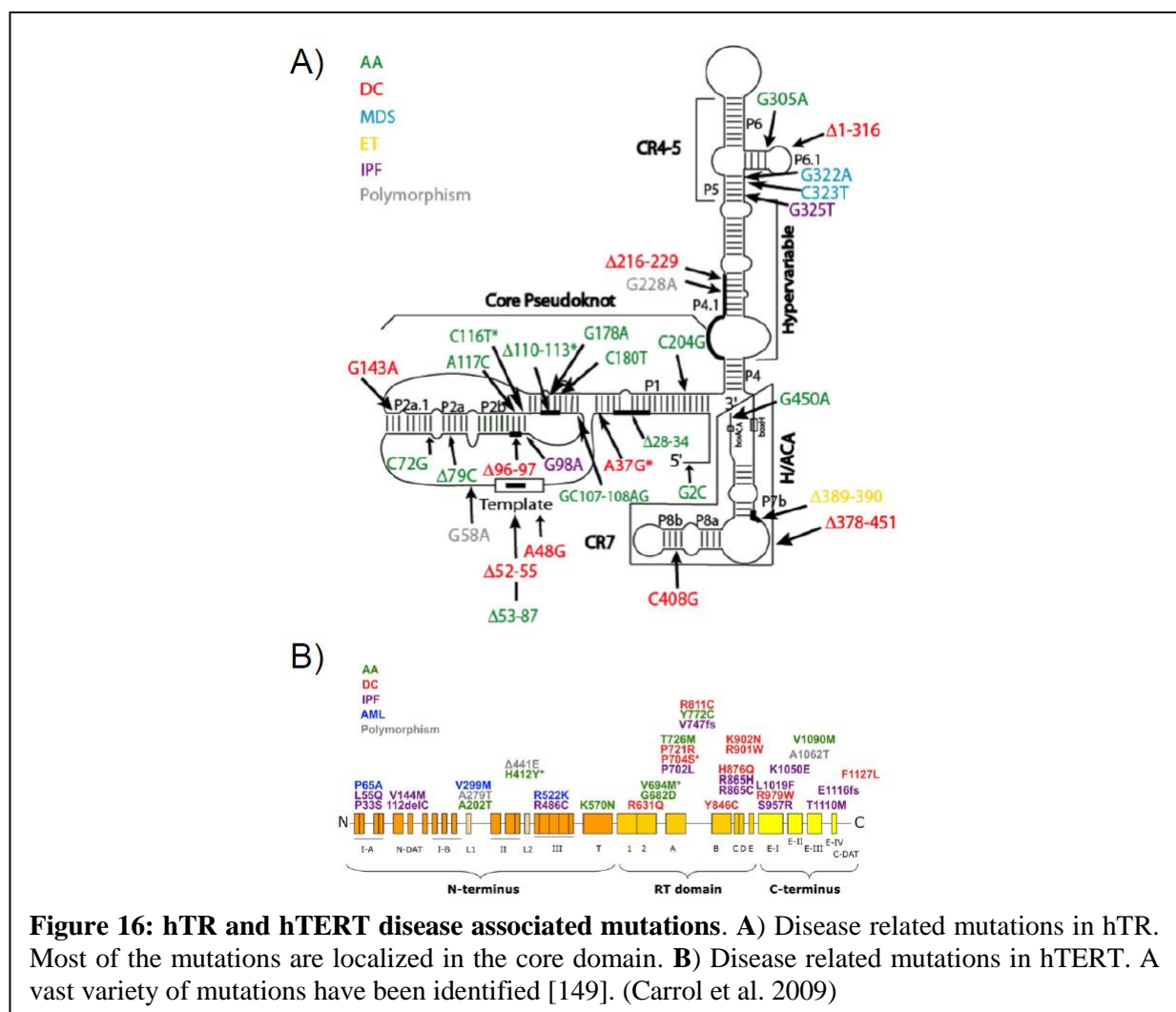


**Figure 16: hTR and hTERT disease associated mutations.** A) Disease related mutations in hTR. Most of the mutations are localized in the core domain. B) Disease related mutations in hTERT. A vast variety of mutations have been identified [149]. (Carroll et al. 2009)

affecting telomerase activity (core domain and CR4/CR5 domain) [140]. In case of the former mutation type telomerase activity can be either be abolished fully or reduced to 50 % by haploinsufficiency [140]. For example, disrupting the BIO box can cause DC [35]. On the other the DC mutation G107C/A108G in stem P3 destabilizes the pseudoknot and therefore cause the dyskeratosis congenita phenotype resulting in an inactive telomerase [141]. Recently, *in vivo* chemical probing revealed that the disease-related mutation G305A impairs telomerase activity by drastically reducing nucleotide addition processivity but keeping repeat addition processivity (RAP) [71]. Also structural analysis of this mutation showed that it does not affect the P6.1 stem nor the formation of the CR4/CR5 domain [71]. Thus suggests that the nucleotide G305 is directly involved in the catalytic process. Therefore investigation of certain positions in human telomerase RNA directly is important in understanding disease formation.

## 1.6 RNA folding

Determining RNA structure is a very difficult task due to the fact that most functional by relevant RNAs are too large for high resolution techniques, like NMR and x-ray crystallography. Thus these techniques often rely on studying truncated variants of the RNA *in vitro*. Also bioinformatic approaches are hindered by the sheer number of folding possibilities and the low sequence conservation of functional RNAs [142]. Thus, studying RNA structure and folding often relies on biochemical approaches, like the powerful tools of chemical probing [143]. Most structural probing studies were performed *in vitro*, after re-folding the transcript under non physiological conditions [143]. Apart from catalytic RNA it is however difficult to assess if the probed conformation is functionally relevant. Moreover, factors, such as the discontinuity and velocity of transcription and translation as well as *trans*-acting factors, like proteins, nucleic acids, metal ions or metabolites may influence RNA folding. Thus, mapping RNA structure *in vivo* would eliminate these variables, but it is essentially harder to achieve. *In vivo* chemical probing provides however the possibility to observe active RNA in its natural environment and allows detecting on structural differences between wild-type and mutant RNA. In lights of these advantages, we recently analyzed the structure of hTR *in vivo* [71]. We identified possible hTR/hTERT interaction site by looking at the DMS pattern of hTR in presence and absence of hTERT and concluded that hTERT interacts with hTR with the P6.1 stem and the adjacent junction J6.1/5[71]. Not only structural information can be obtained with chemical probing. We also used this method to identify possible leads of pseudouridines in hTR [71].

## 2 Scientific aims of this project

Telomerase activity, biogenesis and regulation is well researched. Although there is great effort in regards of obtaining high resolution structure of parts of the telomerase RNA there is little known about structural importance of certain positions of full length *in vivo* hTR. Recent investigations in our lab have given insight into wild-type telomerase RNA in presence and absence of hTERT as well as structural insights into disease mutations of hTR. This investigation raised the question which nucleotides play a crucial role in telomerase activity especially in case of the base pair C123 and G91. Also in this doctoral thesis of Georgeta Zemora 18 Uridines were identified to be methylated by DMS *in vivo* [71]. Some of this methylated Us coincided with those already reported by Kim et al. [126]. Therefore the scientific aims of this project are: i) Identifying important functional and structural positions in the human telomerase RNA according to sequence conservation. ii) Identifying possible pseudouridines giving insight into how pseudouridylation is important in folding of the human telomerase RNA.

### 3 Materials

All solutions were prepared with deionized RNase-free water with a sensitivity of  $> 18 \text{ M}\Omega \text{ cm}$  at  $25^\circ\text{C}$  and either autoclaved or sterile filtered.

#### 3.1 Plasmid constructs

Plasmid constructs for hTERT (pcDNA6-hTERT) and hTR (pBSU1-hTR) used for mutagenesis analysis and transient transfection were supplied by Dr. Joachim Lingner, EPFL, Switzerland [144]. The plasmid vector maps can be seen in **Figure 17**.

##### 3.1.1 Plasmids encoding mutated variants of hTR

Using the Fast cloning method (described in section **4.1 Fast cloning**) the mutations were introduced into the hTR gene cloned into the vector pBSU1-hTR (**Figure 17**). The mutation sites and nucleotides were chosen based on their sequence conservation in vertebrates or on their structural property previously determined by chemical probing in Georgeta Zemoras doctoral thesis [71]. The full list of all mutants created is shown in **Table 1**.

#### 3.2 Cell lines and bacterial strains

For plasmid amplification and cloning we used the *E. coli* XL1-blue: *recA1 endA1 gyrA96 thi-1 hsdR17 wupE44 relA1 lac[F' proAB lacIqZΔM15 Tn10 (Tetr)]*.

As for the cell culture the HEK-293 cell line (HEK: Human Embryonic Kidney) was used for transient transfection. This cell line originates from human embryonic kidney tissue and was immortalized by transformation with adenovirus 5. The number 293 refers to the 293<sup>rd</sup> experiment performed to reach a stable transformation. In addition this cells are also hypotriploid which means that these cells contain 64 chromosomes (less than 3 times the chromosomes).

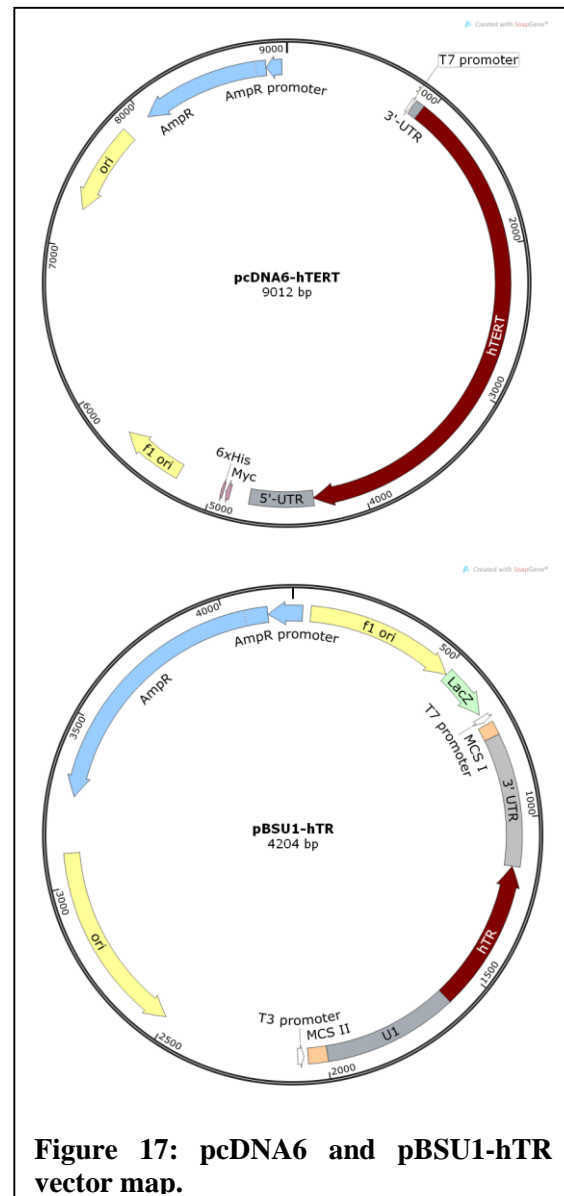


**Figure 17: pcDNA6 and pBSU1-hTR vector map.**

nr.	mutation	plasmid ID	primer sequence
1	U68A	pCW112	Fw: 5' -AAGGGCGAAGGCGCCGTGCTTTTGCT-3'
			Rv: 5' -CGGCGCCTTCGCCCTTCTCAGTTAGGGTT-3'
2	G91A	pCW113	Fw: 5' -GCTCCCCACGCGCTGTTTTTCTCGCTG-3'
			Rv: 5' -ACAGCGCGTGGGGAGCAAAAGCACGGC-3'
3	G91C	pCW168	Fw: 5' -GCGCGGGGGGAGCAAAAGCACG-3'
			Rv: 5' -TCCCCCGCGCTGTTTTTCTCGCTG3'
4	C123A	pCW114	Fw: 5' -TCAGCGGGAGGAAAAGCCTCGGCCTGC-3'
			Rv: 5' -GCTTTTCCTCCCGCTGAAAGTCAGCGAG-3'
5	C123U	pCW115	Fw: 5' -CAGCGGGTGGAAAAGCCTCGGCCTG-3'
			Rv: 5' -GGCTTTTCCACCCGCTGAAAGTCAGCGAG-3'
6	G140A	pCW116	Fw: 5' -TCGGCCTACCGCCTTCCACCGTTCA-3'
			Rv: 5' -AAGGCGGTAGGCCGAGGCTTTTCCG-3'
7	U146-147A	pCW117	Fw: 5' -GGCCTGCCGCCAACCACCGTTCATTCTAGAGC-3'
			Rv: 5' -ACGGTGGTTGGCGGCAGGCCGAGGC-3'
8	A150U	pCW118	Fw: 5' -CCGCCTTCCTCCGTTTATTCTAGAGCAAAC-3'
			Rv: 5' -GAACGGAGGAAGGCGGCAGGCC-3'
9	C152G/G153C/U154A/ U155A/C156G/A157U/ U158A/U159A/C160G/ U161A	pCW163	Fw: 5' -TGCTCTTCTTACTTGCGTGGAAGGCGGCAGGCC-3'
			Rv: 5' -GCCTTCCACGCAAGTAAGAAGAGCAAACAAAAATGTCAGCTGC-3'
10	A164U/G165C/C166G/ A167U/A168U/A169U	pCW164	Fw: 5' -GACATTTTTTTGAAACGACTAGAATGAACGGTGGAAGGCGG-3'
			Rv: 5' -CATTCTAGTCGTTTCAAAAAATGTCAGCTGCTGGCCCG-3'
11	C170A	pCW119	Fw: 5' -AGAGCAAAAAAAAATGTCAGCTGCTGGCCCGTTC-3'
			Rv: 5' -GACATTTTTTTTTTGTCTAGAATGAACGGTGGAAGGCG-3'
12	G268C	pCW169	Fw: 5' -CCCGGGGCGGACCGCGGC-3'
			Rv: 5' -GCCCCGGGCTTCTCCGGAGGC-3'
13	G288C	pCW170	Fw: 5' -GGCAGTCGGTGCCTCCGGAGAAG-3'
			Rv: 5' -GCACCGACTGCCACCGCAAGAG-3'
14	G268C/G288C	pCW171	Fw: 5' -CCCGGGGCGGACCGCGGC-3'
			Rv: 5' -GCCCCGGGCTTCTCCGGAGGC-3'
15	G322A	pCW120	Fw: 5' -CTGTCAGCCACGGTCTCTCGGGG-3'
			Rv: 5' -GACCCGTGGCTGACAGAGCCCAACTC-3'
16	G402C	pCW166	Fw: 5' -GGAATCGGGCCGCGCGCGG-3'
			Rv: 5' -CGCGGCCCGATTCCCTGAGCTG-3'
17	C427G	pCW165	Fw: 5' -CTGGGTCCACGTCCACAGCTCAG-3'
			Rv: 5' -ACGTGGACCCAGGACTCGGCTCAC-3'
18	G402C/C427G	pCW167	Fw: 5' -GGAATCGGGCCGCGCGCGG-3'
			Rv: 5' -CGCGGCCCGATTCCCTGAGCTG-3'

**Table 1: Sites of mutation, plasmid IDs and primer sequences for the fast cloning PCR.**

## 4 Methods

### 4.1 Fast cloning

This method is an adapted version of the method described by Shen et al. in 2011 [145]. The basic principle behind this method is that mutated plasmids can be easily obtained by 1) doing an overlap PCR of the target plasmid introducing the mutations and removing the template plasmid with a *DpnI* digest. As for the *in vitro* mutagenesis/cloning strategies, the plasmids are transformed into *E. coli*. Which repairs the single nicks in the plasmids and after plasmid extraction from identified clones they were sequenced. These steps are explained in more detail in **section 4.2** and **section 4.3**.

First of all the primers for the PCR reaction were designed (**Table 1**) to yield a  $T_m$  (melting temperature) of around 60°C using the following equation:

$$T_m = 81.5^{\circ}\text{C} + 16.6^{\circ}\text{C} * (\log_{10}[0.05]) + 0.41^{\circ}\text{C} * (\%GC) - 675/N$$

N ... number of nucleotides in the oligo

$T_m$  ... melting temperature

For the annealing temperature ( $T_a$ ) 5°C were subtracted from the  $T_m$  giving a  $T_a$  of 55°C. The setup of the PCR reaction is shown in **Table 3** and the PCR program in **Table 2**.

10x pfu ultra II buffer	5 µL
template DNA (10 ng/µl)	1 µL
10 µM Fw-primer [f.c. 1 µM]	0.5 µL
10 µM Rv-primer [f.c. 1 µM]	0.5 µL
10 mM dNTP mix [f.c. 2 mM]	1.25 µL
pfu ultra II	1 µL
ddH <sub>2</sub> O	40.75 µL
	50 µL

**Table 3: PCR reaction mix for Fast cloning.**

initial denaturation	95°C	3 min
30 cycles	95°C	10 s
	55°C	30 s
	72°C	3 min
final extension	72°C	5 min
store	4°C	∞

**Table 2: PCR program for Fast cloning.**

To determine the size of the PCR fragment, 1 µL PCR product was loaded onto a 0.8 % native agarose gel. After confirming that the PCR has yielded a product of correct size the template DNA was digested with 1 µL *DpnI* (20 U/µL), which only digests methylated DNA, at 37°C for 1 hour.

<b>10x TBE buffer (Tris/Borate/EDTA):</b> 0.89 M TRIS base, 0.89 M boric acid, 0.02 M EDTA
<b>1x TBE buffer (Tris/Borate/EDTA):</b> 1:10 dilution of 10x TBE buffer with ddH <sub>2</sub> O
<b>10 mM dNTP mix:</b> 1:10 dilution with ddH <sub>2</sub> O of 100 mM dNTP set, sodium salt (Roche)
<b>PfuUltra II Fusion HotStart DNA Polymerase</b> (Agilent/Stratagene)
<b>0.8 % native agarose gel:</b> 0.8 % (w/v) agarose in 1x TBE, was heated until the agarose melted and then cooled until it was touchable. Afterwards 1/1000 of the volume of ethidiumbromide [10 mg/ml] was added.
<b><i>DpnI</i> (20 U/µL)</b> (New England Biolabs)

## 4.2 Transformation of *E. coli*

10 µL of the *DpnI* treated PCR reaction was added to 50 µL *XL1-blue* cell suspension. They were incubated on ice for 20 min. After that the cells were heat shocked at 42°C for 45 s followed by incubation on ice for 2 min. Afterwards 700 µL of LB-medium were added and the cells were put on 37°C for 1 hour. Then the cells were collected by centrifuging at max speed for 1 min at room temperature and plated on a selective LB agar plate (+amp). The plate was placed at 37°C over night.

**LB-medium:** 1 % (w/v) Bacto-Tryptone; 0.5 % (w/v) yeast extract; 0.5 % (w/v) NaCl

**1000x ampicilline [100 mg/mL]** (Sigma-Aldrich)

**LB agar plates (+amp):** 1 % (w/v) Bacto-Tryptone; 0.5 % (w/v) yeast extract; 0.5 % (w/v) NaCl, 2 % (w/v) agar and 100 µg/mL ampicilline

## 4.3 Miniprep and sequencing of plasmid DNA

1 grown colony was picked and inoculated into 5 mL LB-medium containing 5 µL 1000x ampicilline and then incubated at 37°C over night. Then a miniprep with the PureYield™ Miniprep System from Promega was performed to extract the plasmids from the cells and sent for sequencing.

**LB-medium:** 1 % (w/v) Bacto-Tryptone; 0.5 % (w/v) yeast extract; 0.5 % (w/v) NaCl

**1000x ampicilline [100 mg/mL]** (Sigma-Aldrich)

**PureYield™ Miniprep System** (Promega)

## 4.4 Cell culture

Plasmids coding for hTERT and hTR were transiently transfected in HEK-293 cells. The HEK-293 cells were passaged, by dilution 1:10 with DMEM (+10% FBS), every third day. This was achieved by removing the old media and washing the cells with 7 mL of 20x DPBS. Then the DPBS was removed and the attached cells were incubated with 1 mL 1x Trypsin at 37°C and 5 % CO<sub>2</sub> for 3-5 min. After the cells detached from the dish 9 mL of DMEM (+10% FBS) were added. 1 mL of this cell suspension was then transferred into 9 mL DMEM (+10 % FBS) on a new Ø 10 cm cell culture dish. Then the cells were incubated at 37°C and 5 % CO<sub>2</sub>.

**DMEM (+10 % FBS):** Dulbecco's Modified Eagle's Medium – high glucose, Sigma-Aldrich, +10 % Fetal Bovine Serum (Sigma-Aldrich)

**20x DPBS:** Dulbecco's Phosphate Buffered Saline, without calcium chloride and magnesium chloride (Sigma-Aldrich)



**1x Trypsin:** 10x Trypsin solution diluted 1:10 with 1x DPBS (Sigma-Aldrich)

#### 4.4.1 Transient transfection with FuGENE®

The transient transfection of the HEK-293 cells was performed with the transfection reagent FuGENE® (Promega). First the cells were grown to ~90 % confluency. Then the cells were washed and trypsinized

type	hTERT [1 µg/µL]	wt hTR [1 µg/µL]	mutant hTR [1 µg/µL]	FuGENE®	ddH <sub>2</sub> O	total volume
wt hTR	3.2 µL	0.8 µL	-	13.33 µL	132.67 µL	150 µL
mutant hTR	3.2 µL	-	0.8 µL	13.33 µL	132.67 µL	150 µL

**Table 4: Representative transfection mix.** The transfection mix includes 13.33 µL FuGENE and a ratio of 5:1 hTERT:wt hTR encoding plasmids or hTERT:mutant hTR encoding plasmids.

as in a normal passaging event (**4.4 Cell culture**). 500 µL of cell suspension was put in each well of a 6-well-plate containing 1.5 mL DMEM (+10 % FBS). Followed by an incubated at 37°C and 5 % CO<sub>2</sub> overnight. After 24 hours of incubation the cells reached a confluency between 80 and 90 %. The medium was renewed with 1.8 mL DMEM (+10% FBS). Beforehand 150 µL of transfection reagent were mixed with 4 µg plasmid DNA in a ratio of 5:1 with respect to the hTERT:hTR encoding plasmids. An example is given in **Table 4: Representative transfection mix**. The transfection mix for each well was assembled and incubated at room temperature for 20 min. Afterwards the mix was pipetted into medium in a spiral fashion to prevent extreme local pH changes which can lyse the cells. Subsequently that the cells were incubated at 37°C and 5 % CO<sub>2</sub> for 12-16 hours. After this period the cells were expanded on Ø 10 cm cell culture dishes per well and again incubated at 37°C and 5 % CO<sub>2</sub> for 48 hours.

**DMEM (+10 % FBS):** Dulbecco's Modified Eagle's Medium – high glucose, Sigma-Aldrich, +10 % Fetal Bovine Serum (Sigma-Aldrich)

**20x DPBS:** Dulbecco's Phosphate Buffered Saline, without calcium chloride and magnesium chloride (Sigma-Aldrich)

**1x Trypsin:** 10x Trypsin solution diluted 1:10 with DPBS (Sigma-Aldrich)

#### 4.4.2 RNA extraction

This section describes the extraction of total RNA from transient transfected HEK-293 cells with TRI Reagent® (Sigma-Aldrich). 48 hours post-expansion (~60 hours post-transfection) the transfected cells reached >90 % confluency on an Ø 10 cm cell culture dish. The medium was removed and the adherent cells then incubated with 4 mL TRI Reagent® at room temperature for 5 min. Afterwards the phenol solution was transferred into a new 14 mL falcon and 800 µL chloroform was added (200 µL per 1 mL TRI Reagent®), vortexed and incubated at room temperature for 10 min. Then the solution was centrifuged at 12,000 x g at 4°C for 10 min. After centrifugation the aqueous phase was transferred into

a new 14 mL falcon and the equal volume of 2-propanol was added. The solution was then vortexed intensively, incubated at room temperature for 10 min and then centrifuged again at 12,000 x g at 4°C for 10 min. After removing the supernatant, the RNA pellet was washed with was removed and 1 mL 70 % ethanol. The solution together with the pellet was transferred into in the a 1.5 mL Eppendorf tube and centrifuged at 7,000 x g at 4°C for 5 min. The supernatant was removed and the pellet dried at room temperature for 10 min. Then it was resuspended in 30 µL ddH<sub>2</sub>O and the concentration measured with a UV spectrophotometer. The RNA extract was stored at -20°C.

**TRI Reagent®** (Sigma-Aldrich)

**Chloroform** (Merck Millipore)

**2-propanol** (Merck Millipore)

**70 % (v/v) ethanol:** 7 mL Ethanol p.a. ad 10 mL with ddH<sub>2</sub>O

#### 4.4.3 Preparation of cell extracts under native conditions

This is a modified version of the cell extract preparation as described in Cristofario et al. 2007 [50]. 48 hours post-expansion (~60 hours post-transfection) the transfected cells reached a >90 % confluency on an Ø 10 cm cell culture dish. The medium was removed and the cells were washed and trypsinized as described in section **4.4 Cell culture**. The trypsinization reaction was stopped with 7 mL DMEM (+10 % FBS) and the cells were collected by centrifuging at 1,200 x g at 4°C for 5 min. After removing the supernatant 3 mL of cold DPBS were added to wash out remaining trypsin in the pellet. The pellet was vortexed briefly and then centrifuged again at 1,200 x g at 4°C for 5 min. Subsequently the DPBS was discarded and the pellet was resuspended in 300 – 600 µL Chaps Lysis Buffer (volume depending on the confluency and the dish size) and transferred into a 1.5 mL Eppendorf tube. The suspension was incubated on a rotating wheel at 4°C for 30 min. Then the solution was centrifuged at 10,000 g at 4°C for 10 min. The supernatant was aliquoted (50 µL per tube) and shock frozen in liquid nitrogen. The aliquots were stored at -80°C. The protein concentration was calculated using the Bradford method against a BSA standard.

**DMEM (+10 % FBS):** Dulbecco's Modified Eagle's Medium – high glucose, Sigma-Aldrich, +10 % Fetal Bovine Serum (Sigma-Aldrich)

**20x DPBS:** Dulbecco's Phosphate Buffered Saline, without calcium chloride and magnesium chloride (Sigma-Aldrich)

**1x Trypsin:** 10x Trypsin solution diluted 1:10 with DPBS (Sigma-Aldrich)

**Chaps Lysis Buffer:** 10 mM TRIS HCl pH 7.5, 400 mM NaCl, 1 mM MgCl<sub>2</sub>, 1 mM EGTA, 0.5 % CHAPS, 10 % glycerol, 5 mM β-mercaptoethanol, 1x protease inhibitor Sigmafast™ (Sigma-Aldrich)

## 4.5 Direct telomerase activity assay (DTA)

The protocol for the direct telomerase activity assay (DTA) is based on the method described in Cristofari et al., 2007 [50]. This protocol allows assessing the telomere elongation and repeat addition processivity of over-expressed human telomerase complex in cell extracts prepared from transient transfected HEK-293 cells. The DTA reaction was prepared as shown in **Table 5** adding the cell extract at last. The reaction was incubated at

20 µg cell extract (4 µg/µL)	5 µL
10x DTA buffer	2 µL
25 mM dNTP-mix [f.c. 0.5 mM]	0.4 µL
$\alpha$ - <sup>32</sup> P dGTP (10 Ci/µL)	2 µL
10 µM telomeric primer [f.c. 1 µM]	2 µL
0.1 M $\beta$ -mercaptoethanol [f.c. 5 mM]	1 µL
ddH <sub>2</sub> O ad	20 µL

**Table 5: Reaction setup of a direct telomere activity assay (DTA).**

30°C for 1 hour. After adding 5 µL of RNase A solution [10 µg/µL] the sample was incubated at 37°C for 10 min. Then 15 µL Proteinase K (20 mg/mL) solution was added and again incubated at 37°C for 30 min. Afterwards trace amounts of <sup>32</sup>P labelled 100mer oligo were added as a loading control. Subsequently the elongated telomeric primers were precipitated by adding 2 µL 0.5 M EDTA, pH 8.0, 2 µL glycogen [10mg/mL] and 125 µL 0.3 M NaOAc/EtOH and placed at -20°C for 1 hour. After centrifugation (14,000 x g at 4°C for 30 min) the supernatant was removed and the pellet dried at room temperature for 10 min. The dried pellet was resuspended in 10 µL loading buffer and stored at -20°C. Half of the sample was loaded and resolved on an 8 % denaturing PAGE (**Section 4.6.4**).

**10x DTA buffer:** 500 mM Tris HCl pH 8.0, 500 mM KCl, 10 mM MgCl<sub>2</sub>, 10 mM Spermidine

**25 mM dNTP mix:** 25 mM dATP, 25 mM dTTP, 0.1 mM dGTP (Roche)

**$\alpha$ -<sup>32</sup>P GTP (10 Ci/µL)**

**10 µM telomeric primer:** 5'-(T<sub>2</sub>AG<sub>3</sub>)<sub>3</sub>-3', gel purified oligo

**0.1 M  $\beta$ -mercaptoethanol:** 1:14.3 dilution of stock (14.3 M) solution with ddH<sub>2</sub>O (Sigma-Aldrich)

**RNase A (10 mg/ml):** DNases were heat inactivated by incubating the solution on 95°C for 5 min (Applichem)

**Proteinase K (20 mg/mL)** (Applichem)

**0.5 M EDTA pH 8.0** (Ambion)

**Glycogen [10mg/mL]**

**3 M NaOAc pH 5.5** (Ambion)

**0.3 M NaOAc/EtOH:** 1:10 dilution of 3 M NaOAc pH 5.5 with ethanol p.a.

**10x TBE buffer (Tris/Borate/EDTA):** 0.89 M TRIS base, 0.89 M boric acid, 0.02 M EDTA

**1x TBE buffer (Tris/Borate/EDTA):** 1:10 dilution of 10x TBE buffer with ddH<sub>2</sub>O

**Loading buffer:** 7 M urea, 25 % sucrose, 0.25 % bromphenol blue in 1x TBE

## 4.6 Chemical probing

Chemical probing is based on the principle that certain chemicals (e.g. DMS, CMCT, Kethoxal) modify specific atoms of nucleotides, if these are not involved in H-bonds or in interaction with the protein. This modification causes a reverse transcription to stop 1 nucleotide prior to the modified base. Notably, reverse transcription can also be terminated prematurely due to partial RNA degradation, stable RNA structure, G/C-rich sequence stretches or natural post-transcriptional modifications. To differentiate between a natural stop or a modification induced stop of the RT unmodified RNA has to be reverse transcribed as well to display natural stops only.

### 4.6.1 *In vivo* DMS mapping

48 hours post-expansion (~60 hours post-transfection) the cells were trypsinized, harvested by centrifugation (1,200 x g, 4°C, 5 min), resuspended in 1 mL prewarmed DMEM (+10 % FBS) and transferred into a 2 mL Eppendorf tube. Then 4.67 µL 10.7 M DMS [f.c. 50 mM] was added, vortexed briefly and incubated at 37°C for 2 min. To stop the methylation reaction 50 µL 14.3 M β-mercaptoethanol and 50 µL isoamylalcohol were added. The solution was vortexed very well and then centrifuged at 1,200 x g at 4°C for 5 min. The supernatant was removed and 1 mL of cold DPBS as well as 50 µL β-mercaptoethanol were added. Then the cell suspension was vortexed very well and again centrifuged with 700 x g at 4°C for 1 min. The supernatant was removed and the pellet resuspended in 4 mL TRI Reagent® and transferred into a 14 mL Falcon tube. The RNA was extracted as described in section 4.4.2 and subsequently reverse transcribed (see section 4.6.3).

**DMEM (+10 % FBS):** Dulbecco's Modified Eagle's Medium – high glucose (Sigma-Aldrich), +10 % Fetal Bovine Serum (Sigma-Aldrich)

**20x DPBS:** Dulbecco's Phosphate Buffered Saline, without calcium chloride and magnesium chloride (Sigma-Aldrich)

**1x Trypsin:** 10x Trypsin solution diluted 1:10 with DPBS, Sigma-Aldrich (T4174 SIGMA);

**10.7 M Dimethyl sulfate (DMS)** (Sigma-Aldrich)

**14.3 M β-mercaptoethanol** (Sigma-Aldrich)

**Isoamylalcohol** (Merck Millipore)

**TRI Reagent®** (Sigma-Aldrich)

### 4.6.2 Pseudouridine mapping

This method is an adapted version of the method described by Ofengand et al, 2001 [146]. The method itself roots on the fact that N-cyclohexyl-N'-(2-morpholinoethyl)carbodiimide metho-p-toluenesulfonate (CMCT) modifies uridines on the N3 and pseudouridines on the N3 and N1 position (for reference see **Figure 15**). Under mild alkaline conditions (pH 10.4) the modification of uridines are

removed and only the pseudouridines remain modified which then can be analyzed by reverse transcription, because the reverse transcription is halted 1 nucleotide before the modified pseudouridine (**4.6 Chemical probing**).

First of all wild-type human telomerase RNA was transfected (**4.4.1 Transient transfection with FuGENE®**), extracted (**4.4.2 RNA extraction**) and then modified with CMCT. In a total volume of 20 µL, 30 µg of RNA extract was mixed with 15 µL ddH<sub>2</sub>O, 97 µL BEU buffer and 3 µL 1 M CMCT [f.c. 25 mM]. The sample was incubated at 37°C for 20 min. To stop the modification reaction the RNA was precipitated by adding 2 µL glycogen [10 mg/mL], 50 µL 3 M NaOAc pH 5.5 and 600 µL ethanol p.a. After incubating the sample at room temperature for 5 min, it was centrifuged at 14,000 x g at 4°C for 5 min. After removing the supernatant the pellet was washed with 200 µL cold 75 % ethanol (-20°C), vortexed briefly and then the centrifuge step was repeated. The wash step was performed a second time. Then the supernatant was removed and the pellet was dried at room temperature for 10 min. To remove the CMC from uridines the pellet was resuspended in 50 µL 50 mM sodium carbonate buffer, pH 10.4 and incubated at 37°C for 4 hours. Subsequently the RNA was again precipitated by adding 2 µL glycogen [10 mg/mL], 6 µL 3 M NaOAc pH 5.5 and 110 µL ethanol p.a. After incubation at room temperature for 5 min the solution was centrifuged at 14,000 x g at 4°C for 5 min. The supernatant was removed and the pellet was washed again twice with 200 µL 75 % ethanol (-20°C) and centrifugation (14,000 x g, 4°C, 5 min). After the second washing step the pellet was dried for 10 min and then resuspended in 12 µL 25 mM potassium borate buffer. The modified RNA was stored at -20°C. To map the pseudouridines the modified RNA was reverse transcribed (see section 4.6.3).

**1 M N-cyclohexyl-N'-(2-morpholinoethyl)carbodiimide metho-p-toluenesulfonate (CMCT)** (Sigma-Aldrich)

**1 M BGicine pH 8.5** (Sigma-Aldrich)

**0.5 M EDTA pH 8.0** (Ambion)

**BEU buffer:** 7 M urea, 4 mM EDTA, 50 mM Bicine, adjust pH to 8.9-9.0, sterile filter the final solution

**Glycogen [10/mg]**

**3 M NaOAc pH 5.5** (Ambion)

**Ethanol p.a.** (Merck)

**1 M sodium carbonate buffer pH 10.4:** sterile filter the final solution

**50 mM sodium carbonate buffer pH 10.4:** sterile filter the final solution

**25 mM potassium borate buffer pH 8.0:** autoclave the final solution

### 4.6.3 Reverse transcription of chemically modified RNA

DMS and CMCT modifies the RNA either by methylation or by attaching the CMC molecule onto specific nitrogens of the nucleobases (DMS: A-N1, C-N3; CMCT: U-N3, G-N1). This modification

interferes with a reverse transcription causing termination exactly 1 nucleotide prior to the modified nucleotide. A reverse transcription creates a pool of cDNAs which are 1 nucleotide shorter than the corresponding cDNA in the sequencing reaction. In order to identify the site of modification 2 sequencing reactions containing ddNTPs complementary to either A or C were performed as well. To identify natural stop of the reverse transcription, unmodified RNA was reverse transcribed as well. These cDNA pools were then resolved on an 8 % PAGE.

### 5'-end labeling of primers

To allow us detection of cDNAs, the gene-specific primers (**Table 6**) used in the reverse transcription reaction were 5'-end labelled by transferring the  $\gamma$  phosphate of a  $\gamma$ -<sup>32</sup>P-ATP molecule onto the 5'-hydroxyl end of

oligo ID	sequence
hTR-149	5' -GTTTGCTCTAGAAATGAACGGTG-3'
hTR-178	5' -GAACGGGCCAGCAGCTGACA-3'
hTR-238	5' -GCCTCCAGGCGGGGTTTCG-3'
hTR-404	5' -GTCCACAGCTCAGGGAATC-3'
hTR-433	5' -GCATGTGTGAGCCGAGTCC-3'

**Table 6: DNA primers for reverse transcription of hTR.**

the primer. As such, 5 pmol of DNA oligo were mixed with 1  $\mu$ L 10x T4-PNK buffer, 5 U T4 polynucleotide kinase (T4 PNK) enzyme (10 U/ $\mu$ L), 3  $\mu$ L  $\gamma$ -<sup>32</sup>P-ATP (10 Ci/ $\mu$ L) and ddH<sub>2</sub>O (ad 10  $\mu$ L). The sample was incubated at 37°C for 30 min. After adding 1  $\mu$ L 0.5 M EDTA pH 8.0 the sample was heated to 95°C for 1 min followed by an incubation on ice for 2 min. The labelled primers were precipitated by adding 2  $\mu$ L glycogen [10 mg/mL] and 30  $\mu$ L 0.3 M NaOAc/EtOH and incubating at -20°C for 1 hour. Then the solution was centrifuged at 15,000 x g at 4°C for 30 min. The supernatant was then removed and the pellet was dried at room temperature for 10 min. The dried pellet was resuspended in 20  $\mu$ L ddH<sub>2</sub>O.

### Annealing and extension reaction

The reverse transcription consist of two parts the annealing reaction, in which the 5'-labelled oligo anneals to the denaturated target RNA, and the extension reaction, in which the annealed primer is elongated. At first 20  $\mu$ g of total RNA extract, 2  $\mu$ L 4.5x hybridization buffer, 1  $\mu$ L <sup>32</sup>P-labelled primer, in 9  $\mu$ L reaction filled up with ddH<sub>2</sub>O. To denature the RNA the sample was incubated at 95°C for 1 min and primers and then placed on ice for 2 min (snap cooling) to allow the primer to anneal to its target RNA.

After the annealing reaction the extension mix (consisting of 4  $\mu$ L 5x RT buffer, 2  $\mu$ L 10 mM dNTPs, 1  $\mu$ L 0.1 M DTT, 20 U RNasin, 10 U Transcriptor reverse transcriptase and ddH<sub>2</sub>O up to a final volume of 10.5  $\mu$ L for each reaction) was added and the sample was incubated at 55°C for 1 hour. After extension 3  $\mu$ L 1 M NaOH was added and the sample was again incubated at 55°C for 45 min. To neutralize the pH 3  $\mu$ L of HCl were added and the cDNA pools were precipitated by adding 1  $\mu$ L 0.5 M EDTA pH 8.0, 2  $\mu$ L glycogen [10 mg/mL] and 80  $\mu$ L 0.3 M NaOAc/EtOH. The sample is kept at -20°C for 1 hour. Then the solution was centrifuged at 14,000 x g, at 4°C for 30 min. The supernatant was discarded and the pellet was dried at room temperature for 10 min. Afterwards the pellet was

resuspended in 8  $\mu$ L loading buffer. The next step was to load half of the RT samples onto an 8 % denaturing PAGE (**Section 4.6.4**).

**T4 polynucleotide kinase (10 U/ $\mu$ L) (PNK)** (New England Biolabs)

**10x T4 PNK buffer** (New England Biolabs)

**$\gamma$ -<sup>32</sup>P ATP (10 Ci/ $\mu$ L)**

**0.5 M EDTA pH 8.0** (Ambion)

**3 M NaOAc pH 5.5** (Ambion)

**0.3 M NaOAc/EtOH:** 1:10 dilution of 3 M NaOAc with ethanol p.a.

**4.5 hybridization buffer:** 225 mM Hepes pH 7.0, 450 mM KCl

**10 mM ddNTP:** 1:10 dilution with ddH<sub>2</sub>O of 100 mM ddNTP set, sodium salt (Roche)

**5x RT buffer:** provided with Transcriptor reverse transcriptase

**10 mM dNTP mix:** 1:10 dilution with ddH<sub>2</sub>O of 100 mM dNTP set, lithium salt, (Roche)

**0.1 M Dithiothreitol (DTT)**

**Recombinant RNasin® Ribonuclease Inhibitor (30 U/ $\mu$ L )** (Promega)

**Transcriptor reverse transcriptase (20 U/ $\mu$ L)** (Roche)

**1 M NaOH**

**1 M HCl**

**Loading buffer:** 7 M urea, 25 % sucrose, 0.25 % bromphenol blue in 1x TBE

#### 4.6.4 8% denaturing polyacrylamide gel electrophoresis (PAGE)

For the 8 % denaturing polyacrylamide gel electrophoresis (PAGE) glass plates of dimensions 52 x 33 cm (0.4 mm spacers) was used to ensure a nucleotide resolution of the cDNA pool. As such 80 mL of 8 % acrylamide solution were mixed with 400  $\mu$ L 10 % APS and 40  $\mu$ L TEMED. This mix was poured between the glass plates. After polymerization has finished (approx. 1 hour after initiation) the gel was pre-run for 30 min (60 W). Then the samples were loaded and the remaining empty wells were loaded with loading buffer. The gel was run at 60 W for 2-2.5 hours until the bromphenol blue reached the bottom of the gel. Then the gel was transferred onto a Whatman 3M™ paper and dried at 80°C under vacuum for about 1 hour. A phosphorimager screen (GE Healthcare) was exposed to the gel for about 24 to 72 hours and then scanned with a Typhoon scanner (GE Healthcare). The scanned image was then analyzed with Image Quant (V7, GE Healthcare) (**4.6.5 Quantification**).

**10x TBE buffer (Tris/Borate/EDTA):** 0.89 M TRIS base, 0.89 M boric acid, 0.02 M EDTA

**1x TBE buffer (Tris/Borate/EDTA):** 1:10 dilution of 10x TBE buffer with ddH<sub>2</sub>O

**8 % acrylamide solution:** 8 % acrylamide (19:1; acrylamide:bisacrylamide)(Applichem), 7 M urea, 1x TBE

**10 % APS:** 10 % (w/v) ammonium persulfate

**N,N,N',N'-Tetramethylethylenediamine (TEMED)** (Sigma-Aldrich)

**Loading buffer:** 7 M urea, 25 % (w/v) sucrose, 0.25 % (w/v) bromphenol blue in 1x TBE

#### **4.6.5 Quantification of DMS modification pattern**

The lanes were detected and each nucleotide was assigned a band with a fixed width. This data was then extracted into an Excel sheet (Microsoft Excel 2013). Subsequently, the percentage of intensity for each nucleotide was calculated from the total intensity of all bands. A threshold was set to distinguish weak, moderate or strong modifications based on the overall modification intensities. This was also done for the DMS pattern of mutant hTR lane.

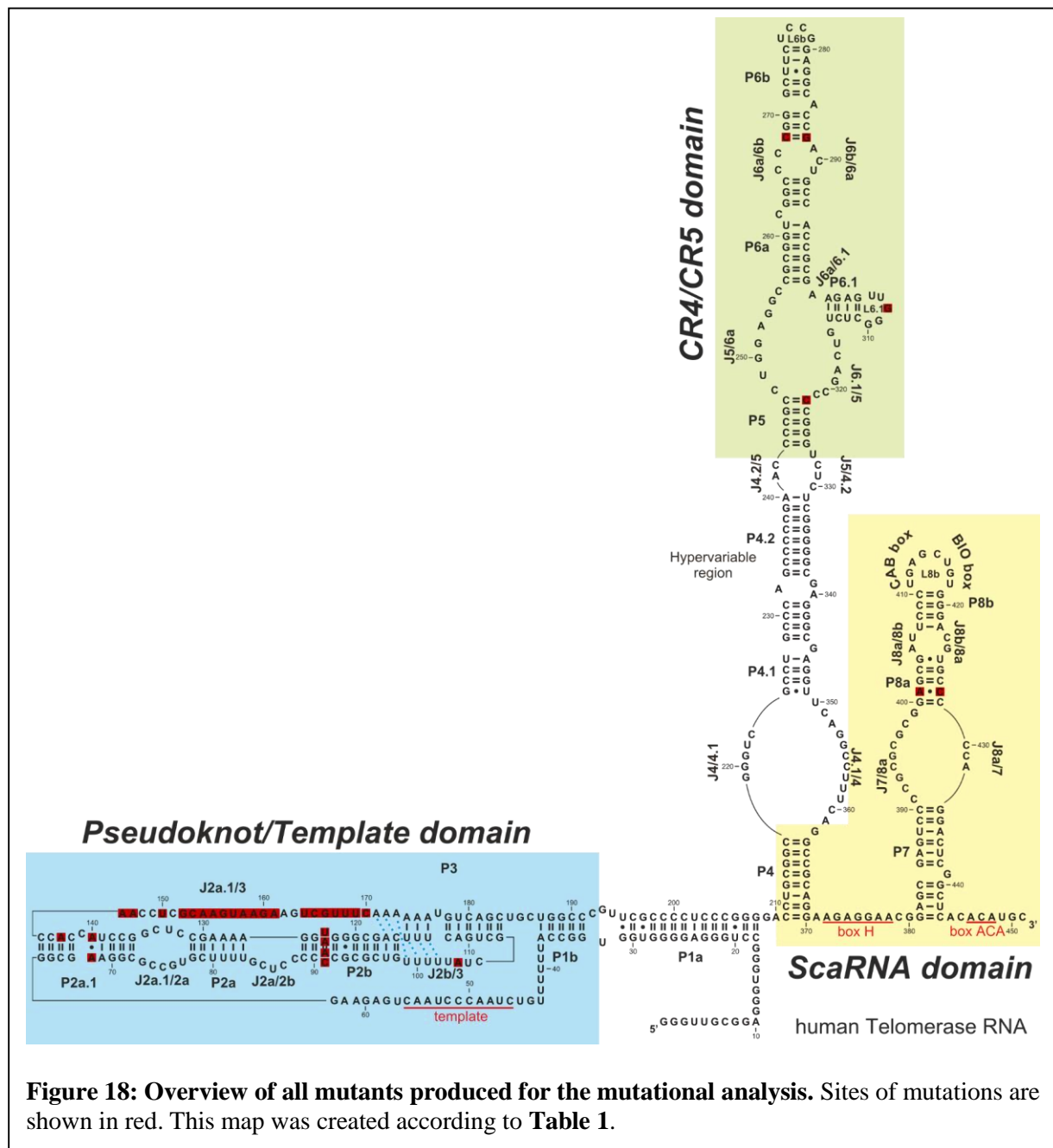


## 5 Results

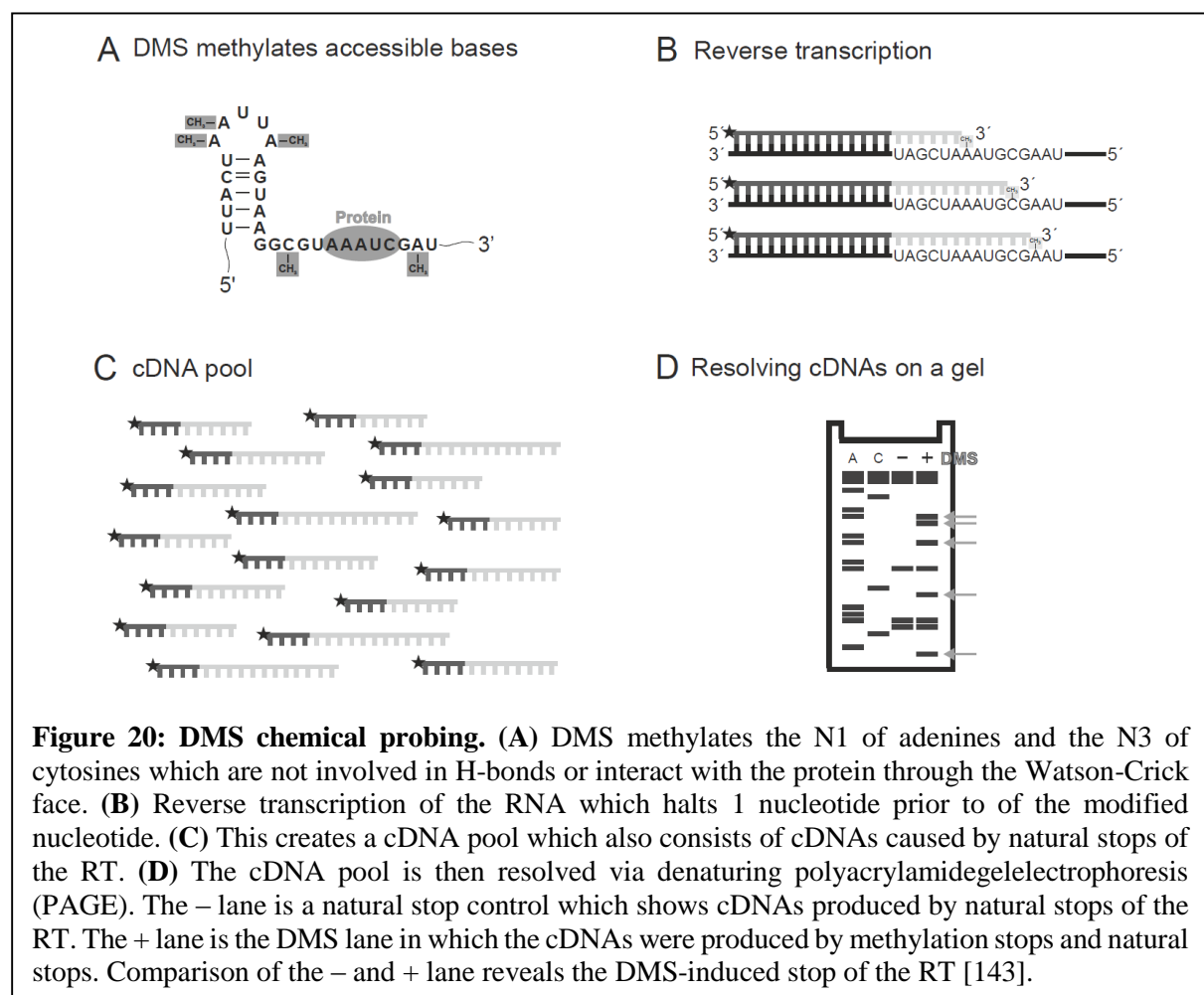
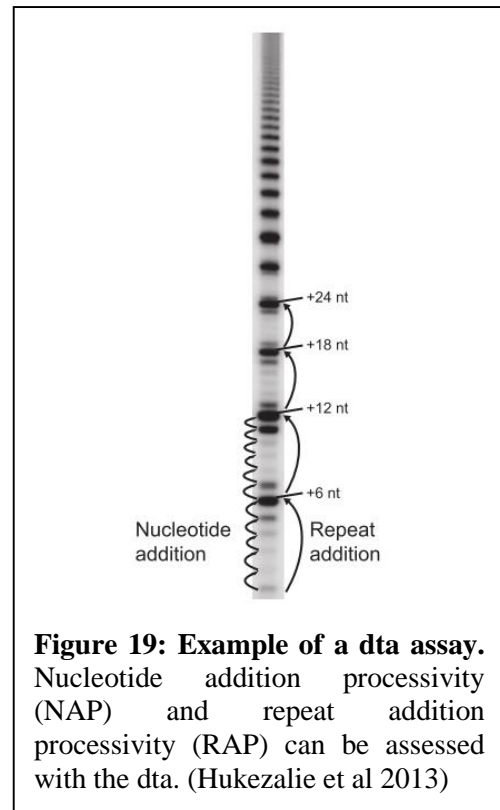
### 5.1 Mutational analysis of human telomerase RNA

#### 5.1.1 Experimental setup

The first step of the mutational analysis of hTR was to prepare the necessary mutant plasmids of hTR carrying mutations at highly conserved or structurally important nucleotides (**Table 1** and **Figure 18**). Afterwards these plasmids were transiently transfected and overexpressed in a ratio 10:1 (hTERT:hTR) into HEK 293 cells and then native cell lysates were prepared. Afterwards these cell lysates, which contain *in vivo* assembled telomerase complex, were tested *in vitro* for their telomerase activity (**section 4.5**). In this assay the ability of the lysate to elongate telomeric primers in presence of  $\alpha$ -<sup>32</sup>P-dGTP, which is incorporated into the added repeats, is tested (**Figure 19**). Thus, it is possible to quantify the



overall nucleotide addition processivity (NAP) and the repeat addition processivity (RAP) of wt and mutant telomerase particles. This assay allowed us to identify hTR residues, which have a functional importance in telomerase activity. To obtain insights into the structural basis underlying telomerase disfunction, we used *in vivo* DMS probing. Dimethyl sulfate (DMS) is able to pass right through cell wall and membranes. In general it modifies the N1 of adenines and the N3 of cytosines. The sites of modification are determined by reverse transcription and plotted on the hTR secondary structure map (Figure 20). This DMS map reveals which nucleotides are chemically accessible and therefore not involved in H-bonds or interaction with any partners (protein, DNA, RNA). To determine the structural consequences of the C123A mutation the *in vivo* DMS modification pattern of the mutant hTR is compared to that of the wt in the presence of hTERT. Using this approach we have previously investigated the differences between the wild type and



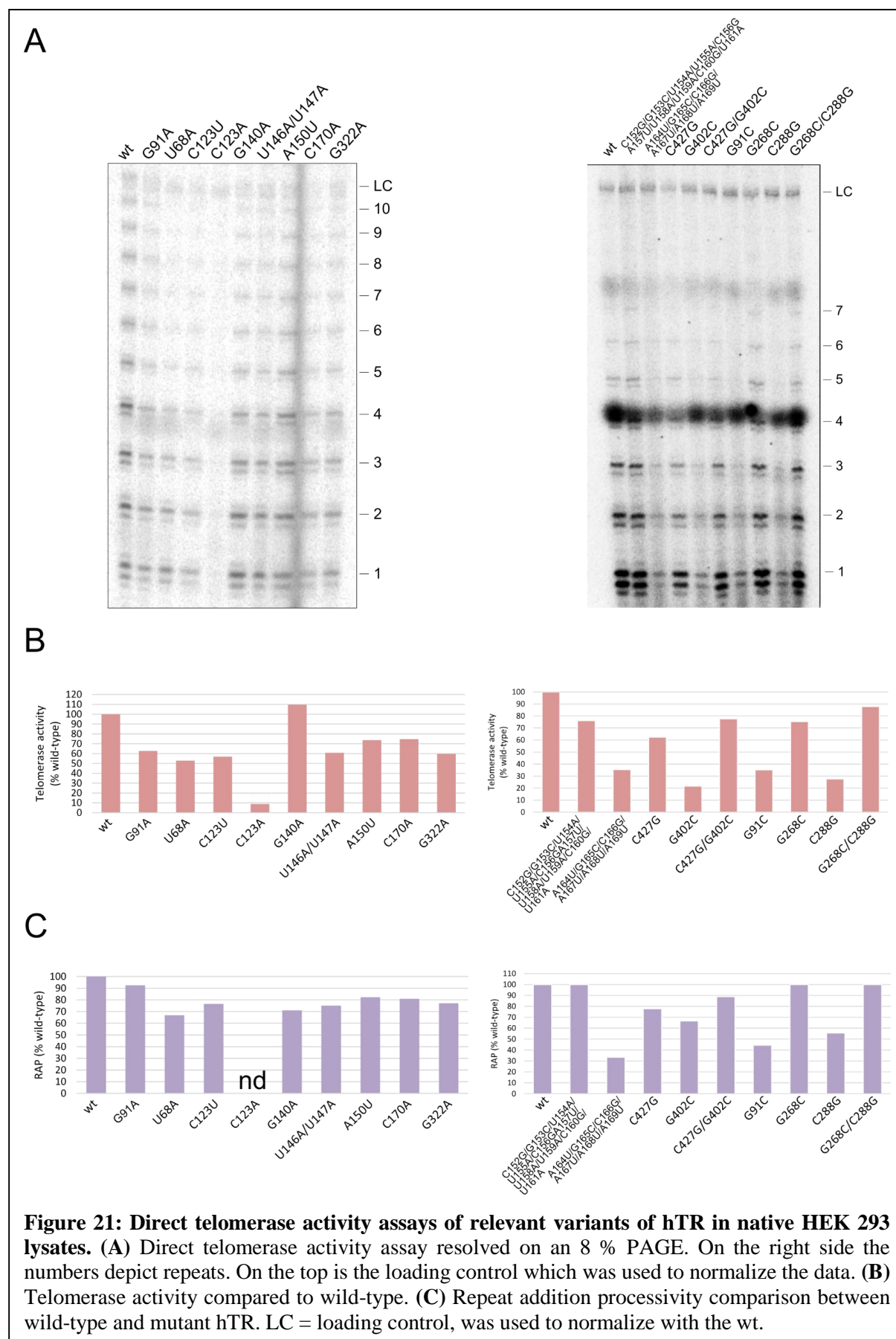
hTR variants carrying disease related mutations [71]. Interestingly, certain disease associated mutations in CR4/CR5 domain neither disrupt the RNP complex nor influence the hTR fold suggesting that these nucleotides may be directly involved in telomerase activity [71]. Mutations in the pseudoknot/template domain seems to have the greatest impact on telomerase activity by disrupting the pseudoknot/triple helical structure [71]. Also fatal mutations in the scaRNA domain influence biogenesis of human telomerase and therefore reduce the levels of mature telomerase [71].

### 5.1.2 The C123A mutation in hTR significantly reduces telomerase activity

A total of 18 hTR mutant variants were tested for their effect on telomerase activity. Of these NAP is only drastically reduced in less than 10 % in the C123A mutant, while RAP is not detectable at all (**Figure 21**). This is interesting mutating the position C123A to U only causes a reduction of 40 %. Also, mutating the proposed base pairing partner of C123, which is G91, to an A or C (G91A or G91C) shows only a 60 % reduction in RAP and NAP (**Figure 21**). This base pair was initially selected, because it showed strong sensitivity to DMS when nucleotides 96 and 97 are deleted [71]. Furthermore, we were interested in determining the importance of nucleotide identity within junction J2a.1/3. Altering nucleobases in the junction J2a.1/3 had only major influence on activity and processivity if these were located near the triple helix (positions in hTR: 164-169). On the other hand exchanging nucleotides within the 5' part of the junction J2a.1/3 showed only a 25% reduction in processivity (positions in hTR: 152-161). Another interesting observation is the base pair G268 and C288 located on top of the stem P6a. It has been shown in NMR structure to form a base triple with C267 and to be associated with protein binding as well [147]. Our analysis revealed that mutating C288G drastically reduces telomerase activity (**Figure 21**). This variant disrupts the base pair and any possible triple base pairing. On the other hand restoring the base pair (G268C/C288G) rescues the activity to nearly wt levels (**Figure 21**). Similarly, disrupting the G402-C427 base pair by mutating G402C strongly impairs NAP but restoring the base pair (G402/C427) brings the activity back to the wt levels (**Figure 21**). From earlier investigations it was suggested that this base pair may form a non-canonical base pair and may be involved in RNA-RNA interactions or interacts with Dyskerin associated H/ACA proteins [71]. G322A is a mutation that is found in patients with aplastic anemia and has previously been reported to reduce the telomerase activity drastically [148]. Interestingly, our DTA showed that there is only a 40 % reduction in NAP. This disparity could be due to the fact that in the previous study telomerase activity was assessed using the less sensitive TRAP assay [148]. We conclude that this mutant reduces telomerase activity but not as drastic as shown previously [148].

In light of these results, the hTR variant C123A appeared to be the most interesting candidate for a residue that is critical for telomerase catalysis activity either due to directly participating in catalysis or due to folding of the core domain. To address the structural basis of the defect in telomerase function of

the C123A variant, the structure of the mutant hTR in presence of hTERT was investigated by *in vivo* DMS chemical probing.



### 5.1.3 The intracellular structure of hTR in complex with hTERT

Mapping of the wt human telomerase RNA was done previously and extensively discussed by Georgeta Zemora [71]. Therefore the mapping of the wild-type hTR structure is limited to confirm the previously found modification pattern [71]. However, mapping the wt hTR structure in the presence of hTERT again was essential to understand the structural perturbation of the C123A. In other words, the structure of the wt + mutant hTR was mapped in parallel and subsequently compared (**Figure 23-Figure 26**). In fact, the obtained *in vivo* DMS pattern of the wt hTR in complex with hTERT is an excellent assessment

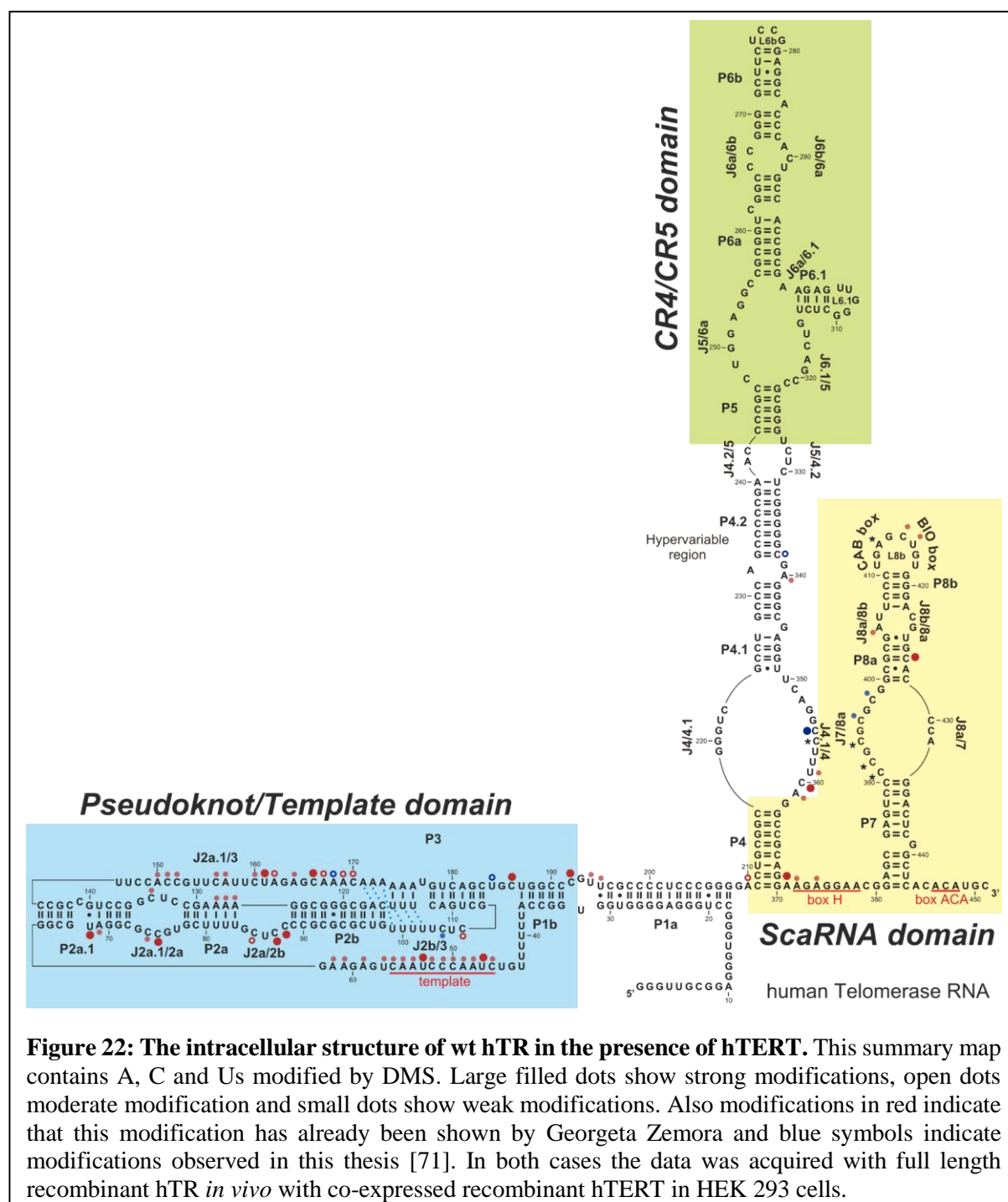


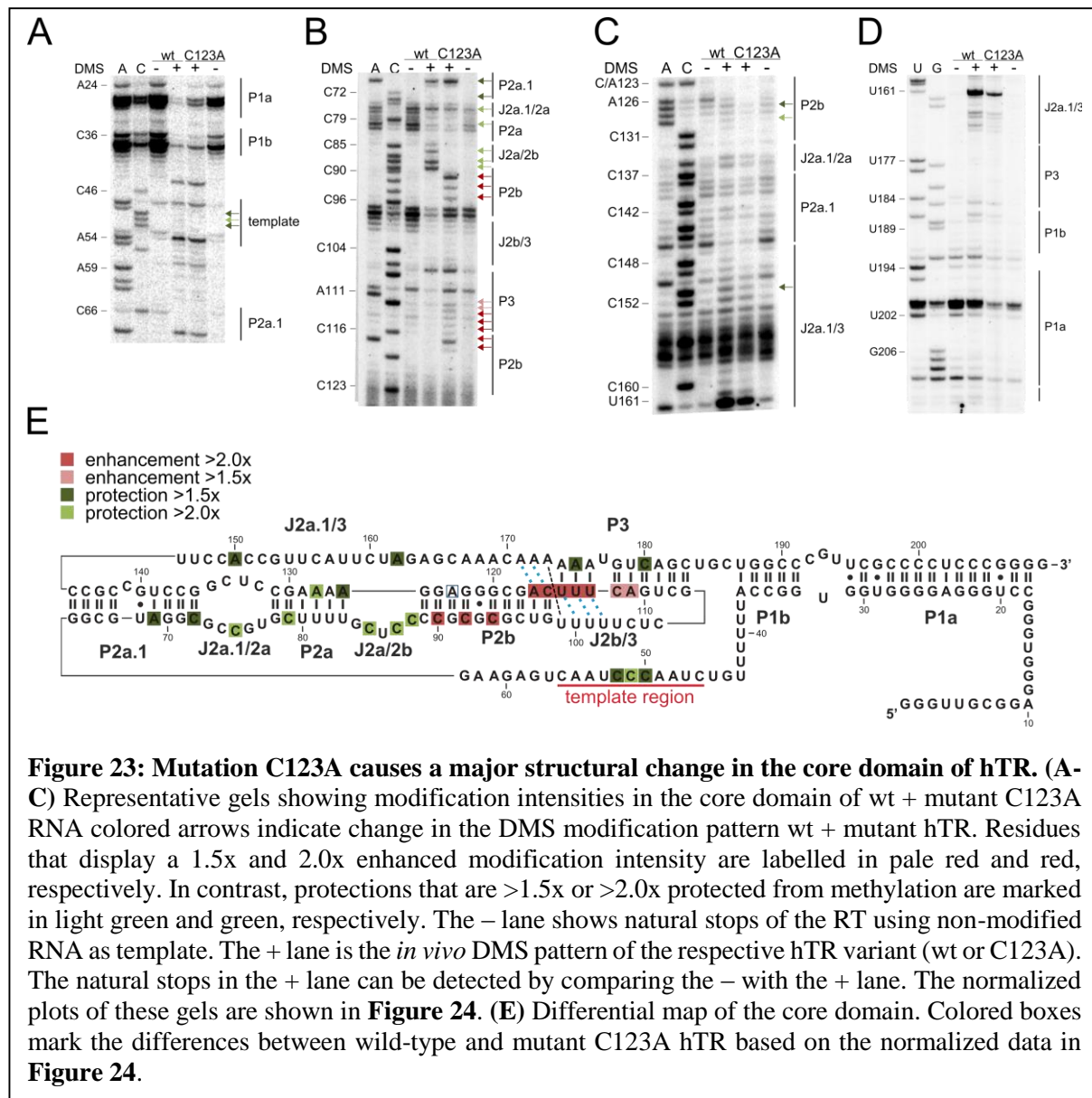
**Figure 22: The intracellular structure of wt hTR in the presence of hTERT.** This summary map contains A, C and Us modified by DMS. Large filled dots show strong modifications, open dots moderate modification and small dots show weak modifications. Also modifications in red indicate that this modification has already been shown by Georgeta Zemora and blue symbols indicate modifications observed in this thesis [71]. In both cases the data was acquired with full length recombinant hTR *in vivo* with co-expressed recombinant hTERT in HEK 293 cells.

with that obtained by G. Zemora [71]. Minor differences in the *in vivo* pattern were observed at residues A168, U184 in the pseudoknot domain and C338, C396 and C398 in or nearby in the scaRNA domain respectively (**Figure 22**). Due to the fact that there are no major DMS modifications in the CR4/CR5 domain it is suggested that hTR is in complex with hTERT. Comparing this data with G. Zemoras and it is possible to conclude that the pseudoknot is formed in the wt. Additionally, the template region shows the same modification pattern as before and is therefore accessible. It has been shown before that mutations in the pseudoknot and template region disrupt the pseudoknot and subsequently abolish telomerase activity without influencing the binding of hTERT to hTR [71]. Apparently most disease-linked and functionally relevant nucleotides do not affect the binding of hTERT to hTR but mess with the conformational arrangement of the pseudoknot/triple helix [71].

#### 5.1.4 The C123A mutation causes misfolding in the core domain of hTR

The mutant variant C123A of the hTR was shown to have no detectable repeat addition processivity and a drastically reduced (less than 10 %) nucleotide addition processivity (**Figure 21**). Thus, we concluded that this position must play a crucial role in the telomerase catalytic activity or in folding of hTR and in turn telomerase RNP assembly. *In vivo* DMS chemical probing demonstrated that the C123A mutation causes a major structural rearrangement of the core domain by disrupting the pseudoknot (**Figure 23**). Positions in junction J2a/2b (C85, C87 and C88) are heavily protected, whereas positions C90, C92 and C94 in P2b are strongly modified, in contrast to wt hTR (**Figure 22** and **Figure 23**). The former seem to be involved in base pairing and the later suggests that these are not involved in base pairing anymore. Additionally, positions A111, C112, U113, U114, U115, C116 and A117 are very strongly modified compared to the wild-type. These strong modifications indicate that the P3 helix cannot form. As such it is not surprising that triple helical scaffold at P3 does not form either (**Figure 23**), as indicated by enhanced modification by residues A111-A117. Interestingly, A171-A173, which form base triples with A117-U97 and C116-G98, respectively, do not display an enhanced modification and A175 and C180 in P3 are less intense modified in the mutant hTR. This suggests that upon disruption of P3 these residues may also engage alternative base pairs, e.g. with Us in J2b/3. At last, changes were also observed in the template region, as C50-C52 became more protected from DMS. Aside from major changes observed in the core domain of the hTR, no differences in the DMS pattern were detected in the other domain except for C360 and C367 (**Figure 25** and **Figure 26**). Since the CR4/CR5 domain has been identified as the main binding site of hTERT and we previously observed conformational changes in this region upon hTERT presence *in vivo*, the nearly identical modification pattern of wt and C123A mutant hTR variants in the CR4/CR5 element implies that the mutation C123A does not interfere with hTERT binding. Along this line the C123A mutation does not affect the structure of the scaRNA domain and in

turn biogenesis of telomerase is unlikely to be influenced by C123A. Thus the defect in telomerase activity of the C123A appears to be caused by structural perturbation in the pseudoknot.





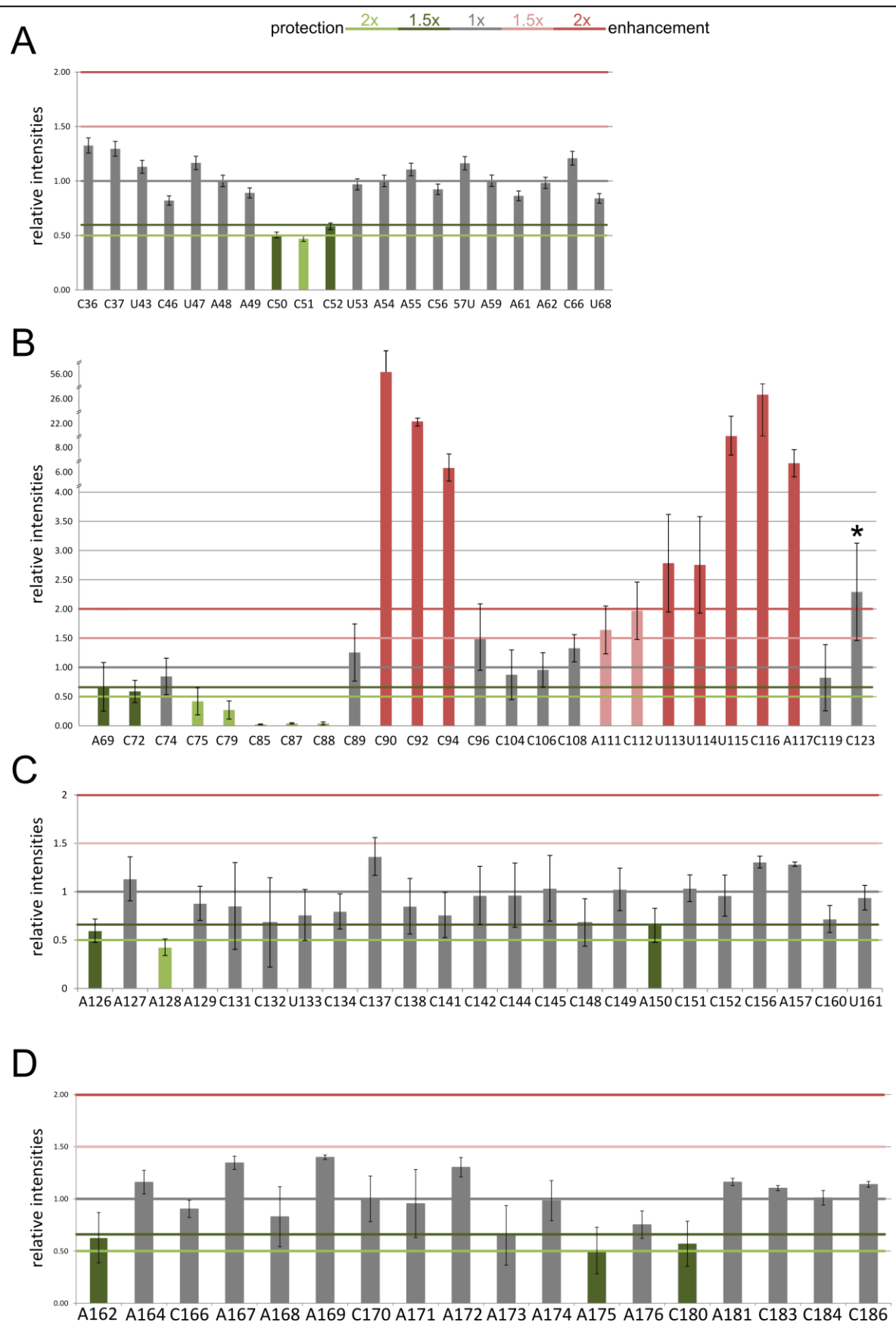


**Figure 24: Normalized plots of the modification intensities of residues in the core domain. (A-D)** These plots are the normalized and quantified data of the gels shown in Figure 23. A > 2 fold enhancement (dark red) refers to a stronger modification in the mutant than in the wt. This applies for 1.5-fold (pale red) enhancement. As well a ratio of 1 (gray) indicates no change in modification. In contrast, residues that are modified to a lesser extend in the C123A mutant, are shown in dark





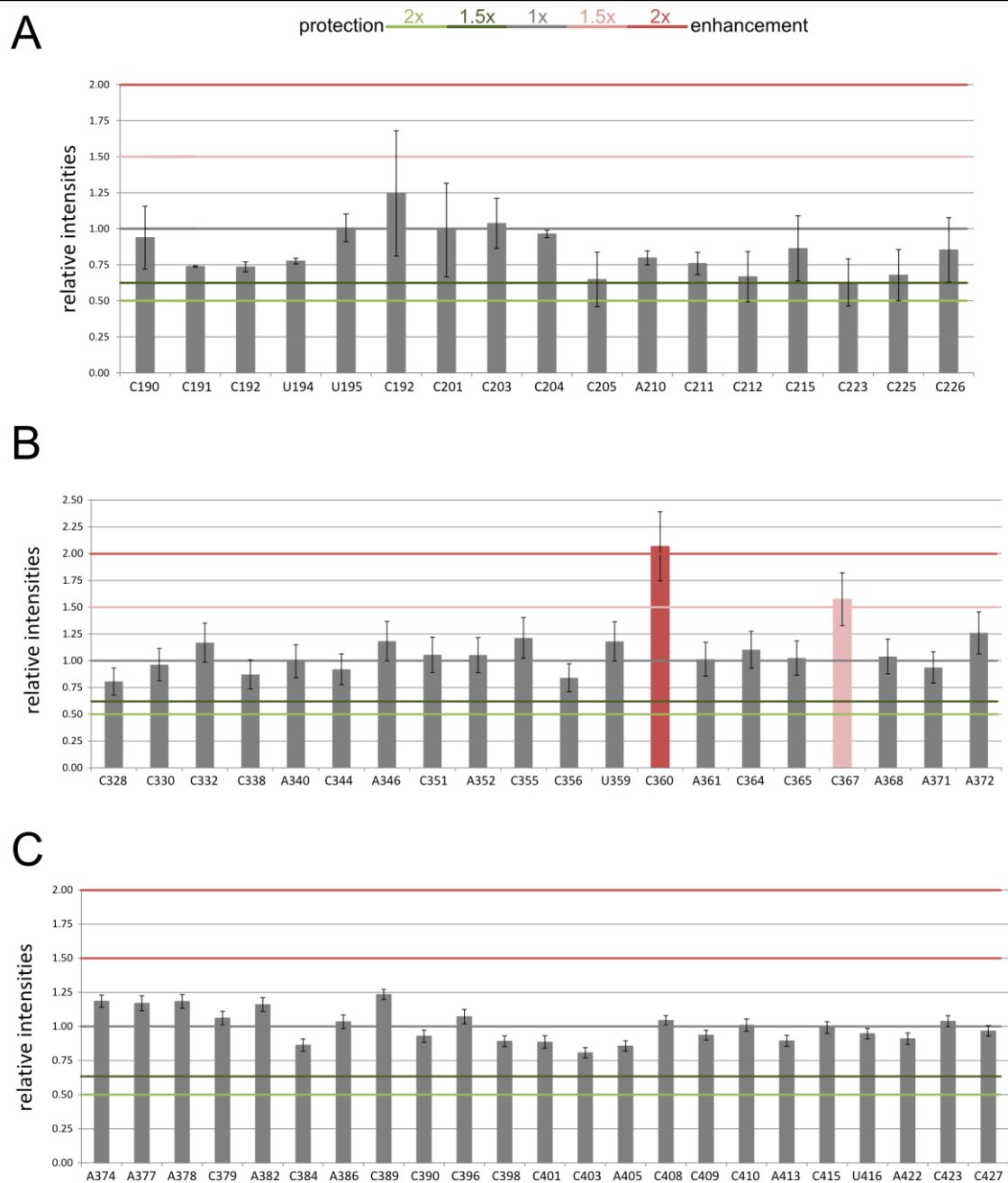


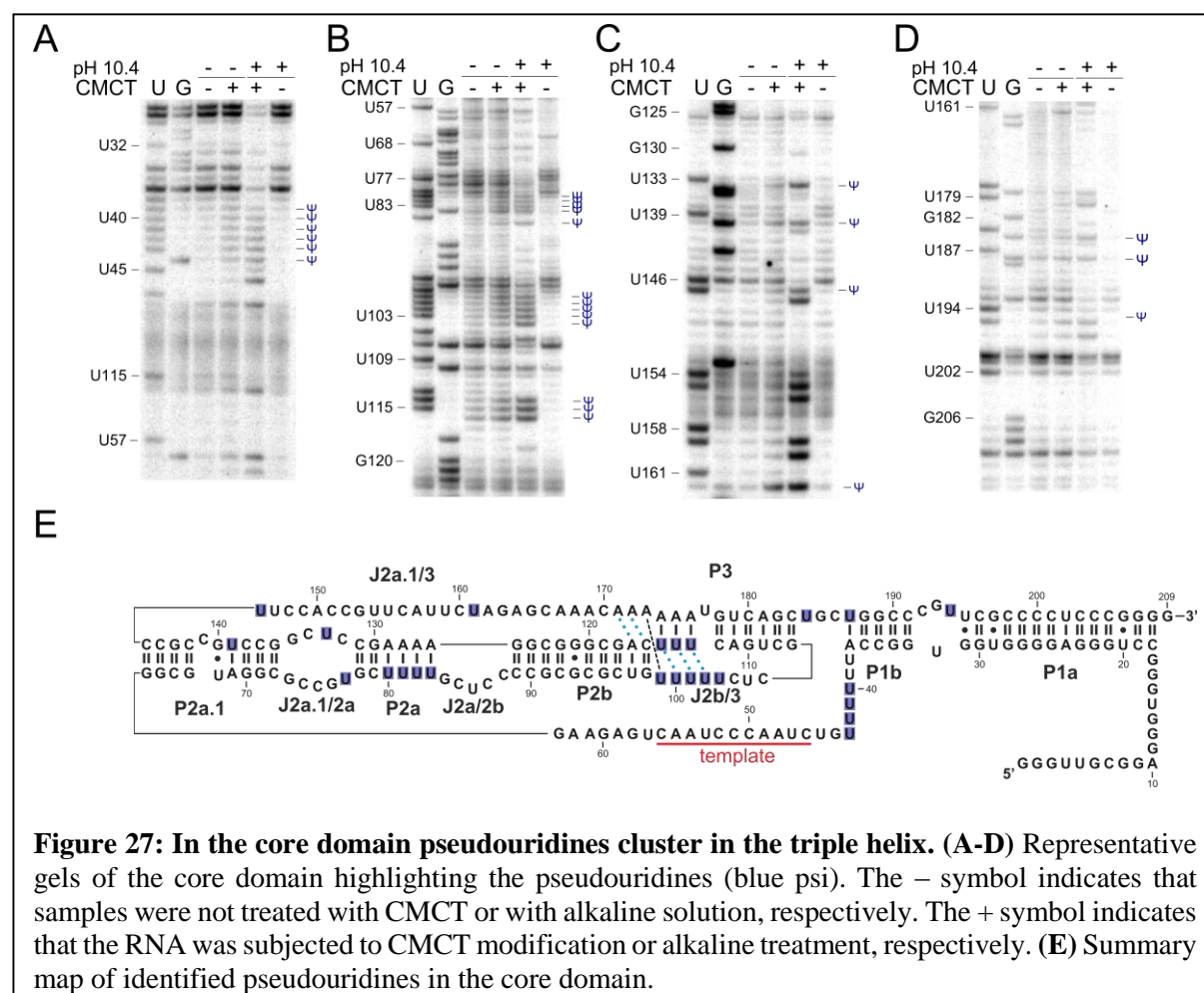
**Figure 26: Normalized plots of the CR4/CR5 and the scaRNA domain showing slightly folding rearrangements in the C123A hTR mutant. (A-C)** These plots are the normalized and quantified data of the gels shown in Figure 23. A > 2 fold enhancement (dark red) refers to a stronger modification in the mutant than in the wt. This applies for 1.5-fold (pale red) enhancement. As well a ratio of 1 (gray) indicates no change in modification. In contrast, residues that are modified to a lesser extend in the C123A mutant, are shown in dark green (<0.67) or bright green (<0.5). The asterisk marks natural stops and thus are not DMS modifications.

## 5.2 Post-transcriptional modification of human telomerase RNA

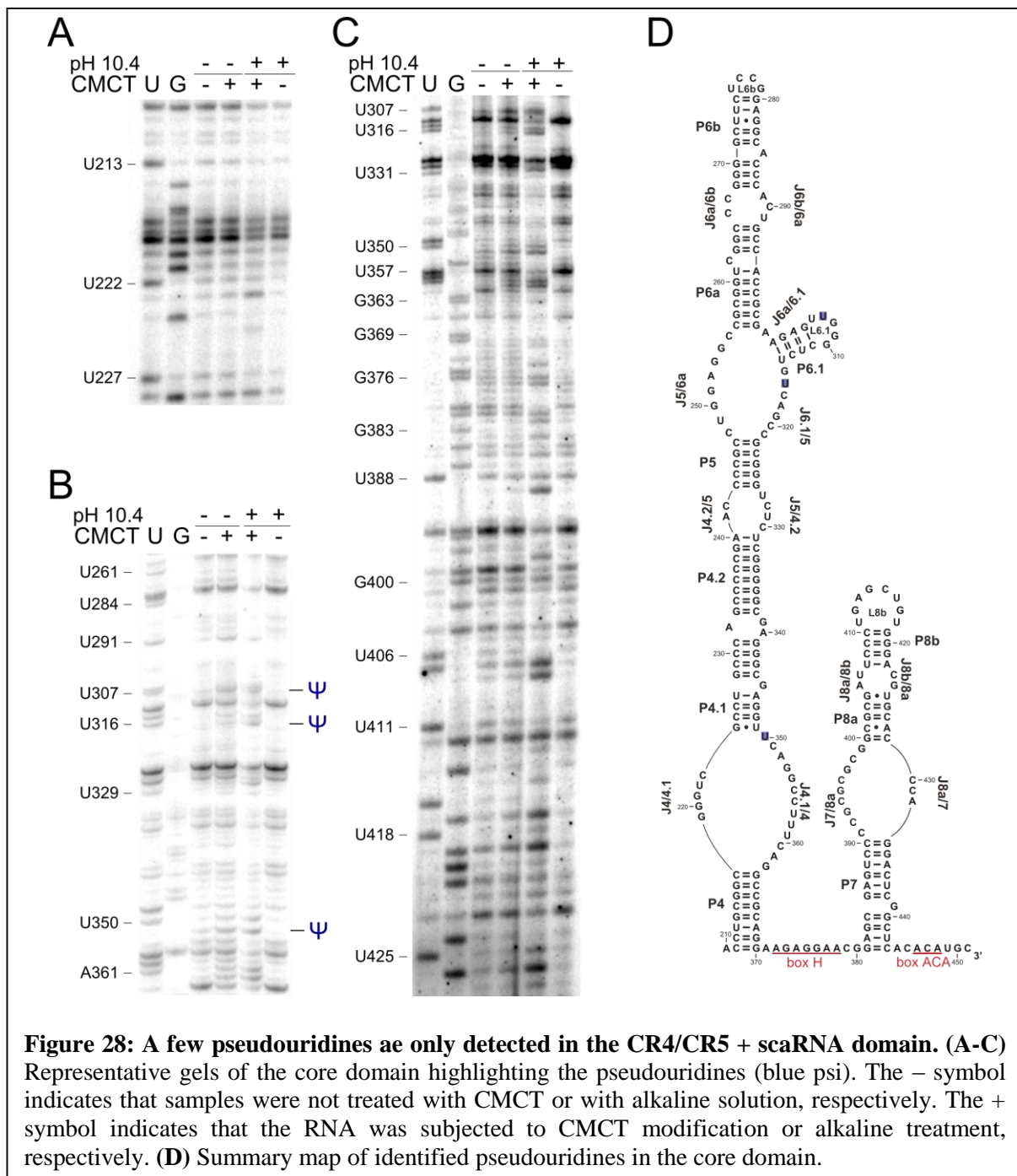
Pseudouridines are a type of post-transcriptional modification found in many RNAs, while rRNAs being the most prominent example [124]. In these RNAs pseudouridines play a role in RNA structure formation and stabilization [126]. The pseudouridines are isomers of uracils, as these have a ring nitrogen (H-NA) at the Hoogsteen face instead of an additional H-donor (**Figure 15**). CMCT is able to modify this N1 position in addition to N3 position, which is also present in uracils. The experimental procedure in detecting pseudouridines is very similar to that of DMS chemical probing (**Figure 20**). It involves isolation of total cellular RNA, which is subjected to CMCT modification followed by treating the modified RNA under alkaline conditions to remove CMCT from the N3 position.

### 5.2.1 Pseudouridines detected with CMCT probing

Although the procedure of pseudouridine detection is straight forward there is a lot of adjustment necessary. The method initially described by Ofengand et al. was performed on rRNA. In case of hTR significant adjustments were necessary. Specifically, the RNA concentration and the CMCT concentration had to be optimized to obtain a better resolution and to reliably detect pseudouridines. Despite our efforts in optimizing the conditions of CMCT modification and alkaline treatment several uridines were indicated to be pseudouridines. Interestingly it appears that all uracils involved in



formation of the triple helical scaffold of the pseudoknot are pseudouridines (U113-U115 and U99-U103). Strikingly, our initial analysis CR4/CR5 and scaRNA domains did not reveal the presence of pseudouridines in these structural elements of hTR (**Figure 27** and **Figure 28**) except for U306/U307, U316 and U350. Of the pseudouridines previously detected by Kim et al, we were only able to detect U307 and U316 as well [71]. Notably, in contrast to our study, Kim et al did not perform the controls done by us and studied endogenous hTR. As pseudouridines were identified in recombinant hTR, this suggests that overexpressed hTR is subject to proper biogenesis which is in line with the observed telomerase activity.



## 6 Discussion

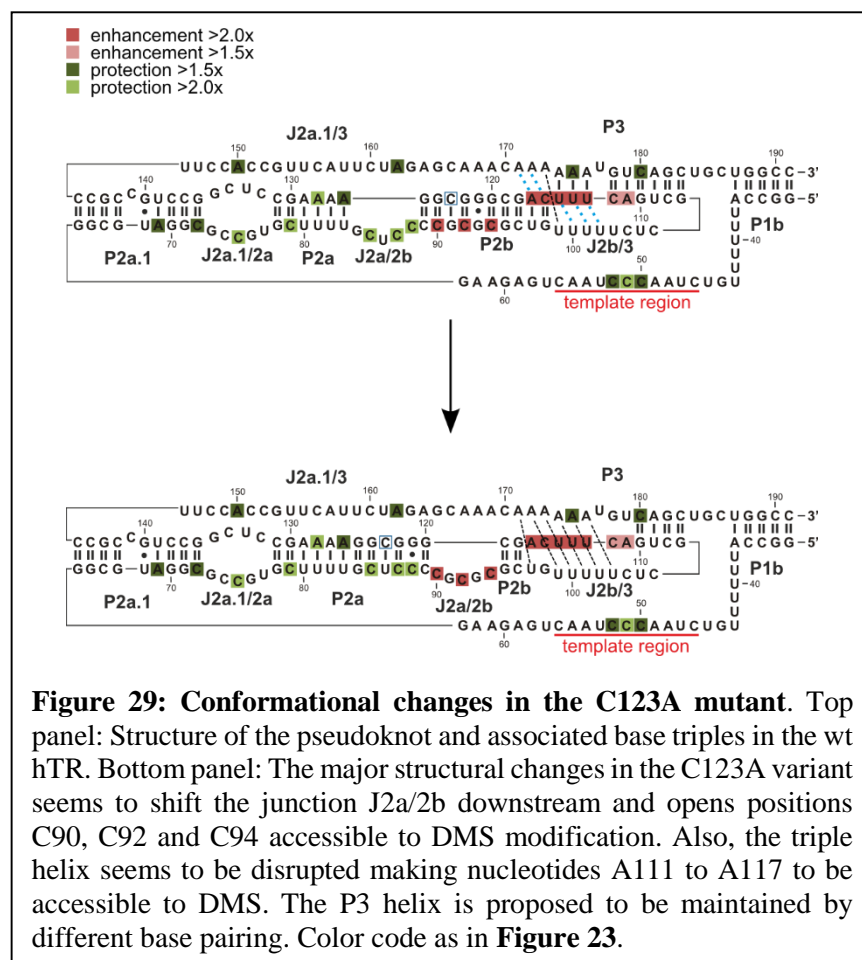
### Mutational analysis of telomerase NAP and RAP in respect to sequence conservation

Numerous studies found on identifying RNA and protein residues essential for telomerase activity [7]. For example, mutational analysis conducted in the core domain revealed that interchanging base pairs reduces telomerase activity [106]. Disease-associated mutations that affect telomerase assembly, structure and activity [149]. Extending a previous study in our lab, we aimed at identifying residues essential for telomerase activity. The direct telomerase activity assay (**Figure 21**) revealed that nearly all mutants tested showed a reduction in telomerase activity except for G140A. To better understand if a nucleotide itself or base pairing is critical for telomerase activity, the proposed base pairs C268-G288 in P6 and G402-C427 in P8a were disrupted. While C288G strongly affects telomerase activity, introducing a C•C mismatch (G268C) barely reduces telomerase activity. This indicates that having a C at position 288 is important. However, it was possible to rescue telomerase activity by restoring base pairing (G268C/C288G). A similar observation was obtained for the G402-C427 bp as only G402C reduced telomerase activity. This was surprising, because C427 was strongly methylated *in vivo* by DMS [71]. Apparently, in both cases certain non-canonical base pair and Watson Crick base pair are compatible with the geometry required for a functional enzyme. Specifically, interfering with the C268-G288 base pair may disrupt an interaction within the TRBD domain of hTERT, while the G402-C427 base pair may contribute to telomerase biogenesis. As for the wobble base pair U68-G140 only U68 shows strong conservation (96 %). Altering this wobble base pair to a G•A non-canonical pair (U68) reduces telomerase activity to 50 %, while changing it to a Watson-Crick base pair (G140A) enhances telomerase activity by 10 % (**Figure 21**). This implies that base identity at position 68 outweighs a specific base pairing configuration. Surprisingly, despite the high sequence conservation of A150 in J2a.1 (96 %) exchanging it to a uracil (A150U) did not result in a drastic decrease in telomerase activity (reduced by 75 %). In addition, we studied junction J2a/3 by mutating either its 5' part, which is close to P2a.1, or its 3' part adjacent to P3. As for the 5' part of J2a.1/3 it seems that the sequence is not of importance for telomerase function. This is in contrast to the 3' part of J2a.1/3, as the respective mutant has reduced nucleotide addition processivity (to 35 %) and repeat addition processivity (to 35 %). Altogether this suggests that secondary structure of the hTR plays an important role in telomerase activity. In disease related mutations of hTR it has been shown that most of these mutations disrupt the integrity of stems [106][107]. As such we were interested in the G91-C123 base pair in stem P2a mutating the invariant residue G91 to A or C only lowered the telomerase activity to ~60 % or 35 %, respectively. Similarly, despite its base pairing partner C123 is also highly conserved (92 %) and seems to be interchangeable with U, which is also indicated with our data of C123U. In contrast C123A drastically reduced NAP and abolished RAP. This observation would explain as to why a C123A has been identified in any patient suffering from pre-mature aging syndrome, as this mutation might be lethal, which would coincide with the fact that it is not found in mammals due to its severe effect.

Telomerase activity itself gives no direct insight into structural changes although it may hint at interesting mutations, like C123A.

### C123 plays an important role for folding of the pseudoknot and associated triple helix

Several lines of evidence indicated the pseudoknot with its triple helical scaffold to contribute to telomerase catalysis. In fact, we recently demonstrated that disease linked mutations in the pseudoknot do not only affect the pseudoknot structure but also the geometry of the template region. Thus the pseudoknot seem to be important for proper positioning of the template of the active site of hTERT [114]. As such, it was of interest to also study the role of the extended pseudoknot for telomerase function. At first we focus on the C123-G91 base pair, as both residues are >96 % conserved and in the previously studied pseudoknot mutants, C123 became accessible to DMS [71]. Indeed, C123A severely reduced telomerase activity (**Figure 21**). To determine the cause for the loss of telomerase function, *in vivo* chemical probing was employed to assess the conformational changes induced by the C123A



mutation. Importantly, biogenesis of telomerase seems not to be impaired due to the fact that there were sufficient amounts of telomerase RNA for reverse transcription. Also, no major changes between wt and mutant DMS pattern were observed in the CR4/CR5 region, which is the main binding site of hTERT,

thus suggesting that the human telomerase RNA is part of the telomerase complex [150]. In contrast to the CR4/CR5 and scaRNA domain, numerous changes in the pseudoknot/template domain were observed. Most of these cluster at the pseudoknot and adjacent junction J2a/2b and stem P2a. The DMS pattern of C123A does not only reveal that the pseudoknot and associated triple helix isn't formed, but that the template geometry is affected. This correlates with the fact that the pseudoknot is suspected to function as a structure to align the template correctly into the active site of hTERT [67][71]. Taking a closer look at the induced conformational change, it was striking that a single stranded element was protected from modification, while base paired residues (C90, C92 and C94) become accessible to DMS, but not their interaction partner (G120, G122 and G124). To make a long story short, it was possible for us to discern non-native interaction, within C123A mutant (**Figure 29**). In particular, stem P2a is extended by base pairs formed by C89-G84 and G120-G125. On the other hand, A171-A176 may interact with U97-U103 thereby extending P2b. Thus, C123A mutation appears to induce a misfold within the core domain of hTR, and in turn abolishes telomerase function. It is likely that such a mutation would be lethal.

### **Pseudouridines seem to crowd in the core domain with possible stabilizing effect**

Pseudouridines were found to contribute to folding and stability of non-coding RNAs before [146][124]. While pseudouridines have been identified in human telomerase RNA, their effect on structure is barely fully understood. In case of P6.1, pseudouridines at position 306 and 307 were shown to alter the overall topology of the P6.1 loop and to increase the stability of P6.1 [126]. Here we attempt to identify pseudouridines throughout the entire hTR modelling, which was transiently expressed in HEK293 cells. A total of 29 pseudouridines were detected by CMCT mapping. Interestingly, the majority of residues in the pseudoknot domain, specifically in the triple helix. Potentially, these pseudouridines are required for stability of the triple helical scaffold and in thus enhance telomerase catalysis. How much influence pseudouridylation has on the overall structure of the hTR remains unsolved.

## 7 References

- [1] Q. Zhang, N.-K. Kim, and J. Feigon, “Architecture of human telomerase RNA.,” *Proc. Natl. Acad. Sci. U. S. A.*, vol. 108, no. 51, pp. 20325–32, Dec. 2011.
- [2] T. M. Nakamura, G. B. Morin, K. B. Chapman, S. L. Weinrich, W. H. Andrews, J. Lingner, C. B. Harley, and T. R. Cech, “Telomerase catalytic subunit homologs from fission yeast and human.,” *Science*, vol. 277, no. 5328, pp. 955–9, Aug. 1997.
- [3] J. Feng, W. D. Funk, S. S. Wang, S. L. Weinrich, A. A. Avilion, C. P. Chiu, R. R. Adams, E. Chang, R. C. Allsopp, and J. Yu, “The RNA component of human telomerase.,” *Science*, vol. 269, no. 5228, pp. 1236–41, Sep. 1995.
- [4] E. H. Blackburn and K. Collins, “Telomerase: an RNP enzyme synthesizes DNA.,” *Cold Spring Harb. Perspect. Biol.*, vol. 3, no. 5, May 2011.
- [5] C. W. Greider and E. H. Blackburn, “Identification of a specific telomere terminal transferase activity in Tetrahymena extracts.,” *Cell*, vol. 43, no. 2 Pt 1, pp. 405–13, Dec. 1985.
- [6] C. Autexier and N. F. Lue, “The structure and function of telomerase reverse transcriptase.,” *Annu. Rev. Biochem.*, vol. 75, pp. 493–517, Jan. 2006.
- [7] C. W. Greider and E. H. Blackburn, “A telomeric sequence in the RNA of Tetrahymena telomerase required for telomere repeat synthesis.,” *Nature*, vol. 337, no. 6205, pp. 331–7, Jan. 1989.
- [8] J.-L. Chen and C. W. Greider, “Determinants in mammalian telomerase RNA that mediate enzyme processivity and cross-species incompatibility.,” *EMBO J.*, vol. 22, no. 2, pp. 304–14, Jan. 2003.
- [9] A. Sauerwald, S. Sandin, G. Cristofari, S. H. W. Scheres, J. Lingner, and D. Rhodes, “Structure of active dimeric human telomerase.,” *Nat. Struct. Mol. Biol.*, vol. 20, no. 4, pp. 454–60, Apr. 2013.
- [10] S. Sandin and D. Rhodes, “Telomerase structure.,” *Curr. Opin. Struct. Biol.*, vol. 25, pp. 104–10, Apr. 2014.
- [11] T. L. Beattie, W. Zhou, M. O. Robinson, and L. Harrington, “Functional multimerization of the human telomerase reverse transcriptase.,” *Mol. Cell. Biol.*, vol. 21, no. 18, pp. 6151–60, Sep. 2001.
- [12] R. K. Moyzis, J. M. Buckingham, L. S. Cram, M. Dani, L. L. Deaven, M. D. Jones, J. Meyne, R. L. Ratliff, and J. R. Wu, “A highly conserved repetitive DNA sequence, (TTAGGG)<sub>n</sub>, present at the telomeres of human chromosomes.,” *Proc. Natl. Acad. Sci. U. S. A.*, vol. 85, no. 18, pp. 6622–6, Sep. 1988.
- [13] M. C. Miller and K. Collins, “Telomerase recognizes its template by using an adjacent RNA motif.,” *Proc. Natl. Acad. Sci. U. S. A.*, vol. 99, no. 10, pp. 6585–90, May 2002.
- [14] T. de Lange, “Shelterin: the protein complex that shapes and safeguards human telomeres.,” *Genes Dev.*, vol. 19, no. 18, pp. 2100–10, Sep. 2005.
- [15] P. Martínez and M. A. Blasco, “Telomeric and extra-telomeric roles for telomerase and the telomere-binding proteins.,” *Nat. Rev. Cancer*, vol. 11, no. 3, pp. 161–76, Mar. 2011.



- [16] J. D. Griffith, L. Comeau, S. Rosenfield, R. M. Stansel, A. Bianchi, H. Moss, and T. de Lange, "Mammalian telomeres end in a large duplex loop.," *Cell*, vol. 97, no. 4, pp. 503–14, May 1999.
- [17] T. de Lange, "How telomeres solve the end-protection problem.," *Science*, vol. 326, no. 5955, pp. 948–52, Nov. 2009.
- [18] E. L. Denchi and T. de Lange, "Protection of telomeres through independent control of ATM and ATR by TRF2 and POT1.," *Nature*, vol. 448, no. 7157, pp. 1068–71, Aug. 2007.
- [19] H. Xin, D. Liu, M. Wan, A. Safari, H. Kim, W. Sun, M. S. O'Connor, and Z. Songyang, "TPP1 is a homologue of ciliate TEBP-beta and interacts with POT1 to recruit telomerase.," *Nature*, vol. 445, no. 7127, pp. 559–62, Feb. 2007.
- [20] J. C. Y. Wang, J. K. Warner, N. Erdmann, P. M. Lansdorp, L. Harrington, and J. E. Dick, "Dissociation of telomerase activity and telomere length maintenance in primitive human hematopoietic cells.," *Proc. Natl. Acad. Sci. U. S. A.*, vol. 102, no. 40, pp. 14398–403, Oct. 2005.
- [21] A. M. Olovnikov, "A theory of marginotomy. The incomplete copying of template margin in enzymic synthesis of polynucleotides and biological significance of the phenomenon.," *J. Theor. Biol.*, vol. 41, no. 1, pp. 181–90, Sep. 1973.
- [22] P. M. Lansdorp, "Major cutbacks at chromosome ends.," *Trends Biochem. Sci.*, vol. 30, no. 7, pp. 388–95, Jul. 2005.
- [23] C. B. Harley, A. B. Futcher, and C. W. Greider, "Telomeres shorten during ageing of human fibroblasts.," *Nature*, vol. 345, no. 6274, pp. 458–60, May 1990.
- [24] C. B. Harley, H. Vaziri, C. M. Counter, and R. C. Allsopp, "The telomere hypothesis of cellular aging.," *Exp. Gerontol.*, vol. 27, no. 4, pp. 375–82, 1992.
- [25] M. Collado, M. A. Blasco, and M. Serrano, "Cellular senescence in cancer and aging.," *Cell*, vol. 130, no. 2, pp. 223–33, Jul. 2007.
- [26] F. d'Adda di Fagagna, P. M. Reaper, L. Clay-Farrace, H. Fiegler, P. Carr, T. Von Zglinicki, G. Saretzki, N. P. Carter, and S. P. Jackson, "A DNA damage checkpoint response in telomere-initiated senescence.," *Nature*, vol. 426, no. 6963, pp. 194–8, Nov. 2003.
- [27] H. Takai, A. Smogorzewska, and T. de Lange, "DNA damage foci at dysfunctional telomeres.," *Curr. Biol.*, vol. 13, no. 17, pp. 1549–56, Sep. 2003.
- [28] C. B. Harley, "Telomerase and cancer therapeutics.," *Nat. Rev. Cancer*, vol. 8, no. 3, pp. 167–79, Mar. 2008.
- [29] D. Hanahan and R. A. Weinberg, "Hallmarks of cancer: the next generation.," *Cell*, vol. 144, no. 5, pp. 646–74, Mar. 2011.
- [30] J. W. Shay and W. E. Wright, "Telomerase therapeutics for cancer: challenges and new directions.," *Nat. Rev. Drug Discov.*, vol. 5, no. 7, pp. 577–84, Jul. 2006.
- [31] R. A. Greenberg, R. C. Allsopp, L. Chin, G. B. Morin, and R. A. DePinho, "Expression of mouse telomerase reverse transcriptase during development, differentiation and proliferation.," *Oncogene*, vol. 16, no. 13, pp. 1723–30, Apr. 1998.
- [32] Y.-S. Cong, W. E. Wright, and J. W. Shay, "Human telomerase and its regulation.," *Microbiol. Mol. Biol. Rev.*, vol. 66, no. 3, pp. 407–25, table of contents, Sep. 2002.

- [33] C. J. Cairney and W. N. Keith, "Telomerase redefined: integrated regulation of hTR and hTERT for telomere maintenance and telomerase activity.," *Biochimie*, vol. 90, no. 1, pp. 13–23, Jan. 2008.
- [34] M. W. Djojosebroto, Y. S. Choi, H.-W. Lee, and K. L. Rudolph, "Telomeres and telomerase in aging, regeneration and cancer.," *Mol. Cells*, vol. 15, no. 2, pp. 164–75, Apr. 2003.
- [35] T. Vulliamy, A. Marrone, F. Goldman, A. Dearlove, M. Bessler, P. J. Mason, and I. Dokal, "The RNA component of telomerase is mutated in autosomal dominant dyskeratosis congenita.," *Nature*, vol. 413, no. 6854, pp. 432–5, Sep. 2001.
- [36] H. Yamaguchi, G. M. Baerlocher, P. M. Lansdorp, S. J. Chanock, O. Nunez, E. Sloand, and N. S. Young, "Mutations of the human telomerase RNA gene (TERC) in aplastic anemia and myelodysplastic syndrome.," *Blood*, vol. 102, no. 3, pp. 916–8, Aug. 2003.
- [37] M. Armanios, "Telomerase and idiopathic pulmonary fibrosis.," *Mutat. Res.*, vol. 730, no. 1–2, pp. 52–8, Feb. 2012.
- [38] E. H. Blackburn, "Cell biology: Shaggy mouse tales.," *Nature*, vol. 436, no. 7053, pp. 922–3, Aug. 2005.
- [39] K. Collins, "The biogenesis and regulation of telomerase holoenzymes.," *Nat. Rev. Mol. Cell Biol.*, vol. 7, no. 7, pp. 484–94, Jul. 2006.
- [40] K. R. Hukezalie and J. M. Y. Wong, "Structure-function relationship and biogenesis regulation of the human telomerase holoenzyme.," *FEBS J.*, vol. 280, no. 14, pp. 3194–204, Jul. 2013.
- [41] X. Yi, V. M. Tesmer, I. Savre-Train, J. W. Shay, and W. E. Wright, "Both transcriptional and posttranscriptional mechanisms regulate human telomerase template RNA levels.," *Mol. Cell. Biol.*, vol. 19, no. 6, pp. 3989–97, Jun. 1999.
- [42] K. Collins and J. R. Mitchell, "Telomerase in the human organism.," *Oncogene*, vol. 21, no. 4, pp. 564–79, Jan. 2002.
- [43] E. D. Egan and K. Collins, "An enhanced H/ACA RNP assembly mechanism for human telomerase RNA.," *Mol. Cell. Biol.*, vol. 32, no. 13, pp. 2428–39, Jul. 2012.
- [44] U. T. Meier, "The many facets of H/ACA ribonucleoproteins.," *Chromosoma*, vol. 114, no. 1, pp. 1–14, May 2005.
- [45] S. B. Cohen, M. E. Graham, G. O. Lovrecz, N. Bache, P. J. Robinson, and R. R. Reddel, "Protein composition of catalytically active human telomerase from immortal cells.," *Science*, vol. 315, no. 5820, pp. 1850–3, Mar. 2007.
- [46] C. Dez, A. Henras, B. Faucon, D. Lafontaine, M. Caizergues-Ferrer, and Y. Henry, "Stable expression in yeast of the mature form of human telomerase RNA depends on its association with the box H/ACA small nucleolar RNP proteins Cbf5p, Nhp2p and Nop10p.," *Nucleic Acids Res.*, vol. 29, no. 3, pp. 598–603, Feb. 2001.
- [47] J. R. Mitchell, J. Cheng, and K. Collins, "A box H/ACA small nucleolar RNA-like domain at the human telomerase RNA 3' end.," *Mol. Cell. Biol.*, vol. 19, no. 1, pp. 567–76, Jan. 1999.
- [48] J. L. Stern, K. G. Zyner, H. A. Pickett, S. B. Cohen, and T. M. Bryan, "Telomerase recruitment requires both TCAB1 and Cajal bodies independently.," *Mol. Cell. Biol.*, vol. 32, no. 13, pp. 2384–95, Jul. 2012.

- [49] P. Richard, X. Darzacq, E. Bertrand, B. E. Jdy, C. Verheggen, and T. Kiss, "A common sequence motif determines the Cajal body-specific localization of box H/ACA scaRNAs," *EMBO J.*, vol. 22, no. 16, pp. 4283–93, Aug. 2003.
- [50] G. Cristofari, E. Adolf, P. Reichenbach, K. Sikora, R. M. Terns, M. P. Terns, and J. Lingner, "Human telomerase RNA accumulation in Cajal bodies facilitates telomerase recruitment to telomeres and telomere elongation," *Mol. Cell*, vol. 27, no. 6, pp. 882–9, Sep. 2007.
- [51] X. Darzacq, N. Kittur, S. Roy, Y. Shav-Tal, R. H. Singer, and U. T. Meier, "Stepwise RNP assembly at the site of H/ACA RNA transcription in human cells," *J. Cell Biol.*, vol. 173, no. 2, pp. 207–18, Apr. 2006.
- [52] J. Chung, P. Khadka, and I. K. Chung, "Nuclear import of hTERT requires a bipartite nuclear localization signal and Akt-mediated phosphorylation," *J. Cell Sci.*, vol. 125, no. Pt 11, pp. 2684–97, Jun. 2012.
- [53] A. S. Venteicher, Z. Meng, P. J. Mason, T. D. Veenstra, and S. E. Artandi, "Identification of ATPases pontin and reptin as telomerase components essential for holoenzyme assembly," *Cell*, vol. 132, no. 6, pp. 945–57, Mar. 2008.
- [54] M. Takakura, S. Kyo, T. Kanaya, H. Hirano, J. Takeda, M. Yutsudo, and M. Inoue, "Cloning of human telomerase catalytic subunit (hTERT) gene promoter and identification of proximal core promoter sequences essential for transcriptional activation in immortalized and cancer cells," *Cancer Res.*, vol. 59, no. 3, pp. 551–7, Feb. 1999.
- [55] D. Fu and K. Collins, "Purification of human telomerase complexes identifies factors involved in telomerase biogenesis and telomere length regulation," *Mol. Cell*, vol. 28, no. 5, pp. 773–85, Dec. 2007.
- [56] B. E. Jdy, E. Bertrand, and T. Kiss, "Human telomerase RNA and box H/ACA scaRNAs share a common Cajal body-specific localization signal," *J. Cell Biol.*, vol. 164, no. 5, pp. 647–52, Mar. 2004.
- [57] Y. Zhu, R. L. Tomlinson, A. A. Lukowiak, R. M. Terns, and M. P. Terns, "Telomerase RNA accumulates in Cajal bodies in human cancer cells," *Mol. Biol. Cell*, vol. 15, no. 1, pp. 81–90, Jan. 2004.
- [58] R. L. Tomlinson, E. B. Abreu, T. Ziegler, H. Ly, C. M. Counter, R. M. Terns, and M. P. Terns, "Telomerase reverse transcriptase is required for the localization of telomerase RNA to cajal bodies and telomeres in human cancer cells," *Mol. Biol. Cell*, vol. 19, no. 9, pp. 3793–800, Sep. 2008.
- [59] R. L. Tomlinson, T. D. Ziegler, T. Supakorndej, R. M. Terns, and M. P. Terns, "Cell cycle-regulated trafficking of human telomerase to telomeres," *Mol. Biol. Cell*, vol. 17, no. 2, pp. 955–65, Feb. 2006.
- [60] S. Marcand, V. Brevet, C. Mann, and E. Gilson, "Cell cycle restriction of telomere elongation," *Curr. Biol.*, vol. 10, no. 8, pp. 487–90, Apr. 2000.
- [61] D. Fu and K. Collins, "Human telomerase and Cajal body ribonucleoproteins share a unique specificity of Sm protein association," *Genes Dev.*, vol. 20, no. 5, pp. 531–6, Mar. 2006.
- [62] G. Cristofari, K. Sikora, and J. Lingner, "Telomerase unplugged," *ACS Chem. Biol.*, vol. 2, no. 3, pp. 155–8, Mar. 2007.

- [63] N. F. Lue, "Adding to the ends: what makes telomerase processive and how important is it?," *Bioessays*, vol. 26, no. 9, pp. 955–62, Sep. 2004.
- [64] J.-L. Chen and C. W. Greider, "Template boundary definition in mammalian telomerase.," *Genes Dev.*, vol. 17, no. 22, pp. 2747–52, Nov. 2003.
- [65] Y. Yang, Y. Chen, C. Zhang, H. Huang, and S. M. Weissman, "Nucleolar localization of hTERT protein is associated with telomerase function.," *Exp. Cell Res.*, vol. 277, no. 2, pp. 201–9, Jul. 2002.
- [66] J. R. Mitchell and K. Collins, "Human telomerase activation requires two independent interactions between telomerase RNA and telomerase reverse transcriptase.," *Mol. Cell*, vol. 6, no. 2, pp. 361–71, Aug. 2000.
- [67] E. D. Egan and K. Collins, "Biogenesis of telomerase ribonucleoproteins.," *RNA*, vol. 18, no. 10, pp. 1747–59, Oct. 2012.
- [68] C. Autexier, R. Pruzan, W. D. Funk, and C. W. Greider, "Reconstitution of human telomerase activity and identification of a minimal functional region of the human telomerase RNA.," *EMBO J.*, vol. 15, no. 21, pp. 5928–35, Nov. 1996.
- [69] F. Wang, E. R. Podell, A. J. Zaug, Y. Yang, P. Baciú, T. R. Cech, and M. Lei, "The POT1-TPP1 telomere complex is a telomerase processivity factor.," *Nature*, vol. 445, no. 7127, pp. 506–10, Feb. 2007.
- [70] X. Qi, M. Xie, A. F. Brown, C. J. Bley, J. D. Podlevsky, and J. J.-L. Chen, "RNA/DNA hybrid binding affinity determines telomerase template-translocation efficiency.," *EMBO J.*, vol. 31, no. 1, pp. 150–61, Jan. 2012.
- [71] G. Zemora, "Structural insights into the human telomerase RNA," University of Vienna, 2014.
- [72] A. G. Bodnar, M. Ouellette, M. Frolkis, S. E. Holt, C. P. Chiu, G. B. Morin, C. B. Harley, J. W. Shay, S. Lichtsteiner, and W. E. Wright, "Extension of life-span by introduction of telomerase into normal human cells.," *Science*, vol. 279, no. 5349, pp. 349–52, Jan. 1998.
- [73] C. P. Morales, S. E. Holt, M. Ouellette, K. J. Kaur, Y. Yan, K. S. Wilson, M. A. White, W. E. Wright, and J. W. Shay, "Absence of cancer-associated changes in human fibroblasts immortalized with telomerase.," *Nat. Genet.*, vol. 21, no. 1, pp. 115–8, Jan. 1999.
- [74] J. Yang, E. Chang, A. M. Cherry, C. D. Bangs, Y. Oei, A. Bodnar, A. Bronstein, C. P. Chiu, and G. S. Herron, "Human endothelial cell life extension by telomerase expression.," *J. Biol. Chem.*, vol. 274, no. 37, pp. 26141–8, Sep. 1999.
- [75] A. J. Gillis, A. P. Schuller, and E. Skordalakes, "Structure of the *Tribolium castaneum* telomerase catalytic subunit TERT.," *Nature*, vol. 455, no. 7213, pp. 633–7, Oct. 2008.
- [76] H. D. M. Wyatt, S. C. West, and T. L. Beattie, "InTERTpreting telomerase structure and function.," *Nucleic Acids Res.*, vol. 38, no. 17, pp. 5609–22, Sep. 2010.
- [77] K. Arai, K. Masutomi, S. Khurts, S. Kaneko, K. Kobayashi, and S. Murakami, "Two independent regions of human telomerase reverse transcriptase are important for its oligomerization and telomerase activity.," *J. Biol. Chem.*, vol. 277, no. 10, pp. 8538–44, Mar. 2002.
- [78] S. S. R. Banik, C. Guo, A. C. Smith, S. S. Margolis, D. A. Richardson, C. A. Tirado, and C. M. Counter, "C-terminal regions of the human telomerase catalytic subunit essential for in vivo enzyme activity.," *Mol. Cell. Biol.*, vol. 22, no. 17, pp. 6234–46, Sep. 2002.

- [79] S. Huard, T. J. Moriarty, and C. Autexier, "The C terminus of the human telomerase reverse transcriptase is a determinant of enzyme processivity.," *Nucleic Acids Res.*, vol. 31, no. 14, pp. 4059–70, Jul. 2003.
- [80] D. C. F. Sealey, L. Zheng, M. A. S. Taboski, J. Cruickshank, M. Ikura, and L. A. Harrington, "The N-terminus of hTERT contains a DNA-binding domain and is required for telomerase activity and cellular immortalization.," *Nucleic Acids Res.*, vol. 38, no. 6, pp. 2019–35, Apr. 2010.
- [81] M. Mitchell, A. Gillis, M. Futahashi, H. Fujiwara, and E. Skordalakes, "Structural basis for telomerase catalytic subunit TERT binding to RNA template and telomeric DNA.," *Nat. Struct. Mol. Biol.*, vol. 17, no. 4, pp. 513–8, Apr. 2010.
- [82] D. Bosoy, Y. Peng, I. S. Mian, and N. F. Lue, "Conserved N-terminal motifs of telomerase reverse transcriptase required for ribonucleoprotein assembly in vivo.," *J. Biol. Chem.*, vol. 278, no. 6, pp. 3882–90, Feb. 2003.
- [83] W. C. Drosopoulos and V. R. Prasad, "The telomerase-specific T motif is a restrictive determinant of repetitive reverse transcription by human telomerase.," *Mol. Cell. Biol.*, vol. 30, no. 2, pp. 447–59, Jan. 2010.
- [84] T. M. Bryan, K. J. Goodrich, and T. R. Cech, "Telomerase RNA bound by protein motifs specific to telomerase reverse transcriptase.," *Mol. Cell*, vol. 6, no. 2, pp. 493–9, Aug. 2000.
- [85] P. W. Hammond, T. N. Lively, and T. R. Cech, "The anchor site of telomerase from *Euplotes aediculatus* revealed by photo-cross-linking to single- and double-stranded DNA primers.," *Mol. Cell. Biol.*, vol. 17, no. 1, pp. 296–308, Jan. 1997.
- [86] T. J. Moriarty, D. T. Marie-Egyptienne, and C. Autexier, "Functional organization of repeat addition processivity and DNA synthesis determinants in the human telomerase multimer.," *Mol. Cell. Biol.*, vol. 24, no. 9, pp. 3720–33, May 2004.
- [87] M. Mason, A. Schuller, and E. Skordalakes, "Telomerase structure function.," *Curr. Opin. Struct. Biol.*, vol. 21, no. 1, pp. 92–100, Feb. 2011.
- [88] A. J. Zaug, E. R. Podell, and T. R. Cech, "Mutation in TERT separates processivity from anchor-site function.," *Nat. Struct. Mol. Biol.*, vol. 15, no. 8, pp. 870–2, Aug. 2008.
- [89] H. D. M. Wyatt, A. R. Tsang, D. A. Lobb, and T. L. Beattie, "Human telomerase reverse transcriptase (hTERT) Q169 is essential for telomerase function in vitro and in vivo.," *PLoS One*, vol. 4, no. 9, p. e7176, Jan. 2009.
- [90] K. L. Friedman and T. R. Cech, "Essential functions of amino-terminal domains in the yeast telomerase catalytic subunit revealed by selection for viable mutants.," *Genes Dev.*, vol. 13, no. 21, pp. 2863–74, Nov. 1999.
- [91] J. Xia, Y. Peng, I. S. Mian, and N. F. Lue, "Identification of functionally important domains in the N-terminal region of telomerase reverse transcriptase.," *Mol. Cell. Biol.*, vol. 20, no. 14, pp. 5196–207, Jul. 2000.
- [92] F. Bachand and C. Autexier, "Functional regions of human telomerase reverse transcriptase and human telomerase RNA required for telomerase activity and RNA-protein interactions.," *Mol. Cell. Biol.*, vol. 21, no. 5, pp. 1888–97, Mar. 2001.

- [93] A. G. Seto, K. Umansky, Y. Tzfati, A. J. Zaug, E. H. Blackburn, and T. R. Cech, "A template-proximal RNA paired element contributes to *Saccharomyces cerevisiae* telomerase activity.," *RNA*, vol. 9, no. 11, pp. 1323–32, Nov. 2003.
- [94] S. L. Weinrich, R. Pruzan, L. Ma, M. Ouellette, V. M. Tesmer, S. E. Holt, A. G. Bodnar, S. Lichtsteiner, N. W. Kim, J. B. Trager, R. D. Taylor, R. Carlos, W. H. Andrews, W. E. Wright, J. W. Shay, C. B. Harley, and G. B. Morin, "Reconstitution of human telomerase with the template RNA component hTR and the catalytic protein subunit hTERT.," *Nat. Genet.*, vol. 17, no. 4, pp. 498–502, Dec. 1997.
- [95] C. M. Counter, M. Meyerson, E. N. Eaton, and R. A. Weinberg, "The catalytic subunit of yeast telomerase.," *Proc. Natl. Acad. Sci. U. S. A.*, vol. 94, no. 17, pp. 9202–7, Aug. 1997.
- [96] M. Xie, J. D. Podlevsky, X. Qi, C. J. Bley, and J. J.-L. Chen, "A novel motif in telomerase reverse transcriptase regulates telomere repeat addition rate and processivity.," *Nucleic Acids Res.*, vol. 38, no. 6, pp. 1982–96, Apr. 2010.
- [97] A. Kilian, D. D. Bowtell, H. E. Abud, G. R. Hime, D. J. Venter, P. K. Keese, E. L. Duncan, R. R. Reddel, and R. A. Jefferson, "Isolation of a candidate human telomerase catalytic subunit gene, which reveals complex splicing patterns in different cell types.," *Hum. Mol. Genet.*, vol. 6, no. 12, pp. 2011–9, Nov. 1997.
- [98] W.-J. Liu, Y.-W. Zhang, Z.-X. Zhang, and J. Ding, "Alternative splicing of human telomerase reverse transcriptase may not be involved in telomerase regulation during all-trans-retinoic acid-induced HL-60 cell differentiation.," *J. Pharmacol. Sci.*, vol. 96, no. 2, pp. 106–14, Oct. 2004.
- [99] I. Listerman, J. Sun, F. S. Gazzaniga, J. L. Lukas, and E. H. Blackburn, "The major reverse transcriptase-incompetent splice variant of the human telomerase protein inhibits telomerase activity but protects from apoptosis.," *Cancer Res.*, vol. 73, no. 9, pp. 2817–28, May 2013.
- [100] Y. Maida, M. Yasukawa, M. Furuuchi, T. Lassmann, R. Possemato, N. Okamoto, V. Kasim, Y. Hayashizaki, W. C. Hahn, and K. Masutomi, "An RNA-dependent RNA polymerase formed by TERT and the RMRP RNA.," *Nature*, vol. 461, no. 7261, pp. 230–5, Sep. 2009.
- [101] A. J. Ye and D. P. Romero, "Phylogenetic relationships amongst tetrahymenine ciliates inferred by a comparison of telomerase RNAs.," *Int. J. Syst. Evol. Microbiol.*, vol. 52, no. Pt 6, pp. 2297–302, Nov. 2002.
- [102] M. Xie, A. Mosig, X. Qi, Y. Li, P. F. Stadler, and J. J.-L. Chen, "Structure and function of the smallest vertebrate telomerase RNA from teleost fish.," *J. Biol. Chem.*, vol. 283, no. 4, pp. 2049–59, Jan. 2008.
- [103] S. Gunisova, E. Elboher, J. Nosek, V. Gorkovoy, Y. Brown, J.-F. Lucier, N. Laterreur, R. J. Wellinger, Y. Tzfati, and L. Tomaska, "Identification and comparative analysis of telomerase RNAs from *Candida* species reveal conservation of functional elements.," *RNA*, vol. 15, no. 4, pp. 546–59, Apr. 2009.
- [104] J. L. Chen, M. A. Blasco, and C. W. Greider, "Secondary structure of vertebrate telomerase RNA.," *Cell*, vol. 100, no. 5, pp. 503–14, Mar. 2000.
- [105] L. Martin-Rivera and M. A. Blasco, "Identification of functional domains and dominant negative mutations in vertebrate telomerase RNA using an in vivo reconstitution system.," *J. Biol. Chem.*, vol. 276, no. 8, pp. 5856–65, Feb. 2001.

- [106] H. Ly, E. H. Blackburn, and T. G. Parslow, "Comprehensive structure-function analysis of the core domain of human telomerase RNA.," *Mol. Cell. Biol.*, vol. 23, no. 19, pp. 6849–56, Oct. 2003.
- [107] J.-L. Chen, K. K. Opperman, and C. W. Greider, "A critical stem-loop structure in the CR4-CR5 domain of mammalian telomerase RNA.," *Nucleic Acids Res.*, vol. 30, no. 2, pp. 592–7, Jan. 2002.
- [108] J.-L. Chen and C. W. Greider, "Functional analysis of the pseudoknot structure in human telomerase RNA.," *Proc. Natl. Acad. Sci. U. S. A.*, vol. 102, no. 23, pp. 8080–5; discussion 8077–9, Jun. 2005.
- [109] C. A. Theimer, C. A. Blois, and J. Feigon, "Structure of the human telomerase RNA pseudoknot reveals conserved tertiary interactions essential for function.," *Mol. Cell*, vol. 17, no. 5, pp. 671–82, Mar. 2005.
- [110] N.-K. Kim, Q. Zhang, J. Zhou, C. A. Theimer, R. D. Peterson, and J. Feigon, "Solution structure and dynamics of the wild-type pseudoknot of human telomerase RNA.," *J. Mol. Biol.*, vol. 384, no. 5, pp. 1249–61, Dec. 2008.
- [111] N. K. Conrad, "The emerging role of triple helices in RNA biology.," *Wiley Interdiscip. Rev. RNA*, vol. 5, no. 1, pp. 15–29, 2014.
- [112] F. Qiao and T. R. Cech, "Triple-helix structure in telomerase RNA contributes to catalysis.," *Nat. Struct. Mol. Biol.*, vol. 15, no. 6, pp. 634–40, Jun. 2008.
- [113] K. Shefer, Y. Brown, V. Gorkovoy, T. Nussbaum, N. B. Ulyanov, and Y. Tzfati, "A triple helix within a pseudoknot is a conserved and essential element of telomerase RNA.," *Mol. Cell. Biol.*, vol. 27, no. 6, pp. 2130–43, Mar. 2007.
- [114] Q. Zhang, N.-K. Kim, R. D. Peterson, Z. Wang, and J. Feigon, "Structurally conserved five nucleotide bulge determines the overall topology of the core domain of human telomerase RNA.," *Proc. Natl. Acad. Sci. U. S. A.*, vol. 107, no. 44, pp. 18761–8, Nov. 2010.
- [115] R. O. Niederer and D. C. Zappulla, "Refined secondary-structure models of the core of yeast and human telomerase RNAs directed by SHAPE.," *RNA*, Dec. 2014.
- [116] M. D. Stone, M. Mihalusova, C. M. O'connor, R. Prathapam, K. Collins, and X. Zhuang, "Stepwise protein-mediated RNA folding directs assembly of telomerase ribonucleoprotein.," *Nature*, vol. 446, no. 7134, pp. 458–61, Mar. 2007.
- [117] C. J. Bley, X. Qi, D. P. Rand, C. R. Borges, R. W. Nelson, and J. J.-L. Chen, "RNA-protein binding interface in the telomerase ribonucleoprotein.," *Proc. Natl. Acad. Sci. U. S. A.*, vol. 108, no. 51, pp. 20333–8, Dec. 2011.
- [118] J. Huang, A. F. Brown, J. Wu, J. Xue, C. J. Bley, D. P. Rand, L. Wu, R. Zhang, J. J.-L. Chen, and M. Lei, "Structural basis for protein-RNA recognition in telomerase.," *Nat. Struct. Mol. Biol.*, vol. 21, no. 6, pp. 507–12, Jun. 2014.
- [119] A. R. Robart and K. Collins, "Investigation of human telomerase holoenzyme assembly, activity, and processivity using disease-linked subunit variants.," *J. Biol. Chem.*, vol. 285, no. 7, pp. 4375–86, Feb. 2010.
- [120] P. Ganot, M. L. Bortolin, and T. Kiss, "Site-specific pseudouridine formation in preribosomal RNA is guided by small nucleolar RNAs.," *Cell*, vol. 89, no. 5, pp. 799–809, May 1997.

- [121] C. A. Theimer, B. E. Jdy, N. Chim, P. Richard, K. E. Breece, T. Kiss, and J. Feigon, “Structural and functional characterization of human telomerase RNA processing and cajal body localization signals,” *Mol. Cell*, vol. 27, no. 6, pp. 869–81, Sep. 2007.
- [122] W. A. Cantara, P. F. Crain, J. Rozenski, J. A. McCloskey, K. A. Harris, X. Zhang, F. A. P. Vendeix, D. Fabris, and P. F. Agris, “The RNA Modification Database, RNAMDB: 2011 update,” *Nucleic Acids Res.*, vol. 39, no. Database issue, pp. D195–201, Jan. 2011.
- [123] J. Ge and Y.-T. Yu, “RNA pseudouridylation: new insights into an old modification,” *Trends Biochem. Sci.*, vol. 38, no. 4, pp. 210–8, Apr. 2013.
- [124] T. H. King, B. Liu, R. R. McCully, and M. J. Fournier, “Ribosome structure and activity are altered in cells lacking snoRNPs that form pseudouridines in the peptidyl transferase center,” *Mol. Cell*, vol. 11, no. 2, pp. 425–35, Feb. 2003.
- [125] A. T. Yu, J. Ge, and Y.-T. Yu, “Pseudouridines in spliceosomal snRNAs,” *Protein Cell*, vol. 2, no. 9, pp. 712–25, Sep. 2011.
- [126] N.-K. Kim, C. A. Theimer, J. R. Mitchell, K. Collins, and J. Feigon, “Effect of pseudouridylation on the structure and activity of the catalytically essential P6.1 hairpin in human telomerase RNA,” *Nucleic Acids Res.*, vol. 38, no. 19, pp. 6746–56, Oct. 2010.
- [127] J. R. Mitchell, E. Wood, and K. Collins, “A telomerase component is defective in the human disease dyskeratosis congenita,” *Nature*, vol. 402, no. 6761, pp. 551–5, Dec. 1999.
- [128] N. W. Kim, M. A. Piatyszek, K. R. Prowse, C. B. Harley, M. D. West, P. L. Ho, G. M. Coviello, W. E. Wright, S. L. Weinrich, and J. W. Shay, “Specific association of human telomerase activity with immortal cells and cancer,” *Science*, vol. 266, no. 5193, pp. 2011–5, Dec. 1994.
- [129] M. Armanios and E. H. Blackburn, “The telomere syndromes,” *Nat. Rev. Genet.*, vol. 13, no. 10, pp. 693–704, Oct. 2012.
- [130] N. S. Heiss, S. W. Knight, T. J. Vulliamy, S. M. Klauck, S. Wiemann, P. J. Mason, A. Poustka, and I. Dokal, “X-linked dyskeratosis congenita is caused by mutations in a highly conserved gene with putative nucleolar functions,” *Nat. Genet.*, vol. 19, no. 1, pp. 32–8, May 1998.
- [131] H. Yamaguchi, R. T. Calado, H. Ly, S. Kajigaya, G. M. Baerlocher, S. J. Chanock, P. M. Lansdorp, and N. S. Young, “Mutations in TERT, the gene for telomerase reverse transcriptase, in aplastic anemia,” *N. Engl. J. Med.*, vol. 352, no. 14, pp. 1413–24, Apr. 2005.
- [132] A. J. Walne, T. Vulliamy, A. Marrone, R. Beswick, M. Kirwan, Y. Masunari, F.-H. Al-Qurashi, M. Aljurf, and I. Dokal, “Genetic heterogeneity in autosomal recessive dyskeratosis congenita with one subtype due to mutations in the telomerase-associated protein NOP10,” *Hum. Mol. Genet.*, vol. 16, no. 13, pp. 1619–29, Jul. 2007.
- [133] T. J. Vulliamy, A. Marrone, S. W. Knight, A. Walne, P. J. Mason, and I. Dokal, “Mutations in dyskeratosis congenita: their impact on telomere length and the diversity of clinical presentation,” *Blood*, vol. 107, no. 7, pp. 2680–5, Apr. 2006.
- [134] F. Zhong, S. A. Savage, M. Shkreli, N. Giri, L. Jessop, T. Myers, R. Chen, B. P. Alter, and S. E. Artandi, “Disruption of telomerase trafficking by TCAB1 mutation causes dyskeratosis congenita,” *Genes Dev.*, vol. 25, no. 1, pp. 11–6, Jan. 2011.
- [135] L. F. Z. Batista, M. F. Pech, F. L. Zhong, H. N. Nguyen, K. T. Xie, A. J. Zaug, S. M. Crary, J. Choi, V. Sebastiano, A. Cherry, N. Giri, M. Wernig, B. P. Alter, T. R. Cech, S. A. Savage, R. A.



- Reijo Pera, and S. E. Artandi, "Telomere shortening and loss of self-renewal in dyskeratosis congenita induced pluripotent stem cells.," *Nature*, vol. 474, no. 7351, pp. 399–402, Jun. 2011.
- [136] A. J. Walne and I. Dokal, "Advances in the understanding of dyskeratosis congenita.," *Br. J. Haematol.*, vol. 145, no. 2, pp. 164–72, Apr. 2009.
- [137] M. Bessler, D. B. Wilson, and P. J. Mason, "Dyskeratosis congenita.," *FEBS Lett.*, vol. 584, no. 17, pp. 3831–8, Sep. 2010.
- [138] B. P. Alter, G. M. Baerlocher, S. A. Savage, S. J. Chanock, B. B. Weksler, J. P. Willner, J. A. Peters, N. Giri, and P. M. Lansdorp, "Very short telomere length by flow fluorescence in situ hybridization identifies patients with dyskeratosis congenita.," *Blood*, vol. 110, no. 5, pp. 1439–47, Sep. 2007.
- [139] R. Rashid, B. Liang, D. L. Baker, O. A. Youssef, Y. He, K. Phipps, R. M. Terns, M. P. Terns, and H. Li, "Crystal structure of a Cbf5-Nop10-Gar1 complex and implications in RNA-guided pseudouridylation and dyskeratosis congenita.," *Mol. Cell*, vol. 21, no. 2, pp. 249–60, Jan. 2006.
- [140] J.-L. Chen and C. W. Greider, "Telomerase RNA structure and function: implications for dyskeratosis congenita.," *Trends Biochem. Sci.*, vol. 29, no. 4, pp. 183–92, Apr. 2004.
- [141] L. R. Comolli, I. Smirnov, L. Xu, E. H. Blackburn, and T. L. James, "A molecular switch underlies a human telomerase disease.," *Proc. Natl. Acad. Sci. U. S. A.*, vol. 99, no. 26, pp. 16998–7003, Dec. 2002.
- [142] R. Schroeder, A. Barta, and K. Semrad, "Strategies for RNA folding and assembly.," *Nat. Rev. Mol. Cell Biol.*, vol. 5, no. 11, pp. 908–19, Nov. 2004.
- [143] N. Sachsenmaier, S. Handl, F. Debeljak, and C. Waldsich, "Mapping RNA structure in vitro using nucleobase-specific probes.," *Methods Mol. Biol.*, vol. 1086, pp. 79–94, Jan. 2014.
- [144] G. Cristofari and J. Lingner, "Telomere length homeostasis requires that telomerase levels are limiting.," *EMBO J.*, vol. 25, no. 3, pp. 565–74, Feb. 2006.
- [145] C. Li, A. Wen, B. Shen, J. Lu, Y. Huang, and Y. Chang, "FastCloning: a highly simplified, purification-free, sequence- and ligation-independent PCR cloning method.," *BMC Biotechnol.*, vol. 11, p. 92, Jan. 2011.
- [146] J. Ofengand, M. Del Campo, and Y. Kaya, "Mapping pseudouridines in RNA molecules.," *Methods*, vol. 25, no. 3, pp. 365–73, Nov. 2001.
- [147] T. C. Leeper and G. Varani, "The structure of an enzyme-activating fragment of human telomerase RNA.," *RNA*, vol. 11, no. 4, pp. 394–403, Apr. 2005.
- [148] H. Ly, R. T. Calado, P. Allard, G. M. Baerlocher, P. M. Lansdorp, N. S. Young, and T. G. Parslow, "Functional characterization of telomerase RNA variants found in patients with hematologic disorders.," *Blood*, vol. 105, no. 6, pp. 2332–9, Mar. 2005.
- [149] K. A. Carroll and H. Ly, "Telomere dysfunction in human diseases: the long and short of it!," *Int. J. Clin. Exp. Pathol.*, vol. 2, no. 6, pp. 528–43, Jan. 2009.
- [150] D. Fu and K. Collins, "Distinct biogenesis pathways for human telomerase RNA and H/ACA small nucleolar RNAs.," *Mol. Cell*, vol. 11, no. 5, pp. 1361–72, May 2003.

## 8 Acknowledgements

In this section I would like to thank all people who supported me in the last few years in starting and finishing my studies.

First of all, I would like to thank Mag. Dr. Christina Waldisch for giving me, almost 3 years ago, the opportunity to work in her lab and to gain a lot of expertise in working in a lab. Starting with the bachelor thesis and now concluding my work with my master thesis I am very thankful for all support and guidance in the last years.

Secondly, I would like to thank my family and friends, which supported me emotionally to be able to study worry-free and have a place where I could always go for help. Especially in this respect I would like to thank Estella Veigel. She is the most amazing person I have ever met. She is kind, beautiful, and intelligent and I love and will love her forever. Thank you for your support!

Special thanks I would like to direct at the ‘Stipendienstelle Wien’ and the republic of Austria, which gave me the opportunity through a ‘Selbsterhalterstipendium’ to study molecular biotechnology first at FH Campus Wien and then for the master molecular biology with specialization in biochemistry at the University of Vienna.

## 9 Appendix

### 9.1 Abstract

The human telomerase is a ribonucleoprotein-complex (RNP) consisting of an RNA part, the human telomerase RNA (hTR), a protein part, the human telomerase reverse transcriptase (hTERT), and accessory proteins like Dyskerin Nop10, Nhp2, Tcab1 and Gar1. The main function of this complex is the maintenance of the telomeres by *de novo* synthesis of hexameric repeats (5'-TTAGGG-3') onto the end of chromosomes after each replication cycle to counteract the end replication problem. In somatic cells telomerase is not expressed and cannot elongate telomeres, therefore after a certain number of cell divisions the short telomeres cause senescence and cell death. For highly proliferative cells, like stem cells, the telomerase expression is up-regulated and telomere length is maintained. Also in 90 % of all cancer types the telomerase is highly up-regulated. This has led biomedical research to focus on ways to use this fact in new therapies. A dysfunctional telomerase enzyme can cause diseases, like dyskeratosis congenita, aplastic anemia, idiopathic pulmonary fibrosis, which are all connected to shortened telomeres and the senescence of highly proliferative cell like stem cells. Mutations in hTERT, hTR and accessory proteins can cause such phenotypes. Single mutations in hTR have been identified to cause such phenotypes and reduce or abolish telomerase activity. These changes seem to influence folding and conformation of the human telomerase RNA. Despite the fact that there are great efforts to obtain high resolution data on telomerase RNA, the information on full length hTR is scarce. In this thesis we analyzed the telomerase activity of hTERT bound to mutant hTR in which highly conserved residues or structurally interesting nucleotides were altered. Of the analyzed mutants, C123A affected telomere function most severely. In fact, nucleotide addition processivity was reduced to <10%, while repeat addition processivity was abolished. Exploring the structural consequences of this single point mutation revealed that disrupting the G91-C123 base pair in P2a perturbs formation of the pseudoknot and associated triple helix, thereby inducing misfolding of the core domain. In contrast, this mutation does not appear to affect binding of hTERT to the CR4/CR5 domain and to interfere with telomere biogenesis. As pseudouridines are known to play a role in stabilizing and folding of non-coding RNAs, it was of interest to identify potential pseudouridines within hTR. In fact, a total of 29 pseudouridines were observed clustering in the pseudoknot/template domain. Specifically, all Us within the triple helical scaffold appear to be pseudouridines, potentially involved in stabilizing this structural element essential for telomerase function.

## 9.2 Zusammenfassung

Die humane telomerase ist ein Ribonukleoprotein-komplex, welcher aus einer RNA, der humanen telomerase RNA (hTR) und einem protein-teil, der humanen telomerase reversen Transkriptase (hTERT) besteht, sowie Anhangs Proteinen wie Dyskerin, Nop10, Nhp2, Tcab1 und Gar1. Die Hauptfunktion dieses Komplexes ist die Instandhaltung der Telomere durch *de novo* synthese von hexameren Sequenzen (5'-TTAGGG-3') an das Ende von Chromosomen nach jedem Replikationszyklus um dem ‚End replication‘ Problem entgegen zu wirken. Somatische Zellen ist wird Telomerase nicht exprimiert und kann daher die Telomere nicht verlängern. Folglich werden die Telomere zu kurz was Zell Seneszenz und den Tod der Zelle zur Folge hat. In hoch-proliferativen Zellen, wie Stammzellen, ist die Telomerase Expression hoch reguliert und die Länge der Telomere kann beibehalten werden. In 90% aller Krebstypen ist die Telomerase hochreguliert. Diese Erkenntnis hat die biomedizinische Wissenschaft dahin gebracht neue Therapien in diese Richtung zu entwickeln. Ein nicht-funktionierendes Telomerase Enzym kann Krankheiten auslösen wie, dyskeratosis congenita, aplastische Anemie and idiopathische pulmonare Fibrose, welche alle in Verbindung zu kurzen Telomeren und Seneszenz in hoch-proliferativen Zellen steht. Mutationen in hTERT, hTR und Anhangs Proteinen können so einen Phänotyp auslösen. Punktmutationen in hTR wurden in Zusammenhang mit so einem Phänotyp und können die telomerase Aktivität reduzieren oder gar komplett vernichten. Trotz des Aufwands hoch auflösende Strukturdaten über die telomerase RNA zu erhalten gibt es nur wenige Informationen über die gesamte hTR. In dieser Arbeit wir analysierten die telomerase Aktivität von hTERT gebunden an mutierte hTR, von hoch konservierten Positionen oder strukturell interessanten Nukleotiden verändert wurden. Von diesen Mutanten die Mutante C123A hat die telomerase Aktivität am meisten beeinflusst. Tatsächlich ‚nucleotide addition processivity‘ wurde auf unter 10 % reduziert, während die ‚repeat addition processivity‘ komplett beseitigte. Genauere Betrachtung der strukturellen Veränderungen dieser Punktmutation zeigte, dass die Auflösung des Basenpaares G91-C123 in P2a die Formierung des Pseudoknoten und der assoziierten dreifach Helix stört und dabei eine Missfaltung der Kern Domäne verursacht. In Kontrast, diese Mutation scheint die Bindung von hTERT in der CR4/CR5 Domäne nicht zu beeinträchtigen und beeinflusst somit nicht die Biogenese der Telomerase. Wir wissen, dass Pseudouridine eine wichtige Rolle im Stabilisieren und in der Faltung von nicht-kodierenden RNAs spielt, deshalb ist es von großem Interesse Pseudouridine in hTR zu identifizieren. Tatsächlich haben wir 29 Pseudouridine beobachtet und festgestellt dass diese in der Pseudoknoten/Template Domäne vermehrt auftreten. Im speziellen scheinen alle Us in der dreifach-Helix Pseudouridine zu sein. Deshalb ist anzunehmen, dass diese Pseudouridine wichtig sind für die Stabilität und Funktion dieses Elements.

### 9.3 Book Chapter: Mapping RNA structure *In vitro* using Nucleobase-specific probes

## Chapter 5

### Mapping RNA Structure In Vitro Using Nucleobase-Specific Probes

Nora Sachsenmaier, Stefan Handl, Franka Debeljak,  
and Christina Waldsich

#### Abstract

RNAs have to adopt specific three-dimensional structures to fulfill their biological functions. Therefore exploring RNA structure is of interest to understand RNA-dependent processes. Chemical probing *in vitro* is a very powerful tool to investigate RNA molecules under a variety of conditions. Among the most frequently used chemical reagents are the nucleobase-specific probes dimethyl sulfate (DMS), 1-cyclohexyl-3-(2-morpholinoethyl) carbodiimide metho-p-toluenesulfonate (CMCT) and  $\beta$ -ethoxy- $\alpha$ -ketobutyraldehyde (kethoxal). These chemical reagents modify nucleotides which are not involved in hydrogen bonding or protected by a ligand, such as proteins or metabolites. Upon performing modification reactions with all three chemicals the accessibility of all four nucleobases can be determined. With this fast and inexpensive method local changes in RNA secondary and tertiary structure, as well as the formation of contacts between RNA and its ligands can be detected independent of the RNA's length.

**Key words** *In vitro* chemical probing, DMS, CMCT, Kethoxal, RNA structure, RNA-protein complexes

#### 1 Introduction

In the past, a vast number of noncoding regulatory RNA molecules were discovered, suggesting that RNA is the driving force in the most essential processes in the cell. To shed light on the basic mechanism of these RNA-dependent processes, it is important to explore the structure of an RNA and the assembly with its ligands, like proteins, metabolites or other RNA molecules. The process of folding is hierarchical and describes how RNA undergoes the transition from an unfolded, disordered state to the native, functional conformation [1–9]. Thus, to understand the dynamic process of folding it is crucial to determine the structure of RNA folding intermediates and the conformation of the native state.

A variety of methods have been used to map the structure of RNA *in vitro* [10–13]. A rapid, inexpensive and widely used

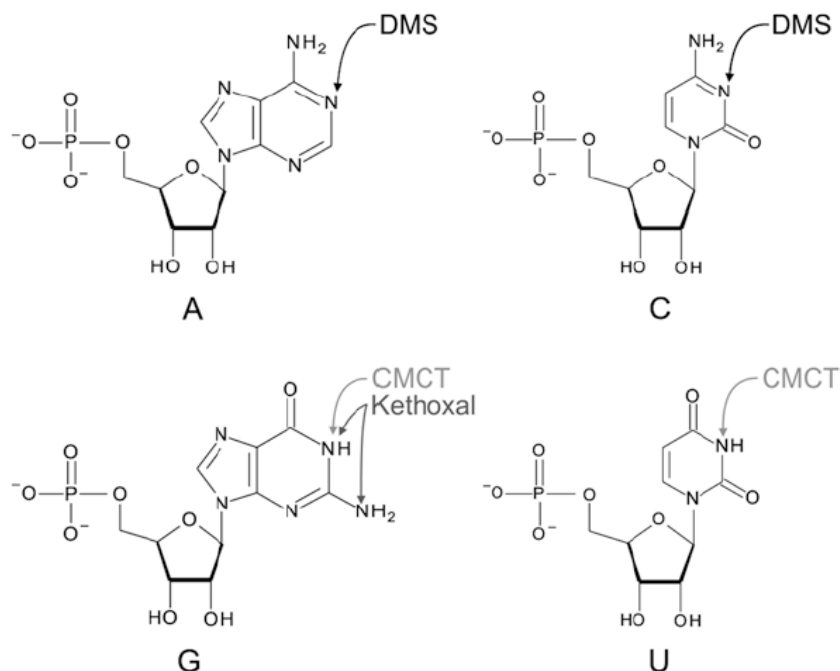


**Fig. 1** The chemical reagents DMS, CMCT, and Kethoxal are nucleobase-specific in their modification reaction. DMS methylates N1 of adenine and N3 of cytosine. CMCT modifies mainly N3 of uracil and to a lesser extent the N1 of guanine, whereas Kethoxal modifies guanine at the N1 and N2 positions. *DMS* dimethyl sulfate, *CMCT* 1-cyclohexyl-3-(2-morpholinoethyl) carbodiimide metho-p-toluenesulfonate, *Kethoxal*  $\beta$ -ethoxy- $\alpha$ -ketobutyraldehyde

method to obtain structural information on RNAs is chemical probing in vitro. This technique employs the commercially available chemical reagents DMS, CMCT and Kethoxal that react with specific atoms of different nucleobases (Fig. 1), if they are not engaged in H-bonds [10, 14, 15]. While DMS methylates the N1 of adenine and N3 of cytosine, CMCT modifies the N1 of guanine and N3 of uracil and Kethoxal specifically attacks the N1 and N2 of guanine. Thus, it is possible to investigate the accessibility of all four nucleobases. The sites of modification can then be determined by reverse transcription (RT) using a radioactively or fluorescently labeled complementary DNA oligo [10, 14, 15], because the bulky modification groups at the Watson-Crick position of the nucleotides leads to termination of the reverse transcription (Fig. 2). After separating the cDNA pool on a standard denaturing polyacrylamide gel, residues, which are not involved in secondary or tertiary structure formation and/or are not protected from modification by binding to a ligand, become visible as strong DMS-dependent RT stops (or CMCT- and Kethoxal-dependent stops), which can be mapped onto the secondary structure of a given RNA. This provides a good picture of the specific structure adopted

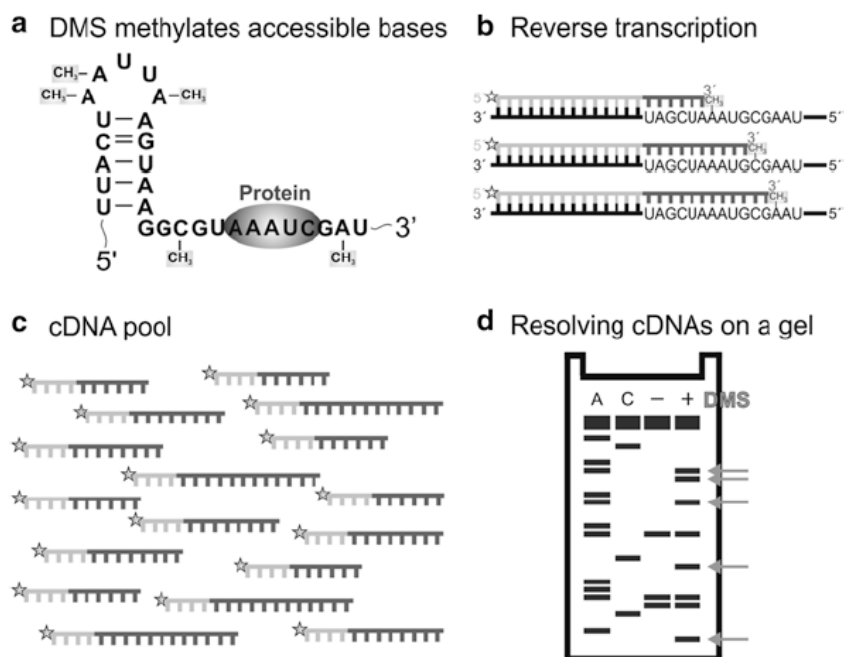


**Fig. 2** Experimental framework of in vitro chemical probing with DMS. **(a)** Only A and C residues that are not engaged in H-bonding and are not interacting with proteins (or another ligand) are accessible to DMS and can thus be methylated. **(b)** Using a 5' end-labeled primer, the sites of modification can be mapped by reverse transcription, as they cause a stop in the extension by the reverse transcriptase due to the bulky methyl group. RNA is shown in *black*, the annealed primer in *dark gray* and the extension by the RT in *light gray*; the *star* indicates the 5' end-label of the primer. **(c)** The generated cDNA pool is then resolved on a standard denaturing polyacrylamide gel **(d)**, resulting in a distinct modification pattern for a given RNA. A and C denote sequencing lanes; *lane 3* is the RT stop control to detect natural stops of the extension (unmodified RNA is used in RT reaction); *lane 4* shows the DMS pattern of the RNA (*gray arrows*)

by the RNA. As such, the conformation of different stable intermediates along a folding pathway can be explored with this method. In addition, residues that interact with a protein (or another ligand) and the concomitant structural changes induced by the protein can also be characterized with this methodology (e.g., [10, 14–23]).

The chemical probing technique can be easily adapted for a given RNA and is largely insensitive to the folding conditions of the RNA and its size. In other words, it can be used to study the structure of RNAs which cannot be easily subjected to NMR and crystallization techniques. Therefore it has proven to be a very powerful tool, as it has been used to map the structure of various RNAs including group I and group II introns, ribosomal RNAs, and ligand-induced conformational changes (e.g., [10, 14–23]). We recently investigated the structure of the human telomerase RNA (hTR) in vitro using DMS chemical probing (Fig. 3; Auer



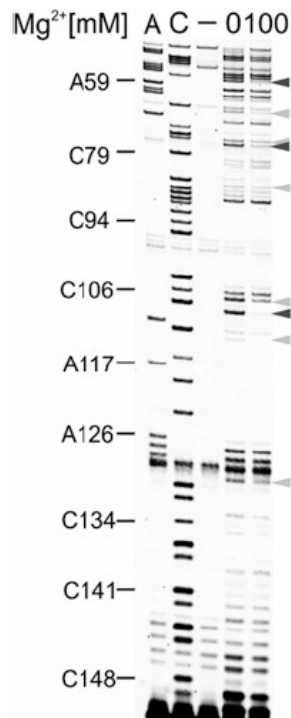


**Fig. 3**  $\text{Mg}^{2+}$ -induced structural changes in human telomerase RNA. Using DMS, which methylates A-N1 and C-N3, if they are not involved in H-bonding, the structure of the human telomerase RNA has been mapped. A and C denote sequencing lanes; *The-lane* is an RT stop control to detect natural stops of the extension (independent of DMS modification; RNA was folded, but not incubated with DMS). Lanes labeled 0 and 100: The *number* refers to the  $\text{Mg}^{2+}$  concentration [mM] used in the folding reaction and both samples were treated with DMS. *Gray arrow heads* indicate residues that became protected from DMS modification upon high  $[\text{Mg}^{2+}]$ ; *light gray arrow heads* indicate weak protections and *dark gray* represents strong protections

*and Waldsich, unpublished*). Comparing the folding states of hTR in the absence and presence of  $\text{Mg}^{2+}$  ions indicates that most of secondary structure of hTR is able to form in the absence of  $\text{Mg}^{2+}$  ions. In contrast, the pseudoknot appears to require high  $[\text{Mg}^{2+}]$  to fold (Fig. 3; *Auer and Waldsich, unpublished*). Also, these chemical probing data imply that the human telomerase RNA holds several interesting tertiary structure features to discover, as supposedly single-stranded residues are protected from modification, suggesting that these are engaged in H-bonding. In summary, chemical probing provides detailed information on the secondary and tertiary structure of a given RNA and can be complemented with other structural probing methods, such as SHAPE and hydroxyl-radical footprinting, or chemogenetic approaches [11–13].



## 2 Materials

Prepare all solutions with RNase-free ultrapure water (deionized water with a sensitivity of  $\geq 18 \text{ M}\Omega \text{ cm}$  at  $25^\circ\text{C}$ ) (*see Note 1*) and store the sterile solutions at room temperature if not stated otherwise. Use RNase-free plasticware and glassware for the experiments.

### 2.1 In Vitro Transcription

1.  $10\times$  transcription buffer: 0.4 M Tris-HCl, pH 7.5, 0.26 M  $\text{MgCl}_2$ , 30 mM spermidine. Store at  $-20^\circ\text{C}$  in the dark.
2. 1 M DTT (dithiothreitol). Store at  $-20^\circ\text{C}$ .
3. 100 mM ribonucleotides rATP, rCTP, rGTP, and rUTP. Store at  $-20^\circ\text{C}$ .
4. RNase inhibitor (40 U/ $\mu\text{L}$ ). Store at  $-20^\circ\text{C}$ .
5. T7 RNA polymerase (homemade). Store at  $-20^\circ\text{C}$ .
6. RNase-free DNase I (2 U/ $\mu\text{L}$ ). Store at  $-20^\circ\text{C}$ .
7.  $10\times$  TBE: 0.89 M Tris base, 0.89 M boric acid, 20 mM EDTA.
8. Glycogen (10 mg/mL). Store at  $-20^\circ\text{C}$ .
9. 0.5 M EDTA, pH 8.0.
10. Ethanol/0.3 M NaOAc, pH 5.0.
11. 70 % (v/v) ethanol.
12. Loading buffer I: 7 M urea, 25 % (w/v) sucrose, 0.025 % (w/v) bromophenol blue, 0.025 % (w/v) xylene cyanol in  $1\times$  TBE.

### 2.2 Purification of In Vitro Transcribed RNA

1. 5 % acrylamide solution: 5 % (v/v) acrylamide/bisacrylamide (19:1), 7 M urea in  $1\times$  TBE (*see Note 2*). Store at  $4^\circ\text{C}$  in the dark.
2. 10 % (w/v) APS (ammonium persulfate). Store at  $4^\circ\text{C}$  (*see Note 3*).
3. N,N,N',N'-tetramethylethylenediamine (TEMED). Store at  $4^\circ\text{C}$ .
4.  $10\times$  TBE: 0.89 M Tris base, 0.89 M boric acid, 20 mM EDTA, pH 8.0 (*see Note 2*).
5. Elution buffer: 100 mM Tris-HCl, pH 7.5, 250 mM NaOAc, pH 5.0, 2 mM EDTA, pH 8.0.
6. Fluor-coated TLC silica gel plate.
7. Short-wavelength UV light source (254 nm).
8. Saran wrap.
9. 0.5 M EDTA, pH 8.0.
10. Glycogen (10 mg/mL). Store at  $-20^\circ\text{C}$ .
11. Ethanol p.A.

12. 70 % (v/v) ethanol.
13. Glass plates (22 (L)×20 (W) cm).
14. Comb and spacer (1.0–1.5 mm thickness).
15. Vertical gel electrophoresis apparatus (adjustable).
16. High voltage power supply.

### **2.3 Chemical Probing**

1. 0.5 M potassium borate buffer, pH 8.0, stock. Store at 4 °C.
2. 0.5 M potassium borate buffer, pH 7.0, stock. Store at 4 °C.
3. 1 M cacodylate buffer, pH 7.5, stock. Store at 4 °C.
4. 2 M KCl.
5. 1 M MgCl<sub>2</sub>.
6. 1-cyclohexyl-3-(2-morpholinoethyl) carbodiimide metho-p-toluenesulfonate (CMCT; 42 mg/mL). Store at –20 °C.
7. 10.7 M dimethyl sulfate (DMS). Store at 4 °C.
8. Kethoxal (37 mg/mL). Store at –20 °C.
9. 25 % (v/v) ethanol.
10. 14.3 M β-mercaptoethanol. Store at 4 °C.
11. 0.5 M EDTA, pH 8.0.
12. Glycogen (10 mg/mL). Store at –20 °C.
13. Ethanol/0.3 M NaOAc, pH 5.0.
14. 70 % (v/v) ethanol.

### **2.4 5' End-Labeling of Primer**

1. [ $\gamma$ -<sup>32</sup>P]-ATP (10  $\mu$ Ci/ $\mu$ L, 6,000 Ci/mmol). Store at 4 °C.
2. 10  $\mu$ M stocks of gene-specific DNA primers. Store at –20 °C.
3. T4 polynucleotide kinase (PNK; 10 U/ $\mu$ L). Store at –20 °C.
4. 10× T4 polynucleotide kinase (PNK) buffer. Store at –20 °C.
5. 0.5 M EDTA, pH 8.0.
6. Glycogen (10 mg/mL). Store at –20 °C.
7. EtOH/0.3 M NaOAc, pH 5.0.
8. 70 % (v/v) ethanol.

### **2.5 Reverse Transcription**

1. 4.5× hybridization buffer: 225 mM K-Hepes, pH 7.0, 450 mM KCl. Store at –20 °C.
2. <sup>32</sup>P- or Cy5-labeled DNA oligos. Store at –20 °C.
3. 5× reaction buffer for the Transcriptor reverse transcriptase (Roche). Store at –20 °C.
4. 10 mM dNTPs mix (Li-Salt). Store at –20 °C.
5. 10 mM ddNTPs. Store at –20 °C.
6. 7.9× extension buffer: 1.3 M Tris-HCl, pH 8.0, 100 mM MgCl<sub>2</sub>, 100 mM DTT. Store at –20 °C.

7. Transcriptor reverse transcriptase (10 U/ $\mu$ L; Roche), or comparable product. Store at  $-20^{\circ}\text{C}$ .
8. AMV reverse transcriptase (10 U/ $\mu$ L). Store at  $-20^{\circ}\text{C}$ .
9. 1 M NaOH.
10. 1 M HCl.
11. 0.5 M EDTA, pH 8.0.
12. Glycogen (10 mg/mL). Store at  $-20^{\circ}\text{C}$ .
13. Ethanol/0.3 M NaOAc, pH 5.0.
14. 70 % (v/v) ethanol.
15. Loading buffer I: 7 M urea, 25 % (w/v) sucrose, 0.025 % (w/v) bromophenol blue, 0.025 % (w/v) xylene cyanol in 1 $\times$  TBE.
16. Loading buffer II: 7 M urea, 25 % (w/v) sucrose in 1 $\times$  TBE.
17. 10 $\times$  TBE: 0.89 M Tris base, 0.89 M boric acid, 20 mM EDTA.

**2.6 Denaturing  
Polyacrylamide Gel  
Electrophoresis (PAGE)**

1. 8 % acrylamide solution: 7 M urea, 8 % (v/v) acrylamide/bisacrylamide (19:1) in 1 $\times$  TBE (*see Note 2*). Store at  $4^{\circ}\text{C}$  in the dark.
2. 10 $\times$  TBE: 0.89 M Tris base, 0.89 M boric acid, 20 mM EDTA (*see Note 2*).
3. 10 % (w/v) APS (ammonium persulfate). Store at  $4^{\circ}\text{C}$  (*see Note 3*).
4. N,N,N',N'-tetramethyl-ethylenediamine (TEMED). Store at  $4^{\circ}\text{C}$ .
5. Glass plates (42 (L) $\times$ 20 (W) cm).
6. Metal plates which cover 2/3 of the glass plates.
7. Comb and spacer (0.4 mm thickness).
8. Vertical gel electrophoresis apparatus (adjustable).
9. High voltage power supply.
10. Whatman 3MM paper.
11. Saran wrap.
12. Phosphorimager exposure cassette and screen (GE Healthcare) or comparable product.
13. Phosphorimager Typhoon TRIO (GE Healthcare) or comparable equipment.

---

## 3 Methods

### 3.1 In Vitro Transcription Using the T7 RNA Polymerase

1. To set up the reaction mix 25  $\mu$ g linear dsDNA template (containing a T7 promoter upstream of the gene of interest) with 100  $\mu$ L 10 $\times$  transcription buffer, 10  $\mu$ L 1 M DTT, 20  $\mu$ L of each 100 mM ribonucleotide stock (rATP, rCTP, rGTP and

rUTP, respectively), 5  $\mu$ L RNase inhibitor (40 U/ $\mu$ L), 40  $\mu$ L T7 RNA polymerase (homemade) and ddH<sub>2</sub>O to a final volume of 1 mL (*see* Notes 1, 4 and 5).

2. Incubate the sample at 37 °C for 4 h.
3. To degrade the template, add 5  $\mu$ L RNase-free DNase I (2 U/ $\mu$ L) and incubate at 37 °C for 30 min.
4. To precipitate the sample, transfer it in a 15 mL tube and add 2  $\mu$ L glycogen (10 mg/mL), 25  $\mu$ L 0.5 M EDTA, pH 8.0, and 2.5 $\times$  volumes of ethanol/0.3 M NaOAc, pH 5.0. Incubate the sample at -20 °C for at least 60 min.
5. Centrifuge the samples at 4 °C for 30 min (18,000 $\times g$ ).
6. Remove the supernatant, wash the pellet with 70 % (v/v) ethanol, and dry it at room temperature for 10 min.
7. Resuspend the pellet in 30  $\mu$ L ddH<sub>2</sub>O and 80  $\mu$ L loading buffer I.

### 3.2 Purification of In Vitro Transcribed RNA

1. To purify the transcript pour a denaturing polyacrylamide gel (*see* Note 4). The percentage of the gel depends on the length of the transcribed RNA (Table 1). In case of human telomerase RNA (451 nt) a 5 % acrylamide solution is used. Use 70 mL of the respective acrylamide solution and mix it with 70  $\mu$ L TEMED and 700  $\mu$ L 10 % (w/v) APS and let it polymerize for at least 60 min.
2. Load the entire sample on the gel and let it run at 20–30 W (the power depends on the percentage of the gel and the time of the gel run depends on the length of the transcript).
3. Disassemble the gel and cover it with a Saran wrap.

**Table 1**  
Dye migration in denaturing polyacrylamide gels

AA solution (%)	Bromophenol blue	Xylene cyanol
5	35 nt	130 nt
6	26 nt	100 nt
8	19 nt	75 nt
10	12 nt	55 nt
20	8 nt	25 nt

Depending on the acrylamide concentration bromophenol blue and xylene cyanol co-migrate with nucleic acid fragments of different length. The appropriate percentage of acrylamide should therefore be chosen with respect to the size of the RNA or DNA molecules to be separated on the denaturing PAGE



4. Detect the transcript band by UV shadowing (254 nm). Place the gel on top of a fluor-coated TLC plate and hold it below a UV light source (254 nm). The TLC plate will appear in a yellow-green color, while the nucleic acid bands in the gel cast a shadow on the TLC plate, thereby becoming visible as a dark band.
5. Cut the marked band with a sterile blade and put the gel piece in a 15 mL reaction tube.
6. Add 3 mL elution buffer per 1 mL transcription reaction.
7. Freeze the sample at  $-80^{\circ}\text{C}$  for at least 30 min.
8. Thaw and vortex the sample.
9. Put the sample on a turning wheel at  $4^{\circ}\text{C}$  for 2–3 h.
10. Centrifuge at  $18,000\times g$  for 10 min.
11. Pour the supernatant in a syringe and press the liquid through a  $0.2\text{ }\mu\text{m}$  sterile filter. If necessary, rinse the syringe with additional 200  $\mu\text{L}$  elution buffer.
12. To precipitate the transcript, add 2  $\mu\text{L}$  glycogen (10 mg/mL) and  $2.5\times$  volumes of ethanol p.A. and keep the sample at  $-20^{\circ}\text{C}$  for at least 60 min.
13. Centrifuge the samples at  $4^{\circ}\text{C}$  for 30 min ( $18,000\times g$ ).
14. Remove the supernatant and dry the pellet at room temperature for 10 min.
15. Resuspend the transcript in 25–50  $\mu\text{L}$  ddH<sub>2</sub>O depending on the size of the pellet. Store the sample at  $-20^{\circ}\text{C}$ .

### 3.3 Chemical Probing of RNA In Vitro

#### 3.3.1 Folding Reaction

1. In a volume of 45  $\mu\text{L}$  assemble 10 pmol RNA with 5  $\mu\text{L}$  1 M KCl and 25  $\mu\text{L}$  160 mM modification buffer. For DMS and Kethoxal reactions use cacodylate buffer, pH 7.5, and for CMCT samples potassium borate buffer, pH 8.0, as modification buffer.
2. Denature the RNA at  $95^{\circ}\text{C}$  for 1 min.
3. Incubate the sample at room temperature for 2 min.
4. Add 5  $\mu\text{L}$  1 M  $\text{MgCl}_2$  (f.c. 100 mM) or 5  $\mu\text{L}$  ddH<sub>2</sub>O to the folded and unfolded RNA samples, respectively, (Fig. 3) and incubate at  $42^{\circ}\text{C}$  for 30 min (*see Note 6*).

#### 3.3.2 Modification Step

1. Add the modification reagent to the RNA samples as indicated in Table 2 (*see Notes 7 and 8*).
2. Incubate the samples at room temperature for 20 min. In case of DMS the samples can be kept at  $37^{\circ}\text{C}$  as well.
3. To stop the reaction, add 1  $\mu\text{L}$   $\beta$ -mercaptoethanol to the DMS-treated samples and 1  $\mu\text{L}$  0.5 M potassium borate buffer, pH 7.0, to the Kethoxal-treated ones (*see Note 9*).

**Table 2****Prepare fresh solutions of the modifying reagents for each experiment**

CMCT	DMS	Kethoxal
Add 10 $\mu$ L of a 42 mg/mL CMCT stock solution; always prepare a fresh stock solution	Add 1 $\mu$ L of a 1.07 M DMS solution; always prepare a fresh 1:10 dilution in ethanol p.A. from the commercially available 10.7 M DMS stock	Add 10 $\mu$ L 7.4 mg/mL Kethoxal solution; always prepare a fresh 1:5 dilution in 25 % (v/v) EtOH from a 37 mg/mL Kethoxal stock

4. Precipitate the samples; add 2  $\mu$ L glycogen (10 mg/mL), 1  $\mu$ L 0.5 M EDTA, pH 8.0, and 2.5 $\times$  volumes of ethanol/0.3 M NaOAc, pH 5.0, and keep them at  $-20^{\circ}\text{C}$  for at least 60 min.
5. Centrifuge the samples at  $4^{\circ}\text{C}$  for 30 min (18,000 $\times g$ ).
6. Remove the supernatant, wash the pellet with 70 % (v/v) ethanol, and dry it at room temperature for 10 min.
7. Resuspend the CMCT-modified sample in 2.5  $\mu$ L 25 mM potassium borate buffer, pH 8.0, per 1 pmol RNA. In case of DMS- and Kethoxal-treated RNA, resuspend the pellet in 2.5  $\mu$ L ddH<sub>2</sub>O per 1 pmol RNA, yielding a concentration of 0.4  $\mu$ M.

### **3.4 5' End-Labeling of DNA Primers**

1. To set up the primer kinase reaction, mix 10 pmol DNA oligo, 10 pmol [ $\gamma$ -<sup>32</sup>P]-ATP (10  $\mu$ Ci/ $\mu$ L, 6,000 Ci/mmol), 2  $\mu$ L 10 $\times$  PNK buffer and add ddH<sub>2</sub>O to a volume of 19  $\mu$ L (*see* Notes 10 and 11). Add 1  $\mu$ L T4 polynucleotide kinase (10 U/ $\mu$ L).
2. Incubate the sample at  $37^{\circ}\text{C}$  for 30 min.
3. Stop the reaction by adding 1  $\mu$ L 0.5 M EDTA, pH 8.0.
4. To denature the enzyme place the sample at  $95^{\circ}\text{C}$  for 1 min, then immediately put the tubes on ice for 2 min.
5. To precipitate the sample, add 2  $\mu$ L glycogen (10 mg/mL) and 2.5 $\times$  volumes of ethanol/0.3 M NaOAc, pH 5.0, and put the tube at  $-20^{\circ}\text{C}$  for at least 60 min.
6. Centrifuge the samples at  $4^{\circ}\text{C}$  for 30 min (18,000 $\times g$ ).
7. Remove the supernatant, wash the pellet with 70 % (v/v) ethanol, and dry it at room temperature for 10 min.
8. Resuspend the oligo in 40  $\mu$ L ddH<sub>2</sub>O and store it at  $-20^{\circ}\text{C}$ .

### **3.5 Detecting the Modification Sites by Reverse Transcription**

1. To set up the annealing reaction mix 2.5  $\mu$ L 0.4  $\mu$ M RNA, 1  $\mu$ L 0.25  $\mu$ M <sup>32</sup>P-labeled primer or 0.5  $\mu$ M Cy5-labeled primer, and 1  $\mu$ L 4.5 $\times$  hybridization buffer (*see* Notes 12–14).
2. Incubate the sample at  $95^{\circ}\text{C}$  for 1 min.

3. Cool the sample either rapidly (snap cooling) by placing it on ice for 2 min or slowly by continuous incubation on a thermomixer until its temperature decreased to 55 °C.
4. For the extension of the <sup>32</sup>P-labeled primer, add 3.4 µL extension mix to the sample consisting of 1 µL 7.9× extension buffer, 0.7 µL 10 mM dNTPs, 1.55 µL ddH<sub>2</sub>O, and 0.15 µL AMV reverse transcriptase (10 U/µL). In case of Cy5-labeled primers, add 14.5 µL extension mix consisting of 4 µL 5× reaction buffer, 2 µL 10 mM dNTPs, 1 µL 0.1 M DTT, 7.5 µL ddH<sub>2</sub>O, 0.5 µL RNase inhibitor (40 U/µL), and 0.5 µL Transcriptor reverse transcriptase (10 U/µL). For the sequencing lanes add 1.5 µL of a 1 mM ddNTP solution to the sample in addition to the extension mix (*see* Notes 13 and 14).
5. Incubate the samples at 55 °C for 60 min to synthesize the cDNA.
6. To degrade the RNA template, add 3 µL 1 M NaOH.
7. Incubate for 30–60 min at 55 °C.
8. Add 3 µL 1 M HCl to neutralize the pH.
9. To precipitate the samples, add 2 µL glycogen (10 mg/mL), 1 µL 0.5 M EDTA, pH 8.0, and 2.5× volumes of ethanol/0.3 M NaOAc, pH 5.0, and incubate them at –20 °C for at least 60 min.
10. Centrifuge the samples at 4 °C for 30 min (18,000×g).
11. Discard the supernatant, wash the pellet with 70 % (v/v) ethanol, and dry it at room temperature for 10 min.
12. Resuspend the cDNA in 10 µL loading buffer I (for <sup>32</sup>P-labeled cDNA) or loading buffer II (for Cy5-labeled cDNA).

**3.6 Denaturing  
Polyacrylamide Gel  
Electrophoresis (PAGE)  
to Separate the  
cDNA Pool**

1. Assemble the glass plates and stabilize them with clamps.
2. Mix 50 mL 8 % acrylamide solution with 500 µL 10 % (w/v) APS and 50 µL TEMED and pour the gel (*see* Note 3).
3. Insert the comb and let the gel polymerize in a horizontal position for at least 60 min.
4. After removing the clamps and the comb adjust the gel in the apparatus and fill the buffer reservoirs with 1× TBE (*see* Note 2).
5. Rinse the wells with 1× TBE.
6. Attach a metal plate to the front of the gel and let it pre-run at 40 W for 30 min (*see* Note 15).
7. Denature the samples at 95 °C for 1 min and then put them on ice.
8. Load half of the sample (5 µL) on the gel. If fluorescently labeled primers were used for reverse transcription, load 2 µL

- of loading buffer I in one of the empty wells as it contains dyes (xylene cyanol and bromophenol blue). This allows following the gel run.
9. Use a darkroom or cover the apparatus with a dark plastic bag if you are working with light sensitive samples.
  10. Run the gel at 40 W for 90–120 min depending on the size of the cDNA fragments to be separated (Table 1).
  11. To disassemble the gel, remove the spacers and carefully detach the coated glass plate from the gel. In case of fluorescently labeled samples, proceed directly to step 15.
  12. Transfer the gel on a Whatman 3MM paper and cover it with Saran wrap.
  13. Dry the gel by applying heat and vacuum (~1 h at 80 °C).
  14. Expose the gel to a phosphorimager screen overnight.
  15. Scan the screen using a phosphorimager Typhoon Trio or equivalent equipment for radioactively labeled cDNA. In case of Cy5-labeled cDNA, scan the gel directly.
  16. For the analysis of the gel (*see* Notes 16–21), use a software like ImageQuant or SAFA [24].

---

## 4 Notes

1. RNA degradation is a frequent problem when working with RNA, therefore some precautions should be considered: Always wear gloves while handling the samples; plasticware and glassware as well as solutions used should be prepared and maintained RNase-free, since autoclaving is not sufficient to inactivate all RNases; always keep RNA on ice while working (unless indicated otherwise) and store it at –20 °C; avoid freezing and thawing of the RNA stock too often; clean the bench and the equipment with “RNaseZap” (Ambion) or a similar product; aliquot the reagents, so if a contamination is encountered, one can simply take a new aliquot without having to remake the stock solutions.
2. To avoid differences in salt concentrations always use the same TBE buffer stock for preparing the acrylamide solution and running the gel.
3. The 10 % (w/v) APS solution can be stored at 4 °C for up to 2 weeks. Alternatively, freeze it in aliquots at –20 °C, which are stable up to 6 months.
4. For in vitro transcription the T7 MegaScript kit (Ambion) can be used alternatively and the transcript can be purified using the MegaClear kit (Ambion).



5. For optimal transcription efficiency it is important to optimize the incubation time as well as the concentration of nucleotides,  $Mg^{2+}$  ions and the DNA template, as these can significantly affect the transcription yield. Increasing the amount of DTT can enhance the yield as well.
6. Incubation temperature and time as well as concentrations of monovalent and divalent ions have to be optimized for a given RNA.
7. Kethoxal and DMS are highly toxic and carcinogenic chemicals which can easily penetrate the skin. Thus, always wear gloves and work under a fume hood to avoid inhaling. For more detailed information about Kethoxal, DMS and CMCT read the Material Safety Data Sheet (MSDS) provided by the manufacturer.
8. It is recommended to perform a concentration series with the chemical reagent to determine the single-hit conditions, i.e., only one modification per RNA molecule should occur. Single-hit conditions typically result in a pool of modified RNA harboring less than one modification and therefore the same amount of full-length cDNA is observed, for example, in the DMS-treated sample and in the unmodified control. If the lanes are fading out (and barely any full-length product is observed), a lower concentration of the modifying reagent should be used.
9. To assure that the DMS reaction is successfully quenched by  $\beta$ -mercaptoethanol, perform a stop control. Therefore add  $\beta$ -mercaptoethanol to the sample before adding the DMS. The stop control should give a pattern comparable to the RT stop control prepared from unmodified RNA.
10. The PNK enzyme and the PNK buffer are highly sensitive to changes in temperature. Therefore aliquot the buffer to avoid frequent freezing and thawing.
11. It is highly recommended to purify the non-labeled DNA oligos using a standard denaturing PAGE in order to remove any organic remnants from the oligo synthesis, since these can impair the end-labeling reaction. Thus, gel-purification of the primer increases the labeling efficiency and in turn the signal intensity. Gel-purification of Cy5-labeled oligos is recommended as well, as it improves the reverse transcription results.
12. Primers have to be designed in a way that they bind efficiently to their target and do not form intramolecular or intermolecular interactions. Their length is typically between 18 and 25 nt and they should preferably contain a G or C at their 3' end. Varying primer length (and its  $T_M$ ) can increase binding efficiency of the oligo to the RNA. To map RNAs consisting of

more than 100 nt, several primers are required to map the modification sites throughout the entire RNA. When designing this primer set, ensure that there is a certain overlap between the sequences mapped by subsequent primers.

13. Experimental conditions like incubation temperature and time, concentrations of dNTPs and ddNTPs (for the sequencing lanes),  $Mg^{2+}$  and RNA have to be adjusted for each construct individually to yield sufficient amounts of cDNA and in turn to obtain a good signal-to-noise ratio. If the ddNTP concentration is too high sequencing lanes tend to give a very faint signal in the upper part of the gel. If the concentration is too low, it may happen that some nucleotides cannot be detected, even though flanking residues are visible.
14. To distinguish between so-called natural stops of the reverse transcriptase enzyme and those induced by DMS (or CMCT, Kethoxal) modification, an RT stop control has to be included. This control is prepared by reverse transcribing RNA, which was refolded but not treated with DMS, CMCT or Kethoxal, thereby revealing the natural stops. These are of different origin: (1) Secondary structures that re-form after denaturing of the RNA as well as (2) G/C sequence stretches can block the reverse transcriptase enzyme and in turn stop the extension. (3) Due to a strain on the backbone RNAs often have “hot spots” for breakage. (4) Partial degradation by RNases results in RT stops as well.
15. If the probes on the gel run unevenly (“smiley effect”), ensure that the gel runs with sufficient temperature (45–55 °C) and attach a metal plate in front of the gel to achieve an equally distributed temperature all over the gel.
16. If the signal to noise ratio is weak, it is often advisable to switch from AMV reverse transcriptase to a more thermostable and sensitive enzyme, like Thermoscript (Invitrogen) or Transcriptor reverse transcriptase (Roche), since these show an improved performance in reverse transcribing highly structured and G/C- rich RNAs.
17. Signals with high intensity allow easier interpretation of data since background noise is reduced to a minimum. A low signal to noise ratio makes it difficult to analyze the gels properly. To avoid this problem, it is recommended to adjust the amount of starting material or loading more sample per lane. Another possibility is to extend the exposure time of the gels.
18. Fuzzy or diffuse bands mostly arise from excess salt in the samples or suboptimal buffer conditions (e.g., gel runs at too high voltage). The samples will not migrate uniformly through the gel and can even get stuck in the wells. To overcome this problem, wash the pellet with 70 % (v/v) ethanol and decrease the

precipitation time. Another solution is to increase the percentage of the gel and the running time, as the salt front will run out of the gel.

19. Dark smears on the gel can result from tiny air bubbles or fibers present in the gel or introduced when loading the samples.
20. Fuzzy bands can occur, if the RNA is not fully degraded after the reverse transcription. In this case it is important to control the pH after adding NaOH or prepare fresh NaOH and HCl stocks.
21. Uneven loading makes quantitation more difficult and less reliable, necessitating a rerun of the gel. It is often helpful to determine the counts of every sample and balance them before loading.

---

## Acknowledgements

This work was supported by the Austrian Science Foundation FWF [grants Y401 and P23497 to C.W.]. We want to thank Katharina Auer for providing the data shown in Fig. 3.

## References

1. Brion P, Westhof E (1997) Hierarchy and dynamics of RNA folding. *Annu Rev Biophys Biomol Struct* 26:113–137
2. Pyle AM, Fedorova O, Waldsich C (2007) Folding of group II introns: a model system for large, multidomain RNAs? *Trends Biochem Sci* 32:138–145
3. Schroeder R, Barta A, Semrad K (2004) Strategies for RNA folding and assembly. *Nat Rev Mol Cell Biol* 5:908–919
4. Sosnick TR, Pan T (2003) RNA folding: models and perspectives. *Curr Opin Struct Biol* 13:309–316
5. Treiber DK, Williamson JR (1999) Exposing the kinetic traps in RNA folding. *Curr Opin Struct Biol* 9:339–345
6. Treiber DK, Williamson JR (2001) Beyond kinetic traps in RNA folding. *Curr Opin Struct Biol* 11:309–314
7. Woodson SA (2000) Compact but disordered states of RNA. *Nat Struct Biol* 7:349–352
8. Woodson SA (2005) Structure and assembly of group I introns. *Curr Opin Struct Biol* 15:324–330
9. Woodson SA (2010) Compact intermediates in RNA folding. *Annu Rev Biophys* 39:61–77
10. Brunel C, Romby P (2000) Probing RNA structure and RNA-ligand complexes with chemical probes. *Methods Enzymol* 318:3–21
11. Shcherbakova I, Mitra S, Beer RH et al (2006) Fast Fenton footprinting: a laboratory-based method for the time-resolved analysis of DNA, RNA and proteins. *Nucleic Acids Res* 34:e48
12. Waldsich C (2008) Dissecting RNA folding by nucleotide analog interference mapping (NAIM). *Nat Protoc* 3:811–823
13. Wilkinson KA, Merino EJ, Weeks KM (2006) Selective 2'-hydroxyl acylation analyzed by primer extension (SHAPE): quantitative RNA structure analysis at single nucleotide resolution. *Nat Protoc* 1:1610–1616
14. Ehresmann C, Baudin F, Mougel M et al (1987) Probing the structure of RNAs in solution. *Nucleic Acids Res* 15:9109–9128
15. Moazed D, Stern S, Noller HF (1986) Rapid chemical probing of conformation in 16 S ribosomal RNA and 30 S ribosomal subunits using primer extension. *J Mol Biol* 187:399–416
16. Brunel C, Romby P, Westhof E et al (1991) Three-dimensional model of *Escherichia coli* ribosomal 5S RNA as deduced from structure

- probing in solution and computer modeling. *J Mol Biol* 221:293–308
17. Moazed D, Noller HF (1986) Transfer RNA shields specific nucleotides in 16S ribosomal RNA from attack by chemical probes. *Cell* 47:985–994
18. Moazed D, Noller HF (1987) Interaction of antibiotics with functional sites in 16S ribosomal RNA. *Nature* 327:389–394
19. Moazed D, Noller HF (1989) Interaction of tRNA with 23S rRNA in the ribosomal A, P, and E sites. *Cell* 57:585–597
20. Moazed D, Robertson JM, Noller HF (1988) Interaction of elongation factors EF-G and EF-Tu with a conserved loop in 23S RNA. *Nature* 334:362–364
21. Moazed D, Samaha RR, Gualerzi C et al (1995) Specific protection of 16 S rRNA by translational initiation factors. *J Mol Biol* 248:207–210
22. Konforti BB, Liu Q, Pyle AM (1998) A map of the binding site for catalytic domain 5 in the core of a group II intron ribozyme. *EMBO J* 17:7105–7117
23. Waldsich C, Masquida B, Westhof E et al (2002) Monitoring intermediate folding states of the *td* group I intron *in vivo*. *EMBO J* 21:5281–5291
24. Das R, Laederach A, Pearlman SM et al (2005) SAFA: semi-automated footprinting analysis software for high-throughput quantification of nucleic acid footprinting experiments. *RNA* 11:344–354



# CURRICULUM VITAE

---

## Stefan Handl, BSc



### PERSÖNLICHE INFORMATIONEN

---

Anschrift:            Arztgasse 64, 1220 Wien (Österreich)  
Telefon:             0699/125 600 67  
E-Mail:              [handl.stefan@gmail.com](mailto:handl.stefan@gmail.com)  
Geburtsdatum:       21.09.1985

### BERUFSERFAHRUNG

---

seit 01/05/2014

#### **Wissenschaftlicher Projektmitarbeiter**

Master thesis: *‘human telomerase RNA: mutational analysis and post-transcriptional modification’*

Beschreibung: Mutationsanalyse und Klonierungen, Aktivitätsassays von nativen Zelllysaten, ‚chemical probing *in vivo*‘ mit DMS und CMCT zur Identifikation der Sekundärstruktur und Veränderungen dieser in der humanen Telomerase RNA, Tutorien und Studentenbetreuung;

Universität Wien, Projektleitung: Mag. Dr. Christina Waldsich  
Dr.-Bohrergasse 7, 1030 Wien (Österreich)

01/06/2012 – 30/04/2014

#### **Wissenschaftlicher Projektmitarbeiter, Teilzeit**

Projekttitel: *‘Two proteins co-opt to promote group I intron folding in vivo’*

Beschreibung: Optimierung der Proteinaufreinigung von Mss116p mit His-Tag über Ni-NTA Säulen und *in vitro* assays zur Bestimmung der Reinheit und Aktivität (ATPase, Splicing), Tutorien und Studentenbetreuung;

Universität Wien, Projektleitung: Mag. Dr. Christina Waldsich  
Dr.-Bohrergasse 7, 1030 Wien (Österreich)

01/07/2007 – 31/08/2009

#### **Sachbearbeiter im Bereich Budget**

Beschreibung: Budgetvollzug, rechnerische Budgetüberwachung von Schulen, Hilfestellung und Schulung von Rechnungsführungspersonal sowie Kostenabrechnung der Nachmittagsbetreuung;

Stadtschulrat für Wien, Abteilung Budget/EDV  
Wipplingerstrasse 28, 1010 Wien (Österreich)

01/04/2007 – 30/06/2007

#### **Rechnungsführer**

04/11/2005 – 31/12/2006

Beschreibung: Verwaltung des Schulbudgets sowie Einkauf, Einnahmenverwaltung und Ausschreibungen;

Stadtschulrat für Wien  
Wipplingerstrasse 28, 1010 Wien (Österreich)

## AUSBILDUNG

---

- seit 01/10/2012      **Master of Science in ‚Molekulare Biologie‘ – Biochemie**  
Universität Wien  
Universitätsring 1, 1010 Wien (Österreich)
- 21/09/2009 – 04/06/2012      **Bachelor of Science in ‚Molekulare Biotechnologie‘**  
University of Applied Life Sciences, FH Campus Wien  
Marxbox, Helmut-Qualtinger-Gasse 2, 1030 Wien (Österreich)
- 01/09/2005 – 16/01/2009      **ORG für Berufstätige (berufsbegleitend)**  
Henriettenplatz 15, 1150 Wien (Österreich)
- 28/02/2005 – 26/10/2005      **Präsenzdienst österreichisches Bundesheer (Sanitäter)**
- 25/09/2001 – 24/12/2004      **Lehre als Verwaltungsassistent und Bürokaufmann**  
Berufsschule für Verwaltungsassistenten  
Panikengasse 31, 1160 Wien (Österreich)

## WEITERE QUALIFIKATIONEN

---

- Sprachkenntnisse:      Deutsch (Muttersprache), Englisch (fließend in Wort und Schrift);
- Soziale Kompetenzen:      Teambildungsfähigkeiten, Projektmanagement, grundlegende Präsentations-  
techniken, Konfliktmanagement und Moderationsfähigkeiten erlernt durch  
Seminare während des Studiums;
- Fachliche Zusätze:      Kenntnisse in GMP/GLP, Qualitäts- und Prozessmanagement,  
Arzneimittelbetriebsordnung (AMBO) und Arzneimittelgesetz (AMG) wurden  
durch das Studium erworben;
- Publikationen:      ‘*Mapping RNA structure in vitro using nucleobase-specific probes.*’ Sachsenmaier, N.,  
Handl, S., Debeljak, F., & Waldsich, C. (2014). *Methods in Molecular Biology*  
(Clifton, N.J.);
- EDV Kenntnisse:      Souveräner Umgang mit Microsoft Office (Word, Excel und PowerPoint),  
Perl, LaTeX, Arbeitserfahrung mit SAP Applikationen;
- Hobbies:      Strategiespiele, Geschichte, Dokumentationen;

Wien, 16.02.2015



Stefan Handl